

Analyzing the Temporal Patterns Associated with the Installation of Monopile Turbines

thru Pile-Driving at Vineyard Wind 1, Massachusetts

by

Tani Valdez Rivas

Dr. Doug Nowacek & Taylor Machette, Advisors

April 25, 2025

Masters project submitted in partial fulfillment of the requirements for the Master of
Environmental Management degree in the Nicholas School of the Environment of

Duke University

Executive Summary

Offshore wind is seen as a means to boost renewable energy production and decarbonize the power sector. However, there is apprehension to adopt offshore wind as its effect on marine life is still unknown. Pile-driving, an impulsive, repetitive, low-frequency sound, during the construction phase of offshore wind can emit noise in the same frequency band that baleen whales, a low-frequency specialist group of mammals, communicate. Previous studies on low-frequency seismic activity show calling rates and sightings decreased during activity. While there have been studies in European waters that examine the effects that pile-driving has on marine mammals, species of interest only include harbor porpoises, a high-frequency cetacean. Thus, there has become a need to understand how baleen whales, which includes mammals that are considered endangered or threatened under the Endangered Species Act and protected under the Marine Mammal Protection Act, are impacted by pile-driving.

For the objective of this study, we used acoustic data to characterize temporal patterns from pile-driving and sound exposure level changes at Vineyard Wind 1, the first commercial-scale offshore wind farm in the United States. Six Rockhoppers, which are passive acoustic monitoring units, were deployed within and surrounding the Vineyard Wind 1 Wind Energy Area. Pile-driving that occurred between September 3rd and December 28th, 2023 was examined. Through Raven Pro, a software used to visualize, measure, and analyze sound, a pile-driving strike detector algorithm was created to automate strike count and calculate start and end times for each individual strike. Additionally, Raven Pro measured the sound exposure level, which is a measure of total acoustic energy. Through R, an open-source language program, the following were calculated: the duration of the piling event (exposure duration), the pulse duration and inter-pulse duration for and between each strike and between each piling period, the strike rate per hour, and the duty cycle. These metrics were compared between the nearest and farthest rockhopper and with pile-driving that occurred at the Egmond aan Zee Offshore Wind Farm within the Dutch Sea.

Key findings include:

1. On average, pile-driving had the following: 3268 strikes per piling event, inter-pulse of 1.47 s, exposure duration of 1.89 hrs, strike rate of 1792.2 strikes/hr, pulse duration of 0.60 s, time interval between pile-driving periods of 111.41 s, and duty cycle of 29.7%.
2. On average, the mean difference between the nearest and furthest recording unit from pile-driving found an increase in average pulse duration by 6.4%, an increase in inter-pulse duration of 0.1%, an increase in duty cycle of 6.4% and decrease in SEL by 8.3 dB.
3. Compared to the Egmond aan Zee Offshore Wind, Vineyard 1 had a less variable exposure duration, a shorter strike rate, a longer pulse and inter-pulse duration, and a higher percentage duty cycle.

Currently, it is difficult to contextualize or make any conclusions to how pile-driving affects baleen whales. The primary reason being that this study was unable to find the sound exposure level as hydrophone calibration information was inaccurate and there is difficulty in determining any relationships between pile driving noise and baleen whale behavior.

Key recommendations include:

1. Long-term monitoring and studies are needed that examine how pile-driving events impact baleen whale behavior and hearing
2. The inclusion of temporal analysis resulting from pile-driving events in future studies

This data will be used to aid in the work being conducted by Project Wildlife and Offshore Wind, a collaborative research program that examines the potential effects that offshore wind energy development has on marine life. It will help inform future management practices and contribute to further research.

Table of Contents

Executive Summary.....	1
<i>Background.....</i>	4
Offshore Wind development and Construction.....	4
Impact of Noise.....	7
<i>Methods.....</i>	13
<i>Results.....</i>	17
<i>Implications.....</i>	21
<i>Discussion & Conclusion.....</i>	23
<i>References.....</i>	26
<i>Appendix.....</i>	31

Background

Offshore Wind development and Construction

As the global demand for energy continues to rise, there's a growing recognition of the limitations and drawbacks associated with reliance on fossil fuels and other non-renewable energy sources. To mitigate this issue, governments and entities have sought to diversify their national energy portfolios. Throughout the 21st century, there has been a notable rise in the adoption and use of Marine Renewable Energy (MRE) as a method to combat climate change. MRE offers a clean and renewable energy source, reduces emissions from greenhouse gases, and aids in the achievement of a sustainable future (Copping et al, 2020). In 2021, the Biden Administration announced the 30x30 initiative, which aims to conserve 30 percent of land, freshwater, and ocean located in the United States by 2030. These efforts included reaching 30 gigawatts (GW) of offshore wind energy capacity by 2030, which could power more than 20 million homes per year, aiding in the expansion of offshore wind development in the United States (The White House, 2021). In 2023, construction began on one of America's first commercial-scale offshore wind farms, Vineyard Wind 1. Located 15 miles from Martha's Vineyard, Vineyard Wind 1 has a total of 62 General Electric Haliade-X turbines, with each turbine capable of generating 13 MW of energy, having a total installation capacity of 800 MW, enough to power 400,000 homes (Musial et al, 2023; Vineyard Wind, 2023).

As offshore wind development and operations have expanded, exposure to anthropogenic noises from offshore wind, such as boats, foundation installation, etc., has increased (Stöber et al, 2019). While offshore wind is regarded as a means to boost renewable energy production and decarbonize the power sector, there are concerns about the effect that it will have on marine species. It can indirectly and directly affect taxa through a variety of means, but noise emissions

produced during turbine installation are thought to be one of the main risks associated with wind farm construction (Brandt et al, 2011; Hastie, et al, 2018).

Offshore wind life cycle consists of planning, construction, installation, maintenance and operation, and decommissioning (Music et al, 2010). As a result, there are a number of noises that radiate from offshore wind operations. During the pre-construction phase, meteorological masts, geological and geotechnical surveys are deployed and conducted to determine local weather information and site suitability, which is critical for wind turbine installation. This requires the use of acoustic ranging/imaging sensors and maintenance from vessels, increasing traffic in the area (Nedwell et al, 2004; Louerio et al, 2023). The construction phase during offshore wind development is usually the shortest phase of the cycle, however noise exposure is a major concern during this phase. During this phase, small and large vessels are used in association with surveying and installation activities. The use of one or more construction vessels, which is used to deploy equipment, is often accompanied by support of personnel vessels (Mooney et al, 2020). This increase in vessel traffic has become an environmental concern as there is increased disturbance from noise levels (Bailey et al, 2014). Depending on vessel size, speed and power engines, vessel noise can reach between 140 and 190 dB re 1 micro pascals (μ Pa) m⁻¹ (Crevello et al, 2023). The longest phase is the operational phase, as most offshore wind farms have an expected life span ranging between 20 - 30 years. During operation, underwater noise from turbines are low-frequency (below 1 kHz), with sound pressure level (SPL) reaching 105 dB re 1 μ Pa and 125 dB re 1 μ Pa 100 m from the source (Tougaard et al, 2008; Mooney et al, 2020). As the decommissioning process is still in its infancy, there is limited knowledge on the noise levels being produced during this phase. When an offshore wind farm is decommissioned, there is the removal of turbines, embedded foundations and transition

pieces, cables, meteorological masts, and offshore substations. The removal of these structures often requires the use of jets or explosives, displacing marine life in the process. Previous studies have estimated that the use of jets have a peak pressure level between 198 - 199 dB re 1 μ Pa at distances of 10 to 50 m from the source with energy concentrated between 250 Hz and 1,000 Hz. As there are significant knowledge gaps, more research needs to be conducted on the noise levels produced during decommissioning (Nedwell et al, 2004; Hinzmann et al, 2017; Mooney et al, 2020). While the effects of decommissioning of offshore wind farms are still being understood, the effects of decommissioning offshore oil and gas structures have been well-studied. Similarly to the decommissioning of offshore wind farms, the removal of offshore oil and gas structures requires the dismantling of large steel structure, pipeline cleaning, and seabed surveys using high technology, machinery, submarines, etc (Shams et al, 2023). The SPL are 30 – 40 dB higher than the baseline measurements (Fernandez-Betelu et al, 2024). Another significant producer of noise during the offshore wind life cycle is pile-driving.

Pile-driving refers to the process of installing turbine monopile and jacket foundations in shallow-water habitats; large hydraulic hammers are used to drive the foundations into the seabed by striking them repeatedly with the necessary energy to drive the piling into a given substrate (Sun et al, 2012). Noise emission from pile-driving is considered to be impulsive, which are characterized as sounds that are brief (<1s), transient, broadband, with high peak sound pressure, rapid rise time, and rapid decay time. Impulsive sounds can be either repetitive or a singular event (National Marine Fisheries Service, 2018; Martin et al, 2020). Pile-driving is measured by its sound exposure level (SEL) and/or peak sound pressure level (Amaral, 2020; Southall et al, 2019). The peak-to-peak sound level, which examines the maximum variation in pressure from positive to negative in a sound wave, is estimated to be 250 dB re 1 μ Pa at 1 m

from the source, i.e., the source level (SL). 100 m from the source, the peak-to-peak sound level is estimated to be 205 dB re 1 μ Pa (Bailey et al, 2010). The zero-to-peak sound level, or peak pressure, examines the maximum variation in pressure from zero to positive (Southall et al, 2007). Peak pressure is estimated to be at 205 dB re 1 μ Pa at 50 m from the source. Peak-to-peak and peak pressure are measured along with the root mean square (RMS) as it provides fixed-average calculations to characterize slow-changing or continuous, non-impulsive noise (Reyff, 2012; Rand, 2024). For piling events, developers often enact a soft start/ramp-up procedure, which slowly increases the sound levels, to provide marine life a warning signal, before sound levels reach a behavioral or injury threshold (Stone et al, 2017; van der Knaap et al, 2022).

Impact of Noise

Marine species utilize a wide range of frequencies to produce and receive sound, which is used for communication, reproduction, navigation, predator avoidance, foraging, etc (Madsen et al, 2006). However, not all marine species have equal hearing capabilities based on behavioral and electrophysiological measurements and predictions on the basis of ear morphology, modeling, behavior, etc. Marine mammals are divided into five hearing groups: low-frequency (LF) cetaceans, high-frequency (HF) cetaceans, very high-frequency (VHF) cetaceans, Phocid, and Sirenians (Southall et al, 2019).

Marine mammal hearing group	Auditory weighting function	Genera (or species) included	Group-specific appendix
Low-frequency cetaceans	LF	Balaenidae (<i>Balaena</i> , <i>Eubalaenidae</i> spp.); Balaenopteridae (<i>Balaenoptera physalus</i> , <i>B. musculus</i>)	1
		Balaenopteridae (<i>Balaenoptera acutorostrata</i> , <i>B. bonaerensis</i> , <i>B. borealis</i> , <i>B. edeni</i> , <i>B. omurai</i> ; <i>Megaptera novaeangliae</i>); Neobalenidae (<i>Caperea</i>); Eschrichtiidae (<i>Eschrichtius</i>)	
High-frequency cetaceans	HF	Physeteridae (<i>Physeter</i>); Ziphiidae (<i>Berardius</i> spp., <i>Hyperoodon</i> spp., <i>Indopacetus</i> , <i>Mesoplodon</i> spp., <i>Tasmacetus</i> , <i>Ziphius</i>); Delphinidae (<i>Orcinus</i>)	2
		Delphinidae (<i>Delphinus</i> , <i>Feresa</i> , <i>Globicephala</i> spp., <i>Grampus</i> , <i>Lagenodelphis</i> , <i>Lagenorhynchus acutus</i> , <i>L. albirostris</i> , <i>L. obliquidens</i> , <i>L. obscurus</i> , <i>Lissodelphis</i> spp., <i>Orcaella</i> spp., <i>Peponocephala</i> , <i>Pseudorca</i> , <i>Sotalia</i> spp., <i>Sousa</i> spp., <i>Stenella</i> spp., <i>Steno</i> , <i>Tursiops</i> spp.); Montodontidae (<i>Delphinapterus</i> , <i>Monodon</i>); Plantanistidae (<i>Plantanista</i>)	
Very high-frequency cetaceans	VHF	Delphinidae (<i>Cephalorhynchus</i> spp.; <i>Lagenorhynchus cruciger</i> , <i>L. australis</i>); Phocoenidae (<i>Neophocaena</i> spp., <i>Phocoena</i> spp., <i>Phocoenoides</i>); Iniidae (<i>Inia</i>); Kogiidae (<i>Kogia</i>); Lipotidae (<i>Lipotes</i>); Pontoporiidae (<i>Pontoporia</i>)	3
Sirenians	SI	Trichechidae (<i>Trichechus</i> spp.); Dugongidae (<i>Dugong</i>)	4
Phocid carnivores in water	PCW	Phocidae (<i>Cystophora</i> , <i>Erignathus</i> , <i>Halichoerus</i> , <i>Histriophoca</i> , <i>Hydrurga</i> , <i>Leptonychotes</i> , <i>Lobodon</i> , <i>Mirounga</i> spp., <i>Monachus</i> , <i>Neomonachus</i> , <i>Ommatophoca</i> , <i>Pagophilus</i> , <i>Phoca</i> spp., <i>Pusa</i> spp.)	5
Phocid carnivores in air	PCA		
Other marine carnivores in water	OCW	Odobenidae (<i>Odobenus</i>); Otariidae (<i>Arctocephalus</i> spp., <i>Callorhinus</i> , <i>Eumetopias</i> , <i>Neophoca</i> , <i>Otaria</i> , <i>Phocarcos</i> , <i>Zalophus</i> spp.); Ursidae (<i>Ursus maritimus</i>); Mustelidae (<i>Enhydra</i> , <i>Lontra feline</i>)	6
Other marine carnivores in air	OCA		

Table 1. Marine Mammal Hearing Groups. Note. Adapted from Southall et al. 2019.

There is concern regarding how cetaceans, in particular, will be affected by noise emissions from pile-driving (Bailey et al, 2010), given that these species utilize a wide range of frequencies to produce and receive sound. Compared to European waters, the North Atlantic right whale (*Eubalaena glacialis*), humpback whale (*Megaptera novaeangliae*), fin whale (*Balaenoptera physalus*), minke whale (*Balaenoptera acutorostrata*), sei whale (*Balaenoptera borealis*), and blue whale (*Balaenoptera musculus*) inhabit areas that overlap with offshore wind development (Davis et al, 2020; Secor et al, 2024). Baleen whales are adapted to living in naturally noisy environments, which includes noises from waves, rain, earthquakes, etc, and are not negatively affected by all anthropogenic noise (Southall et al, 2023). However, there is

limited research on the effects that pile-driving has on marine mammals, especially in regards to baleen whales as the high-intensity, low-frequency noises produced from pile-driving are at the same frequency baleen whales communicate (< 1000 Hz) (Madsen et al, 2006; Cranford et al, 2015; Southall et al, 2019).

The effects of noise exposure on marine mammals can be broadly categorized into five groups: behavioral disturbance, masking, physiological stress, temporary threshold shift, and auditory injury (Southall et al, 2017). Since there are limited studies on the effects of pile-driving on baleen whales, research on seismic airguns can provide insight into their potential impact. Airgun pulses are low-frequency, high amplitude sounds and can propagate over large distances, similar to pile-driving. Calling behavior of bowhead whales were found to increase over no-seismic (no detected airgun pulses) calling rates when seismic airguns were in use. Calling rates increased with received cumulative SEL (cSEL), reaching twice the rate observed in the absence of seismic activity. At a received cSEL of ~127 dB, calling rates started to decrease, and reached zero when the cSEL reached 160 dB (Blackwell et al, 2015; Thode et al, 2020). This was also recorded in blue whales that saw an increase in calling behavior in response to exposure of noise related to seismic exploration (Di Iorio et al., 2010). Certain sound duration and exposure levels can lead to recoverable hearing loss, often referred to as temporary threshold shift (TTS), or induce permanent hearing loss, referred to as permanent threshold shift (PTS) (National Marine Fisheries Service, 2018). Based on peak-to-peak sound level metrics, TTS onset can occur within 10 m to 40 m from the source while PTS onset within 5 m for cetaceans (Bailey et al, 2010). General studies examining seismic surveys have estimated that baleen whale sightings were reduced by an average of 88% across multiple study sites during active and inactive seismic activity periods. It is important to note that sighting density did not decrease, but redistribution

did occur (Kavanagh et al, 2019). In general, low-frequency sounds from seismic airguns can elicit a chronic effect over a greater distance for a longer period of time for baleen whales (Ellison et al, 2011).

Marine mammal hearing group	TTS onset: SEL (weighted)	PTS onset: SEL (weighted)
LF	179	199
HF	178	198
VHF	153	173
SI	186	206
PCW	181	201
OCW	199	219
PCA	134	154
OCA	157	177

Table 2. The temporary threshold shift and permanent threshold shift in non-impulsive noises for various marine mammal hear groups. Note. Adapted from Southall et al, 2019.

Marine mammal hearing group	TTS onset: SEL (weighted)	TTS onset: Peak SPL (unweighted)	PTS onset: SEL (weighted)	PTS onset: Peak SPL (unweighted)
LF	168	213	183	219
HF	170	224	185	230
VHF	140	196	155	202
SI	175	220	190	226
PCW	170	212	185	218
OCW	188	226	203	232
PCA	123	138	138	144
OCA	146	161	161	167

Table 3. The temporary threshold shift and permanent threshold shift to impulsive noises for various marine mammal hearing groups. SEL thresholds in dB re 1 $\mu\text{Pa}^2 \cdot \text{s}$ and SPL thresholds in dB re 1 μPa for LF, HF, and VHF groups. Note. Adapted from Southall et al, 2019.

The effects that offshore wind energy development has on harbor porpoises (*Phocoena phocoena*) have been extensively researched (Tougaard et al, 2005; Carstensen et al, 2006; Tellmann et al, 2012; Brandt et al, 2018). Harbor porpoises are abundant in European waters, where the offshore energy industry is more established compared to the United States; currently there are 125 commercial offshore wind farms in Europe with an installed capacity of around 41 GW while the United States has two commercial offshore wind farms with an installed capacity of 2 GW (Global Energy Monitor, 2024; Renewables Now, 2025). Harbor porpoises have a vocal repertoire consisting solely of narrow-band, high-frequency echolocation clicks (Sørensen et al, 2018). As hearing sensitivity is greatest at frequencies above 100 kHz, their detection of low-frequency sounds is limited by their hearing threshold (Madsen et al, 2006; Lucke et al, 2009). However, they are able to detect individual wind turbines depending on the received level, causing a change in their calling rates, feeding behavior, breathing, and movement that can reduce foraging and mating abilities and can increase chronic stress, impacting their health and fecundity (Tougaard et al, 2005; Dragon et al, 2016; Holdman et al, 2023). Researchers have utilized this species' simple vocal repertoire and used Cetacean Porpoise Detectors (C-PODs) to detect harbor porpoise acoustic presence in relation to pile-driving events (Dähne et al, 2017; Brandt et al, 2018, Voß et al, 2023). Multiple studies have used C-PODs to determine both the distances and received levels (RLs) at which harbor porpoises were disturbed by pile-driving events; When active noise mitigation systems (NMS) were not deployed during piling operations, harbor porpoise detections were found to be significantly reduced up to 15-20 km from the sound source. Detection positive hours (DPH), which indicate harbor porpoise activity,

decreased when noise levels during pile-driving reached 143 dB SEL. Additionally, detection rates decreased up to 50% at distances up to 17 km from the pile-driving site (Brandt et al., 2018). It has also been determined that exposure between 139 and 152 dB re 1 μPa^2 SEL can elicit a response from harbor porpoises (Dähne et al, 2013). However, due to differing study designs, methodology, and data availability, there was uncertainty around the results (Brandt et al, 2018).

Unlike in European offshore wind farms, baleen whales are of major concern in the United States as baleen whale habitat overlaps with existing and future offshore wind leasing areas. The effects that pile-driving has on low-frequency baleen whales is unknown due to a lack of available data, thus there is caution in determining hearing capabilities and sensitivity. Cetaceans with greater hearing sensitivity are more likely to have lower TTS-onset, as the difference between noise levels from a source and their hearing threshold is greater compared to species with lower sensitive hearing. While there is a correlation between hearing sensitivity and susceptibility to noise exposure, they still can be affected by noise frequencies out of their range of best hearing sensitivity (Southall et al, 2019). The loud, low-frequency impulsive noise generated by pile-driving have been hypothesized to have a greater degree of effect on low-frequency cetaceans (Madsen et al, 2006, Szesciorka et al, 2025).

In this paper, I will characterize the temporal patterns resulting from pile-driving used to install turbines at Vineyard Wind 1, one of the first commercial-scale offshore wind farms in the United States. This research will eventually be used to evaluate the potential behavioral responses of cetaceans to pile-driving. I will use passive acoustic monitoring (PAM) data to calculate various temporal variables of piling-driving strikes at distances ranging from 1.4 to 10.8 km from turbine construction sites. I will calculate both the single-strike SEL and

cumulative SEL for all pile-driving events to determine sound changes from the nearest Rockhopper unit to a pile-driving event to the farthest.

Methods

Six “Rockhopper” recording units (Cornell University; <https://www.birds.cornell.edu/ccb/rockhopper-unit/>) were deployed within and surrounding the Vineyard Wind 1 Wind Energy Area (WEA) from August 15th, 2023 to February 13th, 2024 (**Figure 1**). They were contained in a buoyant Vitrovex glass sphere suspended 2m above the sea floor. The hydrophones, which were used to acquire sounds and store wav files on an internal electronic storage media, were mounted 20 cm above the Vitrovex glass sphere to minimize any possible acoustic interference. The Rockhoppers recorded continuously at a 200 kHz sampling rate throughout their six-month deployment.

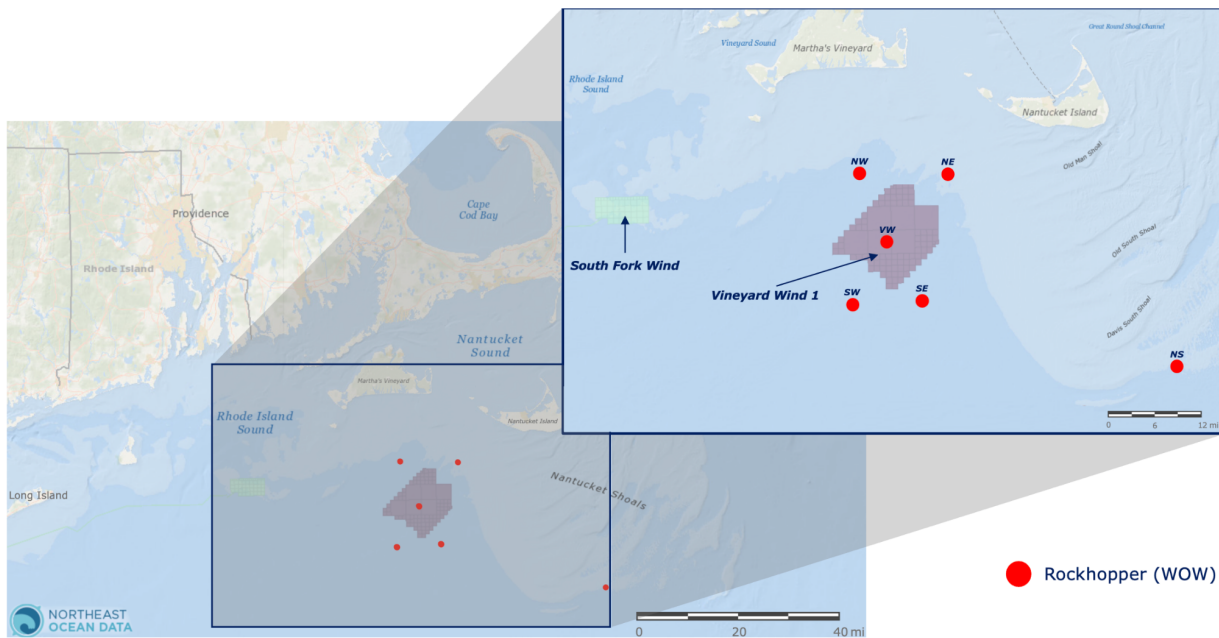


Figure 1. Map of the Vineyard Wind 1 leasing areas and location of Six “Rockhopper” recording units.

Each Rockhopper was equipped with a Xeos satellite tag for tracking each Rockhopper and notified if a Rockhopper surfaced prematurely or was caught in fishing gear. For retrieval,

the acoustic release is sent a series of sounds to release itself and float to the surface for retrieval. After retrieval, audio information is extracted and stored on a server for analysis. In the Cornell fabrication facility, the Rockhopper is cleaned of biofouling and saltwater, unsealed, and depressurized before recorded data can be accessed. The Rockhopper is then refurbished for further deployment. (Klink et al, 2020)

The Rockhopper hydrophone has a nominal or transducer sensitivity, which is a ratio of the electrical output and the acoustical input, of -175.5 dB re 1V/ μ Pa. The pre-amplifier sensitivity varies with frequency. At 10 Hz, the analog system sensitivity is approximately -180 dB re 1V/ μ Pa and at 50 kHz, sensitivity is approximately -140 dB re 1V/ μ Pa. The clipping level of the LTC2512-24 analog-to-digital converter is ± 5 Volts (Klink et al, 2020).

I used Raven Pro, an acoustic software program designed to visualize, measure, and analyze sounds (<https://www.ravensoundsoftware.com/software/raven-pro/>), to calculate the number and duration of pile-driving strikes recorded on the five Rockhoppers deployed within or surrounding the Vineyard Wind 1 WEA.

Vineyard Wind 1 turbines were installed on 30 days during the Rockhopper deployment, with pile-driving events lasting between 1.41 hrs and 4.13 hrs (average: 1.89 hrs) (i.e., **Table 4**) All hour-long Rockhopper recordings were decimated to a 2 kHz sampling rate using Sax-o-matic, an audio file management software (<https://www.birds.cornell.edu/ccb/sox-o-matic/>), to facilitate efficient data processing and analysis, seeing as the impulsive signals resulting from pile-driving tend to have their energy concentrated below 500 Hz (Mooney et al, 2020; Crevello et al, 2023).

Foundation ID	Installation			Exposure		Closest RH	Farthest RH	Distance to nearest RH (km)	Distance to farthest RH (km)
	Date	Start Time	End Time	Duration (hrs)					
AV38	2023/09/03	17:58	19:41	1.72	VW	NW		6	21.3
AN37	2023/09/05	21:50	24:01	2.18	VW	SW		8	22.2
AU38	2023/09/07	19:56	22:40	2.73	VW	NW		4.5	19.6
AS41	2023/09/20	10:59	12:42	1.72	VW	SW		8.7	20.5
AQ36	2023/09/28	11:42	13:10	1.47	VW	SW		4.2	18
AT41	2023/09/29	12:06	13:40	1.57	VW	NW		8.8	21.1
AQ39	2023/10/02	11:09	13:13	2.07	VW	SW		6.6	20.7
AS40	2023/10/03	11:24	13:11	1.78	VW	SW		6.9	19.1
AR38	2023/10/04	11:19	13:03	1.73	VW	SW		4	18.1
AS42	2023/10/12	11:54	13:25	1.52	VW	SW		10.6	21.9
AP39	2023/10/13	19:26	21:18	1.87	VW	SW		7.9	22.2
AN38	2023/10/14	15:52	17:50	1.97	VW	SW		8.5	22.9
AR40	2023/10/16	18:24	19:55	1.52	VW	SW		7.3	20.4
AR41	2023/10/17	16:18	18:03	1.75	VW	SW		9	21.7
AU40	2023/10/19	15:36	17:16	1.67	VW	NW		7.6	21.4
AQ42	2023/10/25	16:32	18:25	1.88	NE	SW		9.8	24.3
AM38	2023/10/26	17:21	18:59	1.63	NW	SW		10.3	24.6
AQ41	2023/10/30	16:44	18:34	1.83	VW	SW		9.7	23
AQ40	2023/10/31	12:48	14:40	1.87	VW	SW		8.1	21.8
AR42	2023/11/01	11:56	13:30	1.57	VW	SW		10.8	23.1
AP40	2023/11/02	16:27	18:37	2.17	VW	SW		9.2	23.3
AN39	2023/11/09	16:11	17:36	1.42	VW	SW		9.4	23.8
AP41	2023/11/10	17:18	18:58	1.67	NE	SW		8.7	24.4
AM39	2023/11/11	16:40	20:48	4.13	NE	SW		8.6	25.4
AT37	2023/11/12	16:49	18:22	1.55	VW	NE		1.9	18.9
AL38	2023/11/13	15:56	17:50	1.90	NW	SW		9	26.3
AS37	2023/11/14	16:20	18:01	1.68	VW	NE		1.4	17.5
AQ34	2023/11/26	13:56	16:26	2.50	VW	SE		6	19.7
AP35	2023/11/30	13:06	14:46	1.67	VW	SE		6.5	20.3
AN36	2023/12/01	20:48	22:26	1.63	VW	SW		7.9	21.5
AR34	2023/12/09	12:26	14:02	1.60	VW	NE		4.8	20.4
AR37	2023/12/14	18:35	20:14	1.65	VW	SW		2.7	17.1
AT33	2023/12/15	20:24	21:59	1.58	VW	NE		6.2	24.1
AS32	2023/12/16	15:11	17:03	1.87	VW	NE		7.9	24.5
AQ35	2023/12/25	12:51	14:49	1.97	VW	SE		4.8	18.7
AS34	2023/12/26	20:00	22:20	2.33	VW	NE		4.2	21.5
AR33	2023/12/27	17:11	19:30	2.32	VW	NE		6.5	21.9
AS33	2023/12/28	13:26	15:39	2.22	VW	NE		6.1	23
Average:				1.89				7.08	21.58

Table 4. The average installation duration of each piling event and its corresponding foundation ID at Vineyard Wind 1. The duration of an event was found by subtracting the last strike and the first ramp-up strike. Also included is the location and distance of the nearest and farthest Rockhopper from the source of pile-driving.

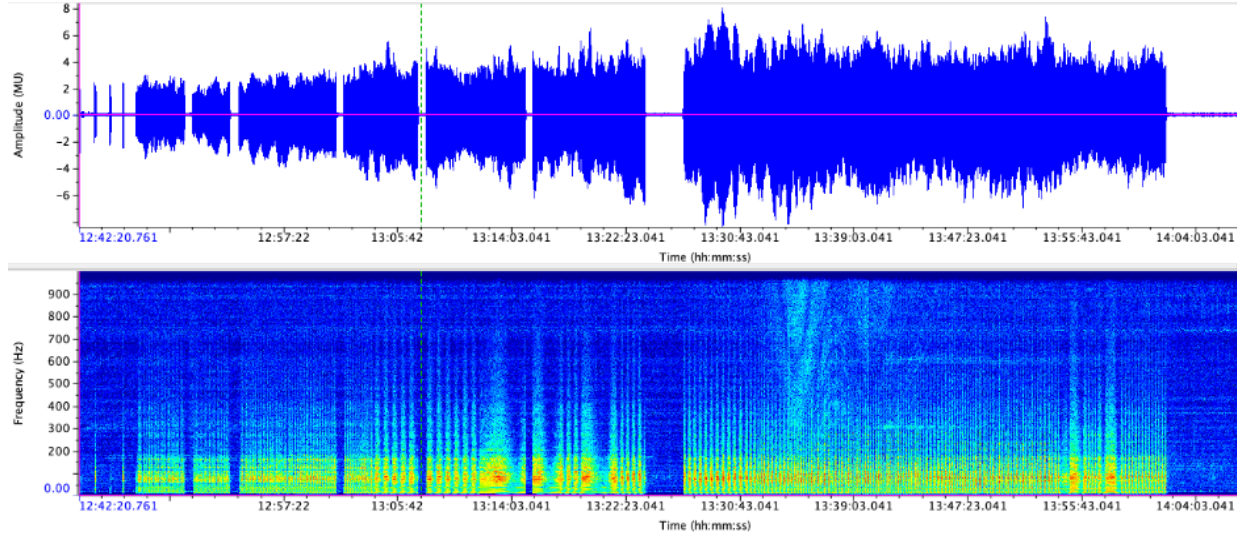


Figure 2. Waveform (top) and spectrogram (bottom) of pile-driving hammer strikes recorded on the VW Rockhopper on December 9th, 2023. Brief pauses between continuous pile-driving strikes ranging from < 1 min to a few min can be seen. Recording Times are in UTC. Spectrogram settings: FFT at 2048 points, 95% overlap, Hann window, 2048 window length, 0.488 Hz resolution, brightness at 50%, and contrast at 60%. Around 13:36 UTC, the spectrogram shows a feature that likely indicates a vessel pass from an unknown ship.

An automated pile-driving strike detector algorithm was created in Raven Pro for Rockhoppers closest to turbine installation. All strikes were manually reviewed to eliminate any false detection of pile-driving and include strikes that were missed by the detector. Notations were made at the beginning and end of each ramp-up period and continuous piling period.

For each strike, the following parameters were measured on Raven Pro:

- The Sound Exposure Level (SEL), which measures the energy of a pulse, defined as the squared instantaneous sound pressure integrated over the pulse duration (dB re 1 $\mu\text{Pa}^2\text{-s}$)
- The 5% and 95% of the total pulse energy

To determine the accuracy of the pile-driving strike detector algorithm, a strike was drawn and selected every two minutes for each contiguous piling period. We then compare the 5% and 95% energy times of the detector output versus the selection boxes manually selected by calculating the absolute difference between the 5% and 95%. From there, we compared whether

these values are higher or lower for pile-driving strikes closer or farther from the Rockhopper unit, or values that occur earlier or later during a pile-driving event.

R Studio, an open-source language program, was used to calculate the duration of the piling event, the average inter-pulse between each strike and between each continuous piling period, the strike rate, the average pulse duration, and duty cycle. The duty cycle, which is the percentage of time that a signal was active or being produced, was calculated by adding the pulse duration from all strikes and dividing it by the total installation time * 100. We randomly selected various installation days to compare how the above temporal metrics varied between the nearest and farthest Rockhopper. Additionally, we found the SEL for nearest and farthest Rockhoppers for these days to compare changes in sound levels.

Results

The analysis reveals notable variations across installations on different days. Continuous strikes per piling event ranged from about 2,649 to 3,834, with an average of 3,194. This indicates differences in the persistence of hammering, potentially influenced by seabed composition or piling resistance. The average inter-pulse interval for continuous strikes over 1-minute and 5-minute periods remained relatively consistent, ranging from approximately 1.25 to 1.80 seconds, with an average of 1.48 s, suggesting a steady hammer strike rhythm. Between continuous pile-driving periods, the inter-pulse ranged between 24.27 s and 957.22 s, with the average being 114.41 s (**Table 5**). A time series of the inter-pulse interval between strikes and each continuous period for each installation day is located in the appendix. While there is limited research examining the effect of intermittent sounds TTS in marine mammals, especially in baleen whales, it was determined that bottlenose dolphins exposed to mid-frequency sonar signals that is characterized having an inter-pulse interval of 0.5 seconds experienced TTS after

five sonar pings, each signal having a SPL of 203 dB re 1 μ Pa (Mooney et al, 2009). Although this study did not calculate peak pressure, a report from the Rand Acoustics found that the impulsive peak noise levels measured during the 2023 construction period reached up to 180 dB over 1 km away and RMS levels above 160 dB at over 3.3 km (Rand, 2023)

Installation times varied between 1.41 and 4.13 hours, with an average of 1.89 hours (**Table 4**). The strike rate ranged from 689.03 to 2,256.12 strikes per hour, with the average being 1,790.38, indicating varying intensity across piling events. The pulse duration for continuous strikes ranged from 0.50 to 0.68 seconds, with the average being 0.61 s, reflecting slight variability in hammer energy delivery but still constant. The duty cycle spanned from 11.7% to 34.3%, with the average being 29.71%, suggesting that some installations maintained more consistent striking patterns while others involved longer pauses or adjustments (**Table 6**).

A 2016 study examined key acoustic metrics (excluding strike counts) and found that exposure duration ranged between 0.25 to 6 hours, there was an average pulse duration of 0.124 seconds, an average inter-pulse duration of 1.3 seconds, an average strike rate of 2,760 strikes per hour, and an average duty cycle of approximately 9.5%. Based on these parameters, the estimated temporary threshold shifts in hearing (TTS) was around 175 dB re 1 μ Pa²s (Kastelein et al, 2016). Studies on harbor porpoises have shown that TTS increases more rapidly during initial noise exposure but plateaus with prolonged exposure, even under intermittent noise conditions with varying duty cycles (Kastelein et al, 2014). Additionally, recovery from TTS tends to occur relatively quickly, typically within an hour, regardless of noise type or exposure duration. It was determined that the inter-pulse interval is an important metric in discerning the extent of noise-induced TTS. While these findings provide insight into TTS onset and recovery in toothed

whales, baleen whales may exhibit different auditory sensitivities and recovery patterns. Considering the strike rates and inter-pulse intervals found in this study, prolonged pile-driving activity could pose a risk of cumulative auditory stress in baleen whales, especially during high duty cycle periods with shorter pauses between strikes and continuous periods.

Foundation ID	Installation Date	Exposure Duration (hrs)	Total Strikes	Continuous Strikes	Avg Inter-pulse (s)	Time Interval Between Periods (s)
AV38	2023/09/03	1.72	3478	3430	1.35	47.05
AN37	2023/09/05	2.18	3693	3645	1.38	258.11
AU38	2023/09/07	2.73	2894	2826	1.37	957.22
AS41	2023/09/20	1.72	3282	3184	1.40	116.44
AQ36	2023/09/28	1.47	2928	2835	1.32	49.87
AT41	2023/09/29	1.57	3059	2974	1.25	209.06
AQ39	2023/10/02	2.07	3828	3726	1.51	186.90
AS40	2023/10/03	1.78	3194	3092	1.40	122.79
AR38	2023/10/04	1.73	2926	2831	1.35	125.04
AS42	2023/10/12	1.52	2972	2861	1.26	127.85
AP39	2023/10/13	1.87	3170	3082	1.55	82.40
AN38	2023/10/14	1.97	3705	3631	1.47	84.84
AR40	2023/10/16	1.52	3167	3082	1.47	56.96
AR41	2023/10/17	1.75	3098	3024	1.42	67.96
AU40	2023/10/19	1.67	2837	2767	1.48	92.74
AQ42	2023/10/25	1.88	3711	3627	1.43	51.44
AM38	2023/10/26	1.63	3685	3640	1.33	38.17
AQ41	2023/10/30	1.83	3539	3497	1.44	80.21
AQ40	2023/10/31	1.87	3417	3369	1.61	38.81
AR42	2023/11/01	1.57	3037	2993	1.44	42.55
AP40	2023/11/02	2.17	3886	3834	1.80	24.27
AN39	2023/11/09	1.42	2703	2659	1.45	88.46
AP41	2023/11/10	1.67	3044	2993	1.60	33.53
AM39	2023/11/11	4.13	2848	2783	1.51	47.94
AT37	2023/11/12	1.55	2944	2890	1.50	27.17
AL38	2023/11/13	1.90	3480	3428	1.62	33.95
AS37	2023/11/14	1.68	3440	3388	1.50	33.82
AQ34	2023/11/26	2.50	3483	3426	1.42	213.52
AP35	2023/11/30	1.67	3215	3168	1.47	45.58
AN36	2023/12/01	1.63	3014	2927	1.43	59.95
AR34	2023/12/09	1.60	3058	2956	1.42	58.09
AR37	2023/12/14	1.65	3155	3056	1.45	54.68
AT33	2023/12/15	1.58	3048	2948	1.36	69.64
AS32	2023/12/16	1.87	3519	3416	1.58	47.87
AQ35	2023/12/25	1.97	3488	3408	1.63	51.68
AS34	2023/12/26	2.33	3888	3807	1.61	69.21
AR33	2023/12/27	2.32	3386	3281	1.74	165.65
AS33	2023/12/28	2.22	2979	2893	1.76	272.12
Average:		1.89	3268.37	3194.13	1.48	111.41

Table 5. The total number and averages of strikes, the number of total strikes within a continuous period, the average inter-pulse interval for continuous strikes for each piling event and its corresponding foundation ID at Vineyard Wind 1.

Foundation ID	Installation Date	Avg Pulse Duration (s)	Strike Rate (Strikes/hr)	Duty Cycle(%)
AV38	2023/09/03	0.60	2026.02	34.27
AN37	2023/09/05	0.62	1691.45	29.28
AU38	2023/09/07	0.59	1058.78	17.28
AS41	2023/09/20	0.64	1911.84	33.48
AQ36	2023/09/28	0.56	1996.36	30.82
AT41	2023/09/29	0.62	1952.55	33.42
AQ39	2023/10/02	0.59	1852.26	30.42
AS40	2023/10/03	0.60	1791.03	28.30
AR38	2023/10/04	0.57	1688.08	26.67
AS42	2023/10/12	0.64	1959.56	34.30
AP39	2023/10/13	0.60	1698.21	28.19
AN38	2023/10/14	0.51	1883.90	26.63
AR40	2023/10/16	0.61	2088.13	31.78
AR41	2023/10/17	0.64	1770.29	31.54
AU40	2023/10/19	0.63	1702.20	30.34
AQ42	2023/10/25	0.59	1970.44	31.97
AM38	2023/10/26	0.57	2256.12	33.56
AQ41	2023/10/30	0.64	1930.36	34.34
AQ40	2023/10/31	0.63	1830.54	32.83
AR42	2023/11/01	0.64	1938.51	34.33
AP40	2023/11/02	0.69	1793.54	32.96
AN39	2023/11/09	0.65	1908.00	32.66
AP41	2023/11/10	0.61	1826.40	31.41
AM39	2023/11/11	0.61	689.03	11.72
AT37	2023/11/12	0.58	1899.35	30.75
AL38	2023/11/13	0.64	1831.58	32.59
AS37	2023/11/14	0.59	2043.56	31.74
AQ34	2023/11/26	0.59	1393.20	13.82
AP35	2023/11/30	0.64	1929.00	34.20
AN36	2023/12/01	0.61	1845.31	31.03
AR34	2023/12/09	0.59	1911.25	31.29
AR37	2023/12/14	0.56	1912.12	29.86
AT33	2023/12/15	0.58	1925.05	31.55
AS32	2023/12/16	0.63	1885.18	32.37
AQ35	2023/12/25	0.63	1773.56	31.20
AS34	2023/12/26	0.59	1666.29	27.20
AR33	2023/12/27	0.65	1461.58	26.20
AS33	2023/12/28	0.62	1343.91	22.57
Average:		0.61	1790.38	29.71

Table 6. The total and average strike rate, average pulse duration, and duty cycle for each piling event and its corresponding foundation ID at Vineyard Wind 1.

Comparing temporal and noise metrics between the farthest and nearest Rockhoppers, in general, pulse duration increased by 6.4%, the inter-pulse duration between strikes increased by 0.1%, the inter-pulse duration between continuous pile-driving period decreased by 0.07%, and the duty cycle increased by 6.37%. On average, single-strike SEL decreased by 8.3 dB.

Installation Date	Foundation ID	Avg Pulse	Avg Inter-Pulse	Duty Cycle	Duration between Periods	SEL (dB)
2023/09/03	AV38	6.1	0.0	6.2	-0.1	-11.1
2023/10/30	AQ41	1.7	-0.5	2.5	-0.1	-6.5
2023/11/02	AP40	5.7	-0.5	6.0	-0.1	-3.2
2023/11/11	AM39	5.8	0.4	4.3	-0.1	-4.9
2023/11/13	AL38	7.5	1.2	7.6	-0.3	-7.4
2023/12/01	AN36	-0.5	0.3	-0.5	0.0	-4.8
2023/12/15	AT33	4.4	0.2	4.3	0.2	-8.9
2023/12/27	AR33	12.0	-0.4	12.0	0.0	-13.1
2023/12/28	AS33	16.0	0.3	16.1	0.0	-14.1
Average		6.5	0.1	6.5	-0.1	-8.2

Table 7. The percent difference of various temporal metrics and absolute difference in sound exposure levels between the nearest and farthest Rockhopper at Vineyard Wind 1. The percentage difference was calculated as $(\text{Farthest} - \text{Nearest}) / \text{Nearest} \times 100$.

Implications

The Bureau of Ocean Energy Management (BOEM) is a regulating body in the United States that leases offshore wind areas in the outer continental shelf. The Outer Continental Shelf Lands Act and Energy Policy Act of 2005 mandates the assessment that activities authorized and permitted by BOEM have on the environment. Ultimately, this ensures that BOEM is in compliance with federal mandates, such as the Endangered Species Act (ESA) and Marine Mammal Protection Act (MMPA). Under the ESA and MMPA, all marine mammals are protected from offshore wind development (CSA Ocean Sciences Inc, 2014; van Parijs et al, 2021). Thus, BOEM has outlined general guidelines for impact pile-driving noises for Offshore Wind Construction and Operations Plans. Reporting recommendations suggest that offshore wind developers include pile and hammer characteristics, which includes which noise attenuation system used and any additional information associated with noise reduction (BOEM, 2023). A NMS that is typically used by developers are bubble curtains. Bubble curtains is a wall of air bubbles which is created through a perforated hose that lies on the seabed or in the water column. There are two forms of bubble curtains that exist: a big bubble curtain (BBC), which has a large radius and a small bubble curtain, which has a small radius. Big bubble curtains are placed 70 m

away from where pile-driving occurs. Typically, BBC can be applied to water depths of 40 m and reduce sound between 7 and 11 dB SEL. Double BBC (DBBC), which is a second hose that is several meters away from the first, can attenuate noise between 8 and 16 dB SEL, depending on the flow rate of the hose. Reportedly, offshore wind construction affected harbor porpoise activity up to 12 km with bubble curtains, a decrease from 18-25 km range of effect without any NMS (CSA Ocean Sciences Inc, 2024; Dahne et al., 2017; Verfuss et al., 2019).

Up until October 31, 2024, Vineyard Wind 1 used Hydro Sound Damper (HSD) systems from Off Noise Solutions GmbH in combination with either single (SBBC) or DBBC from Hydrotechnik Lubeck. Monopiles AT-40, AU-39, and AP-38 were installed with a SBBC 115 m away from the pile with an air delivery rate of $0.448 \text{ m}^3/(\text{min*m})$. Subsequent monopiles were installed DBBC with the second BBC installed 150 m away from piling (Kusel et al, 2024). Studies have sought to understand how the insertion of a bubble curtain changes the sound field and how it impacts sound level reduction, or the insertion loss. Modeling from Bohne et al, 2025 found that from a distance of 200 m from the BC, the insertion loss, which is the difference in the levels of the reference and bubble curtain case determined at the measurement station, decreased from 12 dB to 10 dB. Insertion loss increased from 10 to 12 dB 300 m away from the BC. However, as the distance from the piling increases further, the insertion loss decreases slightly before reaching between 8 and 5 dB at a distance of 5000 m (Bohne et al, 2025). Other studies have found that pile-driving noise from 750 m away from the source measured between 100 Hz and 400 Hz (Bellmann, 2014). While fewer studies have looked at NMS efficiency at longer distances, Nehls et al. found that bubble curtains reduced the disturbance radius to ~5 km and had an average noise mitigation of 11 dB (Nehls et al, 2016). It is important to recognize that bubble curtains attenuate particularly well for noises above 1 kHz (Dahne, et al, 2017).

Behavioral shifts are also critical for this analysis. Exposure to impulsive noise at greater distances, as close as 1.5 km to 9.3 km (Finneran et al, 2000), can result in changes to behavior (Hastie, et al, 2019; Thompson et al, 2020). Analysis done on harbor porpoises found that they may be displaced from distances up to 26 km. Even when these species are not displaced, foraging efficiency and success can be attenuated by impulsive noise, leading to high energy expenditure and limited energy capacity, potentially leaving them vulnerable to starvation (Benhemma-Le Gall et al, 2021; Brandt et al, 2018). However, these species have high frequency hearing, thus behavioral onset is different between them and baleen whales. While this study was unable to determine onset behavioral shifts, the metrics analyzed in this study should be considered moving forward.

Discussion & Conclusion

The purpose of this study was to characterize various temporal metrics from the installation of monopile turbines thru pile-driving at Vineyard Wind 1. It was determined that, on average, the exposure duration lasted for 1.89 hours. Including ramp-up strikes, there was an average of 3,269 strikes for the entire installation period. There was an average strike rate of 1,790 strikes/hr, an average pulse duration of 0.61 s, an average inter-pulse duration of 1.48 s, and an average duty cycle of 29.71%. Excluding time intervals between ramp-up, the duration between each pile-driving period within an installation day for a singular monopile turbine was 111.41 s. Compared to other studies, pile-driving at Vineyard Wind 1 had a less variable exposure duration, a lower strike rate, a longer inter-pulse and pulse duration, and a longer duty cycle (**Table 8**). Although the exact reasons are unknown, a few potential reasons in this variation could be attributed to the composition of the seabed, the tools used, the hammer strike

energy, and weather conditions. A more thorough study should be conducted to determine the differences.

In general, the pulse duration was longer farther away from the source and there was a greater duty cycle. The inter-pulse duration showed more variability; this could be attributed to how the pile-driving strike algorithm detector captured energy. SEL decreased by an average of 8.3 dB between the closest and most distant Rockhopper. It is difficult to determine the significance that pile-driving has on baleen whales at greater distances, but preliminary data has indicated the inter-pulse duration between strikes and between continuous pile-driving periods did not differ at distances lower than 25 km. While most studies have found that recovery in hearing can happen at a short timeframe, all have focused on harbor porpoises. Given the difficulty of studying baleen whales and their life history, the same conclusions cannot be made.

Metric	Valdez Rivas, 2025	Kastelein et al, 2016
Exposure Duration (hrs)	1.89	0.25 to 6
Total Strikes	3268.37	N/A
Continuous Strikes	3194.13	N/A
Strike Rate (Strikes/hr)	1790.38	2760
Avg Inter-pulse (s)	1.48	1.3
Avg Pulse (s)	0.61	0.12
Time between periods (s)	111.41	N/A
Duty Cycle (%)	29.71	9.5

Table 8. Comparison of the averages of various temporal metrics at Vineyard Wind 1 and from the Kastelein et al, 2016 study which examined temporal metrics from the Egmond aan Zee Offshore Wind Farm.

This study faced some limitations; the primary being incorrect hydrophone sensitivity information. Based on the Rand technical report, SEL unweighted values should be near 158.2 dB re 1uPa²s at 1.06 km (Rand, 2023). However, single-strike SEL values measured by Raven Pro using the hydrophone sensitivity information from the Klink et al, 2020 paper was above 300

dB. Attempts to contact Cornell University were unsuccessful as there were delays in response. Additionally, attempts to analyze hammer strike energy from turbines were met with constraints as that information is proprietary of Vineyard Wind 1. The process of obtaining this information is currently stalled with legal reviewing contracts. Overall, understanding these dynamics is crucial for assessing the potential impacts offshore wind development has on baleen whale hearing and behavior. Further research needs to be conducted examining the effects that temporal patterns from pile-driving events have on baleen whales. With this data, it can be used to inform any behavioral or hearing threshold shifts that Project WOW is examining.

References

1. Amaral, J. (2020). The underwater sound from offshore wind farms. *Acoustics Today*, 16(2), 13. <https://doi.org/10.1121/AT.2020.16.2.13>
2. Bailey, H., Brookes, K.L. & Thompson, P.M (2014). Assessing environmental impacts of offshore wind farms: lessons learned and recommendations for the future. *Aquat. Biosyst.* 10, 8. <https://doi.org/10.1186/2046-9063-10-8>
3. Bailey, H., Senior, B., Simmons, D., Rusin, J., Picken, G., & Thompson, P. M. (2010). Assessing underwater noise levels during pile-driving at an offshore windfarm and its potential effects on marine mammals. *Marine Pollution Bulletin*, 60(6), 888-897. <https://doi.org/10.1016/j.marpolbul.2010.01.003>
4. Bellmann, M. A.(2014). Overview of existing noise mitigation systems for reducing pile-driving noise, INTERNOISE and NOISE-CON Congress and Conference Proceedings, vol. 249, pp. 2544–2554, Institute of Noise Control Engineering.
5. Benhemma-Le Gall, A., Graham, I. M., Merchant, N. D., & Thompson, P. M. (2021). Broad-scale responses of harbor porpoises to pile-driving and vessel activities during offshore windfarm construction. *Frontiers in Marine Science*, 8<https://doi.org/10.3389/fmars.2021.664724>
6. Blackwell, S. B., Nations, C. S., McDonald, T. L., Thode, A. M., Mathias, D., Kim, K. H., Greene, J., Charles R, & Macrander, A. M. (2015). Effects of airgun sounds on bowhead whale calling rates: Evidence for two behavioral thresholds. *PloS One*, 10(6), e0125720-e0125720. <https://doi.org/10.1371/journal.pone.0125720>
7. Brandt, M. J., Diederichs, A., Betke, K., & Nehls, G. (2011). Responses of harbour porpoises to pile driving at the horns rev II offshore wind farm in the danish north sea. *Marine Ecology. Progress Series* (Halstenbek), 421, 205-216. <https://doi.org/10.3354/meps08888>
8. Brandt, M. J., Dragon, A., Diederichs, A., Bellmann, M. A., Wahl, V., Piper, W., Nabe-Nielsen, J., & Nehls, G. (2018). Disturbance of harbour porpoises during construction of the first seven offshore wind farms in germany. *Marine Ecology. Progress Series* (Halstenbek), 596, 213-232. <https://doi.org/10.3354/meps12560>
9. BOEM, 2023: Bureau of Ocean Energy Management (BOEM) (2023). Nationwide Recommendations for Impact Pile Driving Sound Exposure Modeling and Sound Field Measurement for Offshore Wind Construction and Operations Plans. Report by Bureau of Ocean Energy Management (BOEM).
10. Bohne, T., & Rolfes, R. (2025). Investigating the influence of a bubble curtain on the underwater sound wave field generated by offshore pile driving. *The Journal of the Acoustical Society of America*, 157(1), 471-481. <https://doi.org/10.1121/10.0034841>
11. Carstensen, J., Henriksen, O. D., & Teilmann, J. (2006). Impacts of offshore wind farm construction on harbour porpoises: Acoustic monitoring of echolocation activity using porpoise detectors (T-PODs). *Marine Ecology. Progress Series* (Halstenbek), 321, 295-308. <https://doi.org/10.3354/meps321295>
12. Cervello, G., Olivier, F., Chauvaud, L., Winkler, G., Mathias, D., Juanes, F., & Tremblay, R. (2023). Impact of anthropogenic sounds (pile driving, drilling and vessels) on the development of model species involved in marine biofouling. *Frontiers in Marine Science*, 10<https://doi.org/10.3389/fmars.2023.1111505>
13. Copping, A.E., Hemery, L.G., Overhus, D.M., Garavelli, L., Freeman, M.C., Whiting, J.M., Gorton, A.M., Farr, H.K., Rose, D.J., & Tugade, L.G. (2020) Potential

Environmental Effects of Marine Renewable Energy Development—The State of the Science. *Journal of Marine Science and Engineering*. 8(11):879.
<https://doi.org/10.3390/jmse8110879>

14. Cranford TW, Krysl P (2015) Fin Whale Sound Reception Mechanisms: Skull Vibration Enables Low-Frequency Hearing. *PLoS ONE* 10(1): e0116222.
<https://doi.org/10.1371/journal.pone.0116222>
15. CSA Ocean Sciences Inc (2014). Quieting Technologies for Reducing Noise During Seismic Surveying and Pile Driving Workshop Report (Report No. BOEM 2014-061). Report by CSA Ocean Sciences Inc. Report for Bureau of Ocean Energy Management (BOEM).
16. Dähne M, Gilles A, Lucke K, Peschko V.. (2013). Effects of pile-driving on harbour porpoises (*Phocoena phocoena*) at the first offshore wind farm in Germany. *Environ Res Lett* 8: 025002
17. Dähne, M. Tougaard, J. Carstensen, J. Rose, A.; Nabe-Nielsen, J. (2017). Bubble Curtains Attenuate Noise from Offshore Wind Farm Construction and Reduce Temporary Habitat Loss for Harbour Porpoises. *Marine Ecology Progress Series*, 580, 221-237.
<https://doi.org/10.3354/meps12257>
18. Dragon, A.C., Brandt, M.I., Diederichs, A., & Nehls, G. (2016). Wind creates a natural bubble curtain mitigating porpoise avoidance during offshore pile driving. *Proc. Mtgs. Acoust.* 27 (1): 070022. <https://doi.org/10.1121/2.0000421>
19. Ellison, W. T., Southall, B. L., Clark, C. W., & Frankel, A. S. (2012). A new context-based approach to assess marine mammal behavioral responses to anthropogenic sounds. *Conservation Biology*, 26(1), 21-28.
<https://doi.org/10.1111/j.1523-1739.2011.01803.x>
20. Fernandez-Betelu, O., Graham, I. M., Malcher, F., Webster, E., Cheong, S., Wang, L., Iorio-Merlo, V., Robinson, S., & Thompson, P. M. (2024). Characterising underwater noise and changes in harbour porpoise behaviour during the decommissioning of an oil and gas platform. *Marine Pollution Bulletin*, 200, 116083-116083.
<https://doi.org/10.1016/j.marpolbul.2024.116083>
21. Finnigan, J. J., Schlundt, C. E., Carder, D. A., Clark, J. A., Young, J. A., Gaspin, J. B., & Ridgway, S. H. (2000). Auditory and behavioral responses of bottlenose dolphins (*Tursiops truncatus*) and a beluga whale (*Delphinapterus leucas*) to impulsive sounds resembling distant signatures of underwater explosions. *The Journal of the Acoustical Society of America*, 108(1), 417-431. <https://doi.org/10.1121/1.429475>
22. Global Energy Monitor. (June 27, 2024). Number of offshore wind farms operating worldwide as of June 2024, by country [Graph]. In Statista. Retrieved February 14, 2025, from
<https://www.statista.com/statistics/264257/number-of-offshore-wind-farms-worldwide-by-country/>
23. Hastie, G. D., Russell, D. J. F., Lepper, P., Elliott, J., Wilson, B., Benjamins, S., & Thompson, D. (2018). Harbour seals avoid tidal turbine noise: Implications for collision risk. *The Journal of Applied Ecology*, 55(2), 684-693.
<https://doi.org/10.1111/1365-2664.12981>
24. Hinzmann, N., P. Stein, J. Gattermann, J. Bachmann, and G. Duff. (2017). Measurements of hydro sound emissions during internal jet cutting during monopile decommissioning. Paper presented at COME 2017—Decommissioning of Offshore Geotechnical Structures.

25. Holdman, A. K., Tregenza, N., Van Parijs, S. M., & DeAngelis, A. I. (2023). Acoustic ecology of harbour porpoise (*phocoena phocoena*) between two U.S. offshore wind energy areas. *ICES Journal of Marine Science*, <https://doi.org/10.1093/icesjms/fsad150>
26. Kavanagh, A. S., Nykänen, M., Hunt, W., Richardson, N., & Jessopp, M. J. (2019). Seismic surveys reduce cetacean sightings across a large marine ecosystem. *Scientific Reports*, 9(1), 19164-10. <https://doi.org/10.1038/s41598-019-55500-4>
27. Kastelein, R. A., Helder-Hoek, L., Covi, J., & Gransier, R. (2016). Pile driving playback sounds and temporary threshold shift in harbor porpoises (*phocoena phocoena*): Effect of exposure duration. *The Journal of the Acoustical Society of America*, 139(5), 2842-2851. <https://doi.org/10.1121/1.4948571>
28. Kastelein, R. A., Hoek, L., Gransier, R., Rambags, M., & Claeys, N. (2014). Effect of level, duration, and inter-pulse interval of 1-2 kHz sonar signal exposures on harbor porpoise hearing. *The Journal of the Acoustical Society of America*, 136(1), 412-422. <https://doi.org/10.1121/1.4883596>
29. Klain, S. C., Satterfield, T., MacDonald, S., Battista, N., & Chan, K. M. A. (2017). Will communities “open-up” to offshore wind? lessons learned from new england islands in the united states. *Energy Research & Social Science*, 34, 13-26. <https://doi.org/10.1016/j.erss.2017.05.009>
30. Klinck, H., Winiarski, D., Mack, R. C., Tessaglia-Hymes, C. T., Ponirakis, D. W., Dugan, P. J., & Matsumoto, H. (2020). The ROCKHOPPER: a compact and extensible marine autonomous passive acoustic recording system. In *Global Oceans 2020: Singapore–US Gulf Coast* (pp. 1-7). IEEE. doi: 10.1109/IEEECONF38699.2020.9388970.
31. Küsel, E.T., C. Graupe, T. J. Stephen, C. Lawrence, M. P. Cotter, and D.G. Zeddies. 2024. Underwater Sound Field Verification: Vineyard Wind 1 Final Report. Document 03233, Version 1.0. Technical report by JASCO Applied Sciences for DEME Group.
32. Lucke, K., Siebert, U., Lepper, P. A., & Blanchet, M. (2009). Temporary shift in masked hearing thresholds in a harbor porpoise (*phocoena phocoena*) after exposure to seismic airgun stimuli. *The Journal of the Acoustical Society of America*, 125(6), 4060-4070. <https://doi.org/10.1121/1.3117443>
33. Loureiro, G., Dias, A., Almeida, J., Martins, A., Hong, S., & Silva, E. (2024). A survey of seafloor characterization and mapping techniques. *Remote Sensing* (Basel, Switzerland), 16(7), 1163. <https://doi.org/10.3390/rs16071163>
34. Madsen, P. T., Wahlberg, M., Tougaard, J., Lucke, K., & Tyack, P. (2006). Wind turbine underwater noise and marine mammals: Implications of current knowledge and data needs. *Marine Ecology Progress Series* (Halstenbek), 309, 279-295. <https://doi.org/10.3354/meps309279>
35. Martin, S. B., Lucke, K., & Barclay, D. R. (2020). Techniques for distinguishing between impulsive and non-impulsive sound in the context of regulating sound exposure for marine mammals. *The Journal of the Acoustical Society of America*, 147(4), 2159-2176. <https://doi.org/10.1121/10.0000971>
36. Mooney, T. A., Nachtigall, P. E., and Vlachos, S. (2009b). “Sonar-induced temporary hearing loss in dolphins,” *Biol. Lett.* 5, 565–567.
37. Mooney, T.A., M.H. Andersson, and J. Stanley. 2020. Acoustic impacts of offshore wind energy on fishery resources: An evolving source and varied effects across a wind farm’s lifetime. *Oceanography* 33(4):82–95, <https://doi.org/10.5670/oceanog.2020.408>.

38. Mooney, T. A., Yamato, M., & Branstetter, B. K. (2012). Hearing in cetaceans: from natural history to experimental biology. *Advances in marine biology*, 63, 197–246. <https://doi.org/10.1016/B978-0-12-394282-1.00004-1>
39. Musial, W., Spitsen, P., Duffy, P., Beiter, P., Shields, M., Hernando, D., Hammond, R., Marquis, M., King, J., & Sathish, S. Offshore Wind Market Report: 2023 Edition. U.S. Department of Energy. <https://www.energy.gov/sites/default/files/2023-09/doe-offshore-wind-market-report-2023-edition.pdf>
40. Musial, W. & Ram, B. (2010) Large-scale offshore wind power in the United States: assessment of opportunities and barriers. Golden, CO, USA: National Renewable Energy Laboratory (NREL).
41. National Marine Fisheries Service: National Marine Fisheries Service. 2018. 2018 Revisions to: Technical Guidance for Assessing the Effects of Anthropogenic Sound on Marine Mammal Hearing (Version 2.0): Underwater Thresholds for Onset of Permanent and Temporary Threshold Shifts. U.S. Dept. of Commer., NOAA. NOAA Technical Memorandum NMFS-OPR-59.
42. Nedwell, J.; Howell, D. (2004). A Review of Offshore Windfarm Related Underwater Noise Sources (Report No. 544 R 0308). Report by Subacoustech Ltd. Report for The Crown Estate.
43. Nehls G, Rose A, Diederichs A, Bellmann M, Pehlke H. (2016). Noise mitigation during pile driving efficiently reduces disturbance of marine mammals. *Adv Exp Med Biol* 875: 755–762.
44. Reyff, J. (2012). Underwater Sounds From Unattenuated and Attenuated Marine Pile Driving. In: Popper, A.N., Hawkins, A. (eds) *The Effects of Noise on Aquatic Life. Advances in Experimental Medicine and Biology*, vol 730. Springer, New York, NY. https://doi.org/10.1007/978-1-4419-7311-5_99
45. Rand, R.W. (2024). "Pile Driving Noise Survey", Rand Acoustics, LLC.
46. Rand, R.W. (2023). "Sonar Vessel Noise Survey", Rand Acoustics, LLC.
47. Renewables Now. (2025, February 13). Offshore wind seen to top 520 GW globally by 2040 (excl. China). Renewables Now. <https://renewablesnow.com/news/offshore-wind-seen-to-top-520-gw-globally-by-2040-excl-china-867006/>
48. Secor, D. H., O'Brien, M. H. P., & Bailey, H. (2024). The flyway construct and assessment of offshore wind farm impacts on migratory marine fauna. *ICES Journal of Marine Science*, <https://doi.org/10.1093/icesjms/fsae138>
49. Shams, S., Prasad, D. M. R., Imteaz, M. A., Khan, M. M. H., Ahsan, A., & Karim, M. R. (2023). An assessment of environmental impact on offshore decommissioning of oil and gas pipelines. *Environments* (Basel, Switzerland), 10(6), 104. <https://doi.org/10.3390/environments10060104>
50. Sørensen, P. M., Wisniewska, D. M., Jensen, F. H., Johnson, M., Teilmann, J., & Madsen, P. T. (2018). Click communication in wild harbour porpoises (*phocoena phocoena*). *Scientific Reports*, 8(1), 9702-11. <https://doi.org/10.1038/s41598-018-28022-8>
51. Southall, B. L., Bowles, A. E., Ellison, W. T., Finneran, J. J., Gentry, R. L., Greene, C. J., Kastak, D., Ketten, D., Miller, J. H., Nachtigall, P. E., Richardson, W. J., Thomas, J., & Tyack, P. L. (2007). Marine mammal noise exposure criteria: Initial scientific recommendations. *Aquatic Mammals*, 33(4).

52. Southall, B. L. (2017). Noise. In B. Würsig and H. Thiewessen (Eds.), *Encyclopedia of Marine Mammals*, 3rd ed. Academic Press, New York, NY, pp. 699-707.
53. Southall, B. L., Finneran, J. J., Reichmuth, C., Nachtigall, P. E., Ketten, D. R., Bowles, A. E., Ellison, W. T., Nowacek, D. P., & Tyack, P. L. (2019). Marine mammal noise exposure criteria: Updated scientific recommendations for residual hearing effects. *Aquatic Mammals*, 45(2), 125-232. <https://doi.org/10.1578/AM.45.2.2019.125>
54. Southall, B. L., Donovan, G. P., Racca, R., Reeves, R. R., Vedenev, A. I., Weller, D. W., & Nowacek, D. P. (2023). Data collection and analysis methods to evaluate potential impacts of seismic surveys and other marine industrial activities on baleen whales. *Ocean & Coastal Management*, 245, 106799. <https://doi.org/10.1016/j.ocecoaman.2023.106799>
55. Stöber, U., & Thomsen, F. (2019). Effect of impact pile driving noise on marine mammals: A comparison of different noise exposure criteria. *The Journal of the Acoustical Society of America*, 145(5), 3252-3259. <https://doi.org/10.1121/1.5109387>
56. Stone C.J., Hall K., Mendes S. & Tasker M.L. (2017) The effects of seismic operations in UK waters: analysis of Marine Mammal Observer data. *Journal of Cetacean Research and Management*, 16, 71-85.
57. Sun, X., Huang, D., & Wu, G. (2012). The current state of offshore wind energy technology development. *Energy*, 41:298–312. <https://doi.org/10.1016/j.energy.2012.02.054>
58. Szesciorka, A.; Severy, M.; Ampela, K.; Hein, C.; Richlen, M.; Haxel, J.; Clerc, J. (2025). Evaluating Tools and Technologies for Monitoring Baleen Whales During Offshore Wind Foundation Installation. Report by Pacific Northwest National Laboratory and National Renewable Energy Laboratory for the U.S. Department of Energy.
59. Teilmann, J., & Carstensen, J. (2012). Negative long term effects on harbour porpoises from a large scale offshore wind farm in the baltic-evidence of slow recovery. *Environmental Research Letters*, 7(4), 1-10. <https://doi.org/10.1088/1748-9326/7/4/045101>
60. Thompson, P. M., Graham, I. M., Cheney, B., Barton, T. R., Farcas, A., & Merchant, N. D. (2020). Balancing risks of injury and disturbance to marine mammals when pile driving at offshore windfarms. *Ecological Solutions and Evidence*, 1(2), n/a. <https://doi.org/10.1002/2688-8319.12034>
61. Tougaard, J.; Carstensen, J.; Teilmann, J.; Bech, N. (2005). Effects of the Nysted Offshore Wind Farm on Harbour Porpoises. Report by National Environmental Research Institute (NERI). Report for ENERGI E2.
62. Tougaard, J.; Madsen, P.; Wahlberg, M. (2008). Underwater Noise from Construction and Operation of Offshore Wind Farms. *Bioacoustics*, 17(1-3), 143-146. <https://doi.org/10.1080/09524622.2008.9753795>
63. van der Knaap, I., Slabbekoorn, H., Moens, T., Van den Eynde, D., & Reubens, J. (2022). Effects of pile driving sound on local movement of free-ranging atlantic cod in the belgian north sea. *Environmental Pollution* (1987), 300, 118913-118913. <https://doi.org/10.1016/j.envpol.2022.118913>
64. van Parijs, Sofie M. et al. (2021). NOAA and BOEM Minimum Recommendations for Use of Passive Acoustic Listening Systems in Offshore Wind Energy Development Monitoring and Mitigation Programs. 8<https://doi.org/10.3389/fmars.2021.760840>

65. Verfuss, U.; Sinclair, R.; Sparling, C. (2019). A review of noise abatement systems for offshore wind farm construction noise, and the potential for their application in Scottish waters (Report No. 1070). Report by Scottish Natural Heritage.
66. Vineyard Wind (2023). Wind fisheries studies and science. Available at:
<https://www.vineyardwind.com/fisheries-science> (Accessed April 29, 2023).
67. Voß, J., Rose, A., Kosarev, V., Vilela, R., van Opzeeland, I. C., & Diederichs, A. (2023). Response of harbor porpoises (*phocoena phocoena*) to different types of acoustic harassment devices and subsequent piling during the construction of offshore wind farms. *Frontiers in Marine Science*, 10^{https://doi.org/10.3389/fmars.2023.1128322}
68. Zhang, Jianhong & Wang, Hao. (2022). Development of offshore wind power and foundation technology for offshore wind turbines in China. *Ocean Engineering*. 266. 113256. ^{10.1016/j.oceaneng.2022.113256.}

Appendix

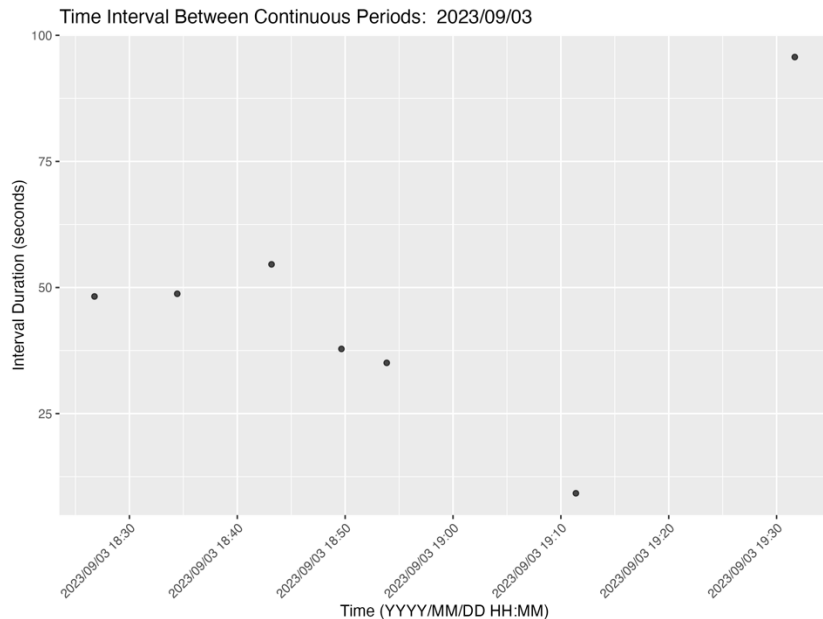


Figure 3. The time interval between continuous periods for the nearest Rockhopper for Foundation ID AV38 on September 3rd, 2023.

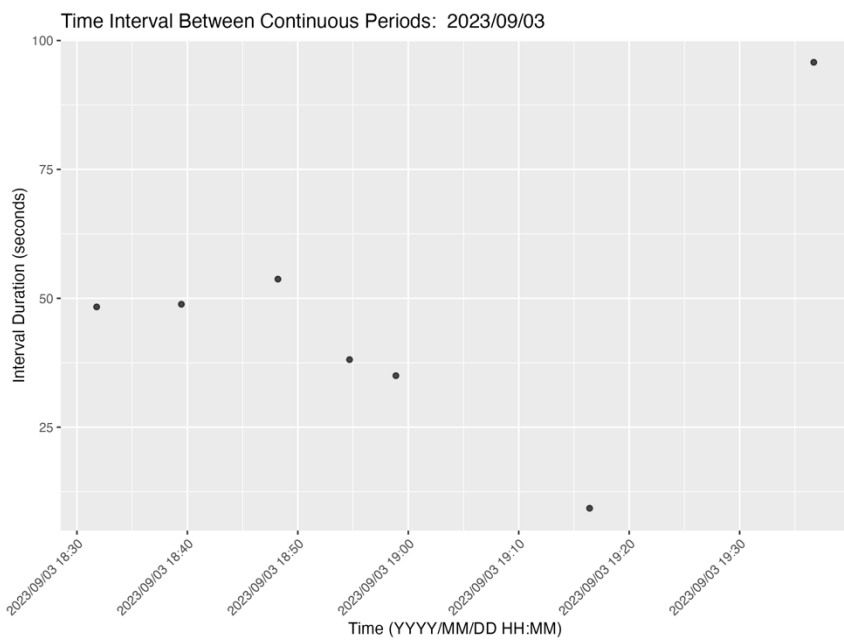


Figure 4. The time interval between continuous periods for the farthest Rockhopper for Foundation ID AV38 on September 3rd, 2023.

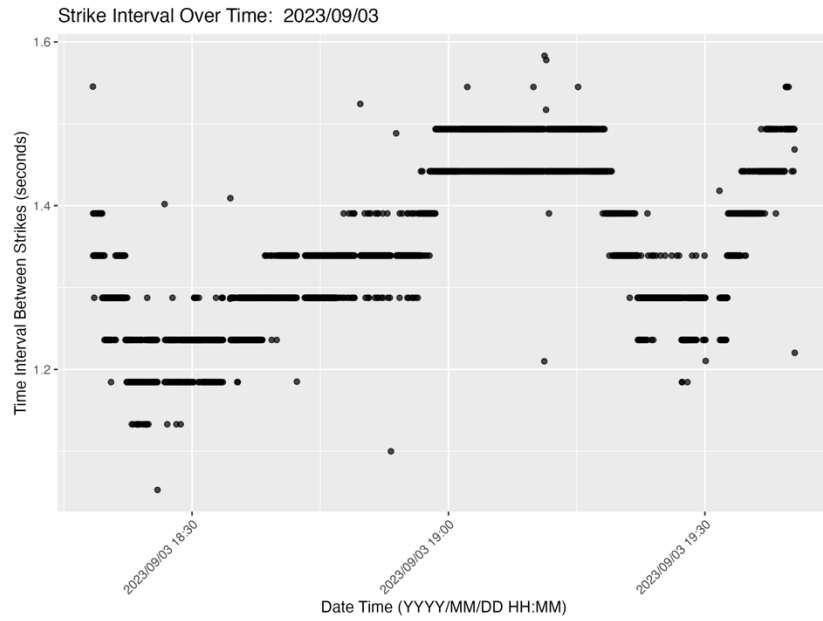


Figure 5. The time interval between strikes in a continuous period for the nearest Rockhopper for Foundation ID AV38 on September 3rd, 2023.

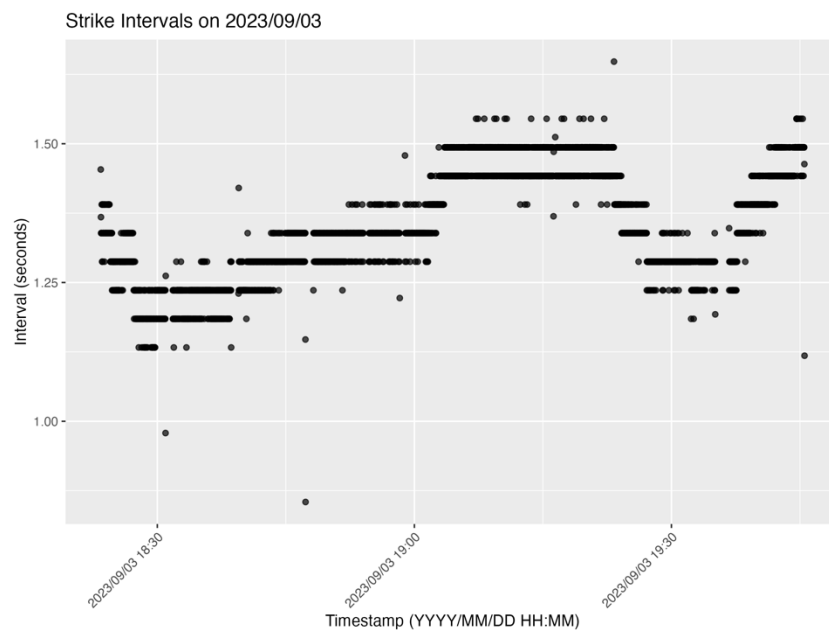


Figure 6. The time interval between strikes in a continuous period for the farthest Rockhopper for Foundation ID AV38 on September 3rd, 2023.

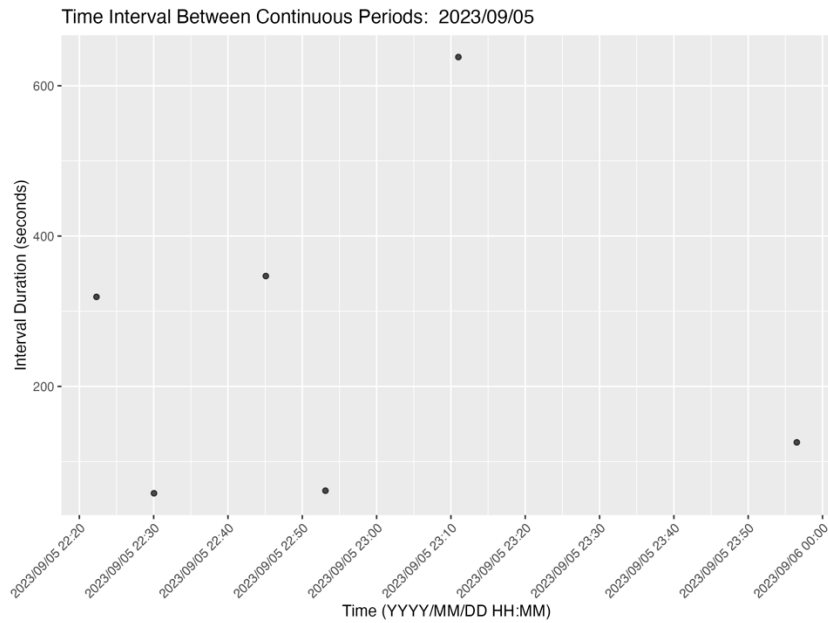


Figure 7. The time interval between continuous periods for the nearest Rockhopper for Foundation ID AN37 on September 5th, 2023.

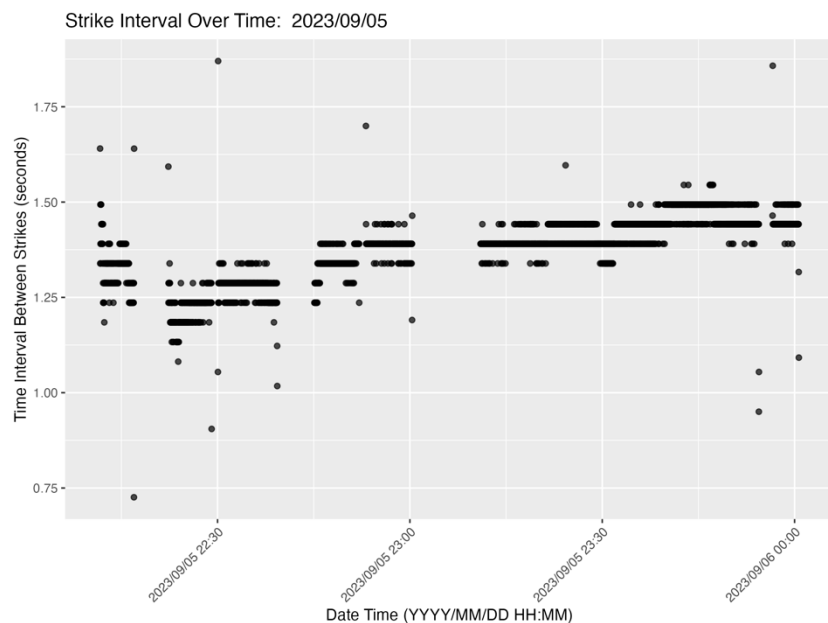


Figure 8. The time interval between strikes in a continuous period for the nearest Rockhopper for Foundation ID AN37 on September 5th, 2023.

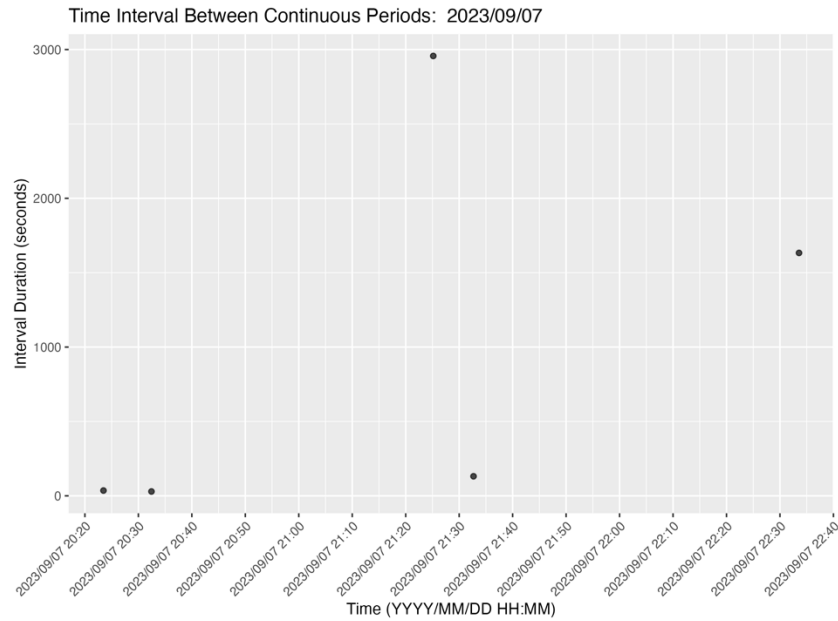


Figure 9. The time interval between continuous periods for the nearest Rockhopper for Foundation ID AU38 on September 7th, 2023.

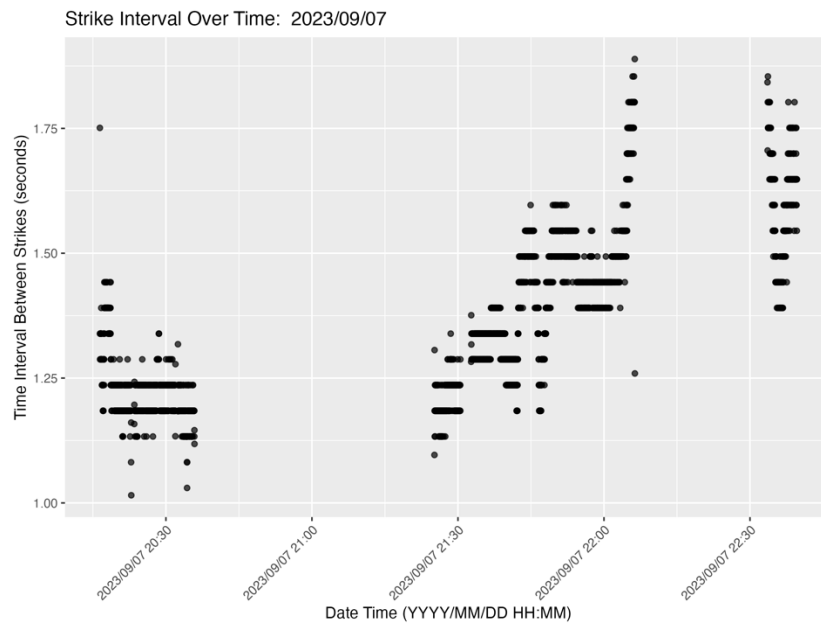


Figure 10. The time interval between strikes in a continuous period for the nearest Rockhopper for Foundation ID AU38 on September 7th, 2023.

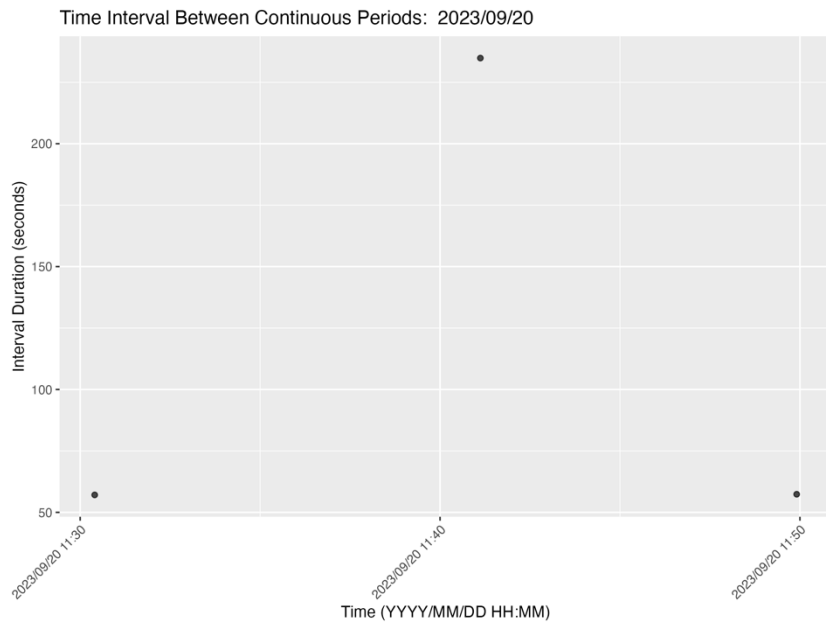


Figure 11. The time interval between continuous periods for the nearest Rockhopper for Foundation ID AS41 on September 20th, 2023.

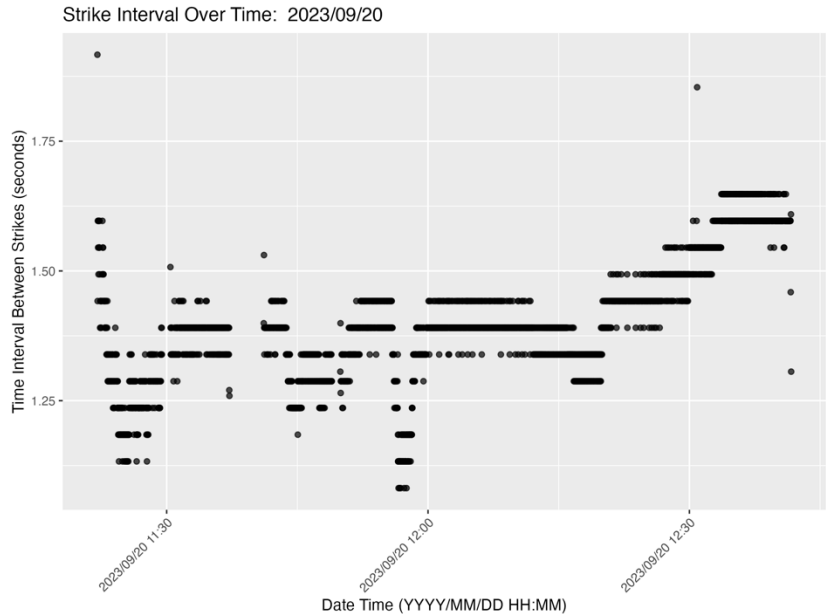


Figure 12. The time interval between strikes in a continuous period for the nearest Rockhopper for Foundation ID AS41 on September 20th, 2023.

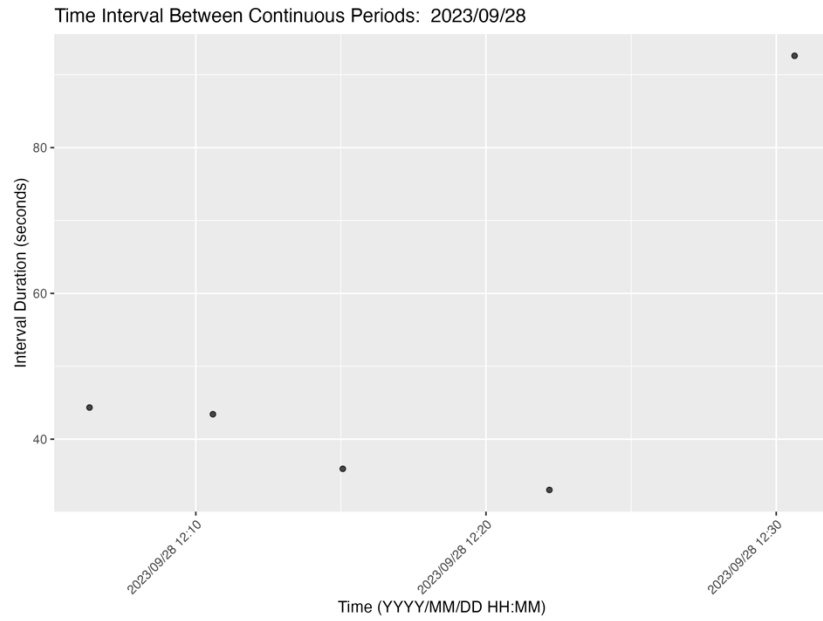


Figure 13. The time interval between continuous periods for the nearest Rockhopper for Foundation ID AQ36 on September 28th, 2023.

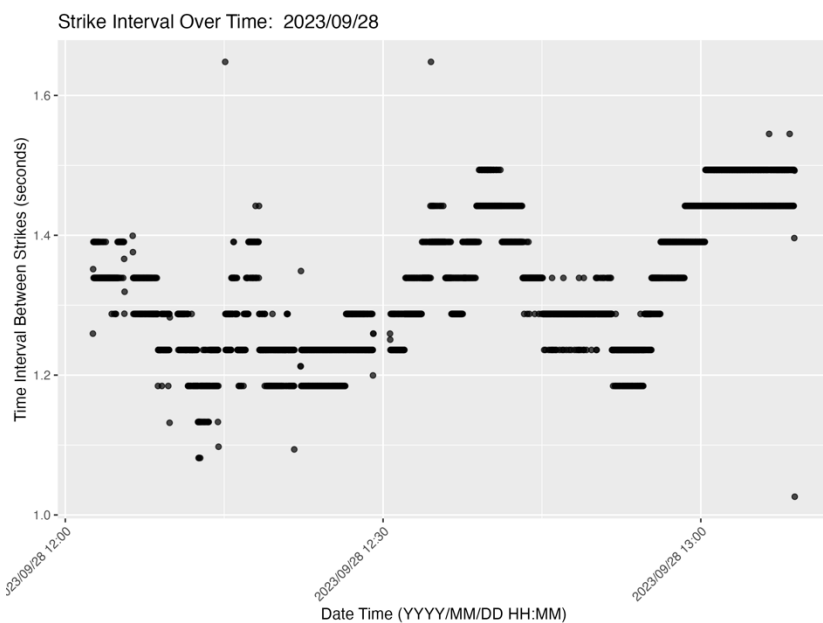


Figure 14. The time interval between strikes in a continuous period for the nearest Rockhopper for Foundation ID AQ36 on September 28th, 2023.

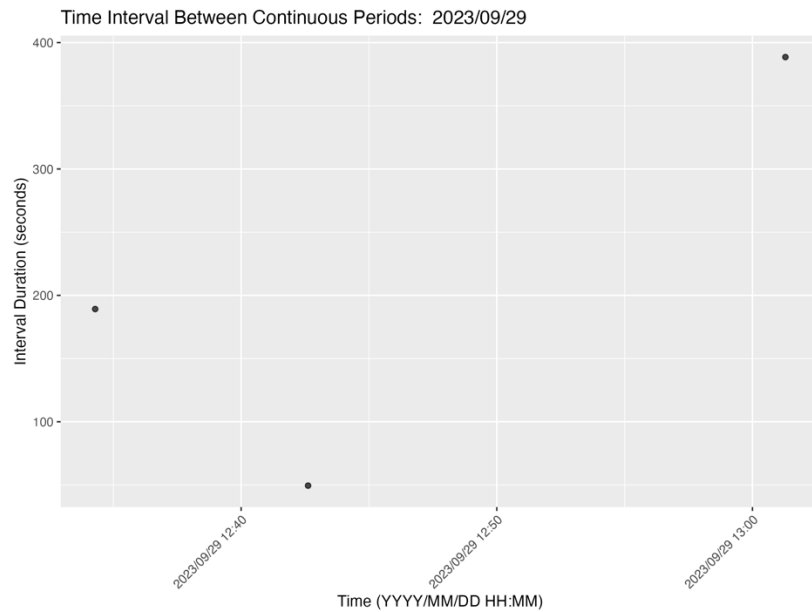


Figure 15. The time interval between continuous periods for the nearest Rockhopper for Foundation ID AT41 on September 29th, 2023.

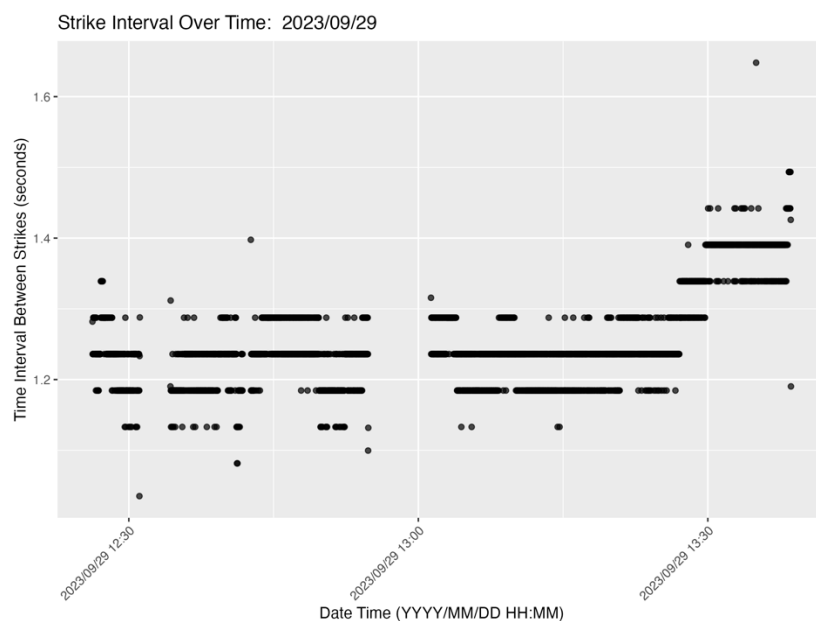


Figure 16. The time interval between strikes in a continuous period for the nearest Rockhopper for Foundation ID AT41 on September 29th, 2023.

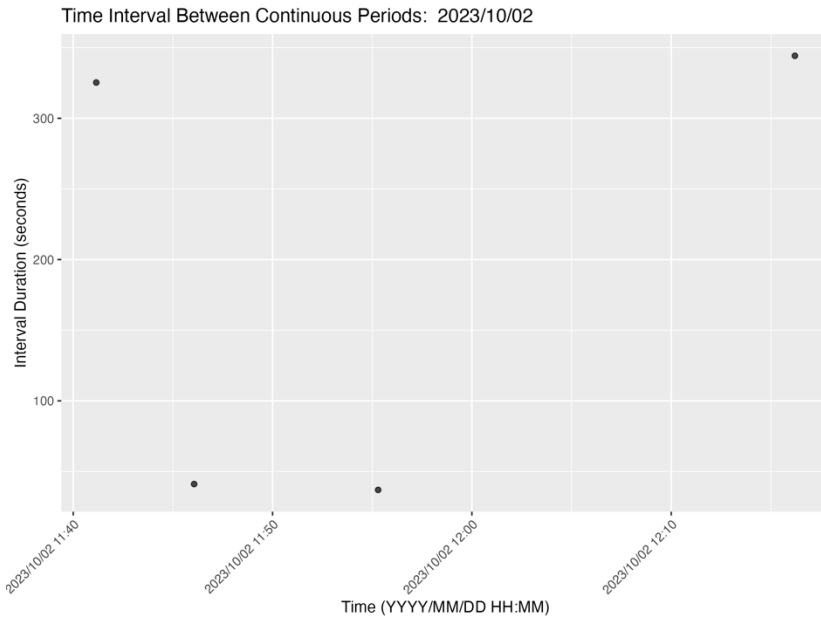


Figure 17. The time interval between continuous periods for the nearest Rockhopper for Foundation ID AQ39 on October 2nd, 2023.

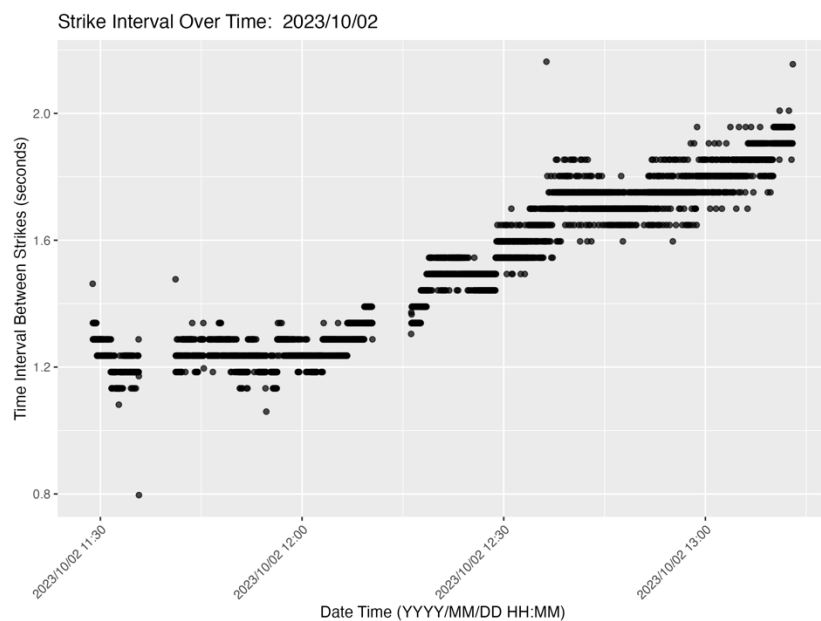


Figure 18. The time interval between strikes in a continuous period for the nearest Rockhopper for Foundation ID AQ39 on October 2nd, 2023.

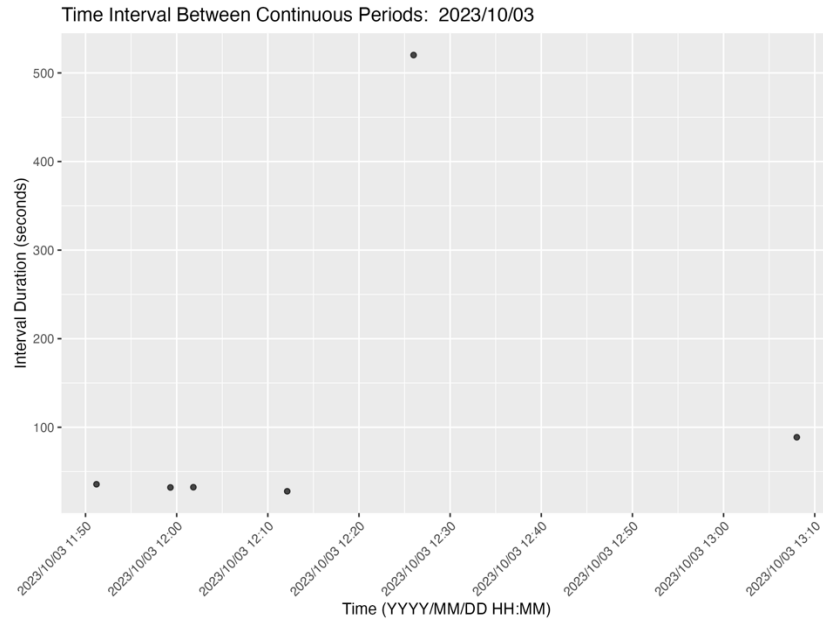


Figure 19. The time interval between continuous periods for the nearest Rockhopper for Foundation ID AS40 on October 3rd, 2023.

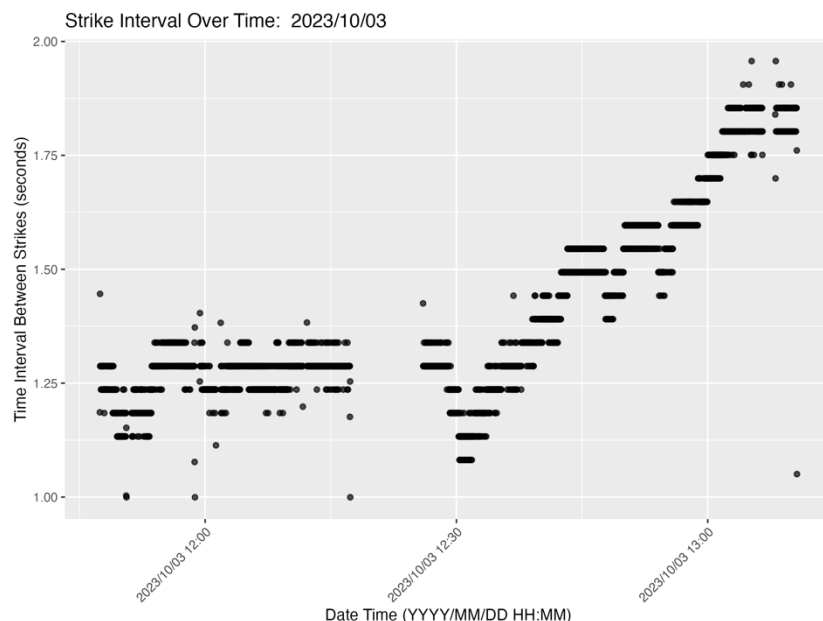


Figure 20. The time interval between strikes in a continuous period for the nearest Rockhopper for Foundation ID AS40 on October 3rd, 2023.

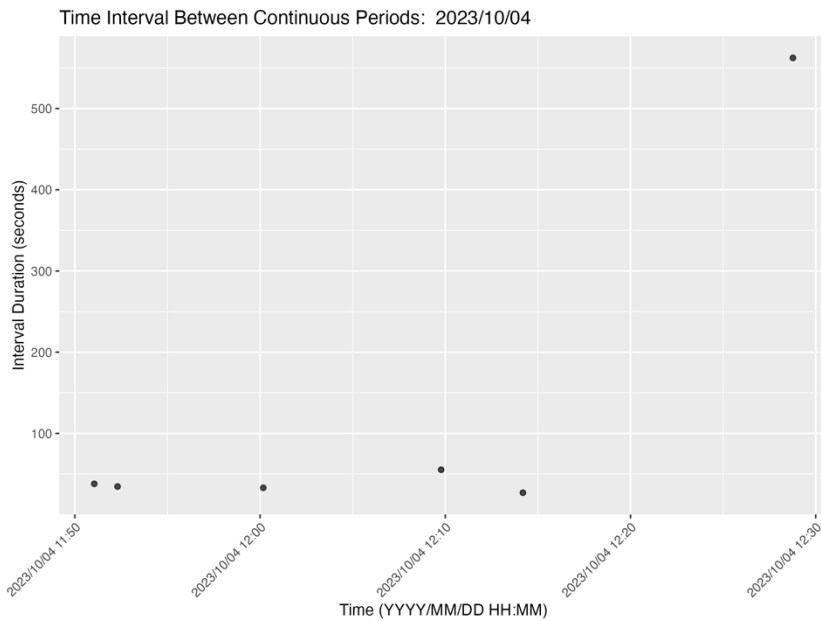


Figure 21. The time interval between continuous periods for the nearest Rockhopper for Foundation ID AR38 on October 4th, 2023.

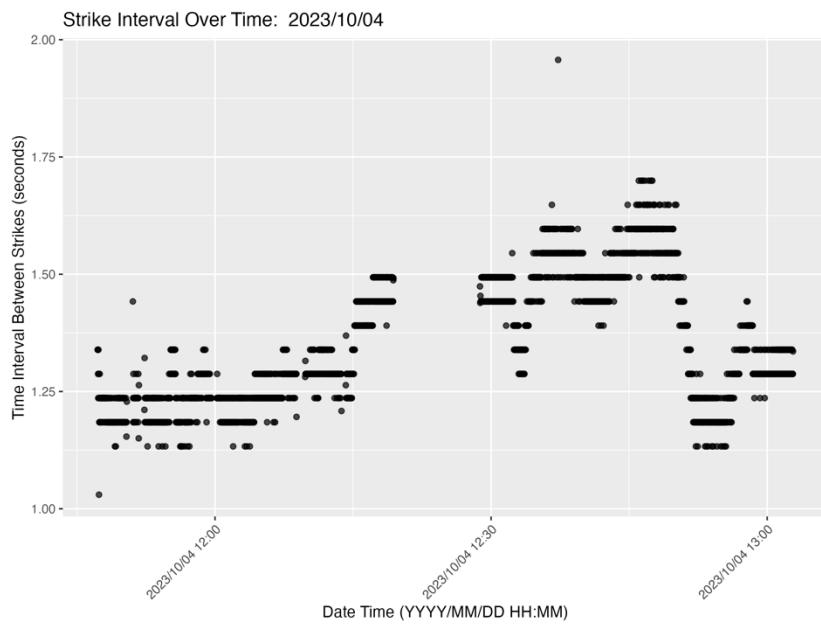


Figure 22. The time interval between strikes in a continuous period for the nearest Rockhopper for Foundation ID AR38 on October 4th, 2023.

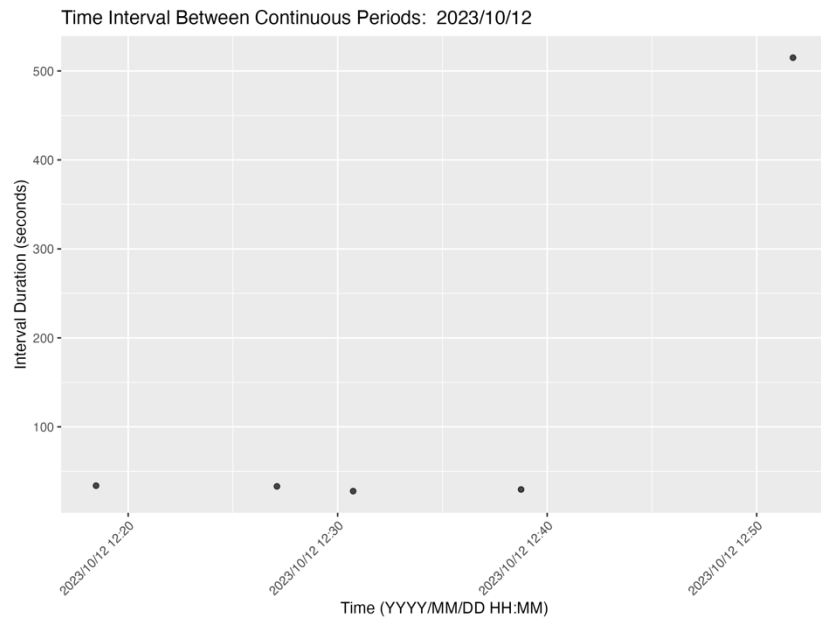


Figure 23. The time interval between continuous periods for the nearest Rockhopper for Foundation ID AS42 on October 12th, 2023.

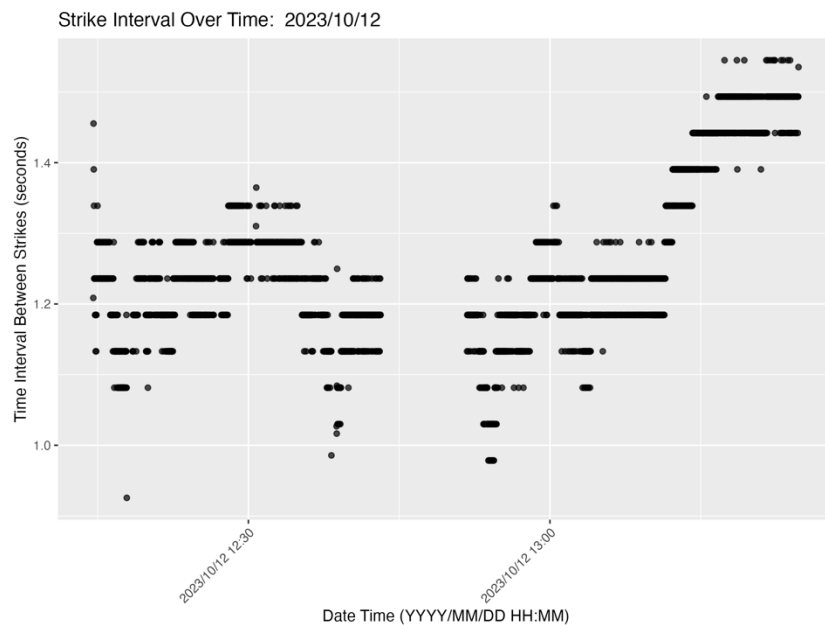


Figure 24. The time interval between strikes in a continuous period for the nearest Rockhopper for Foundation ID AS42 on October 12th, 2023.

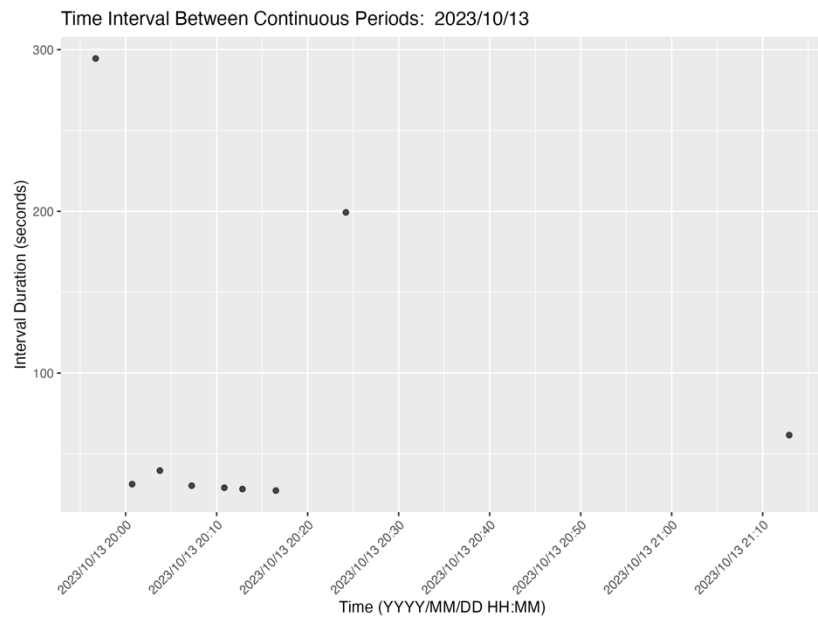


Figure 25. The time interval between continuous periods for the nearest Rockhopper for Foundation ID AP39 on October 13th, 2023.

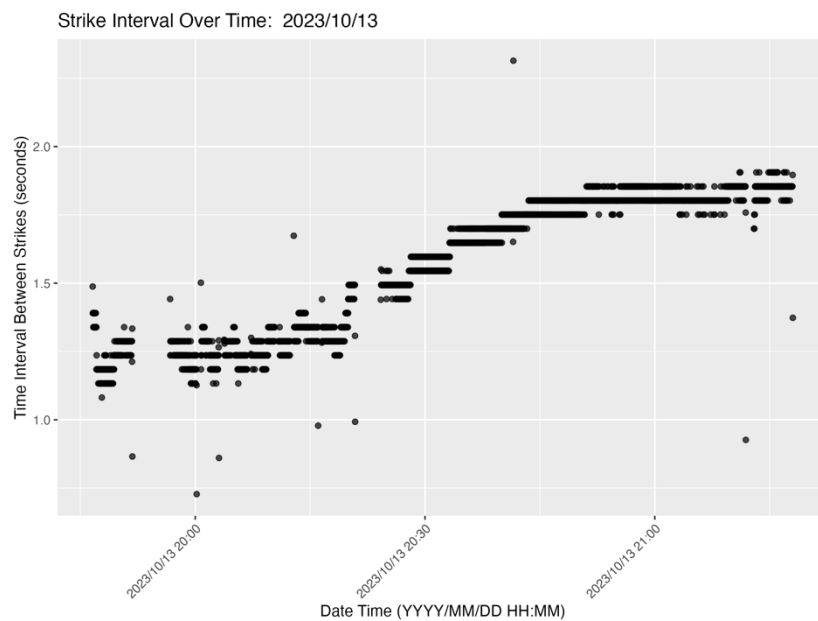


Figure 26. The time interval between strikes in a continuous period for the nearest Rockhopper for Foundation ID AP39 on October 13th, 2023.

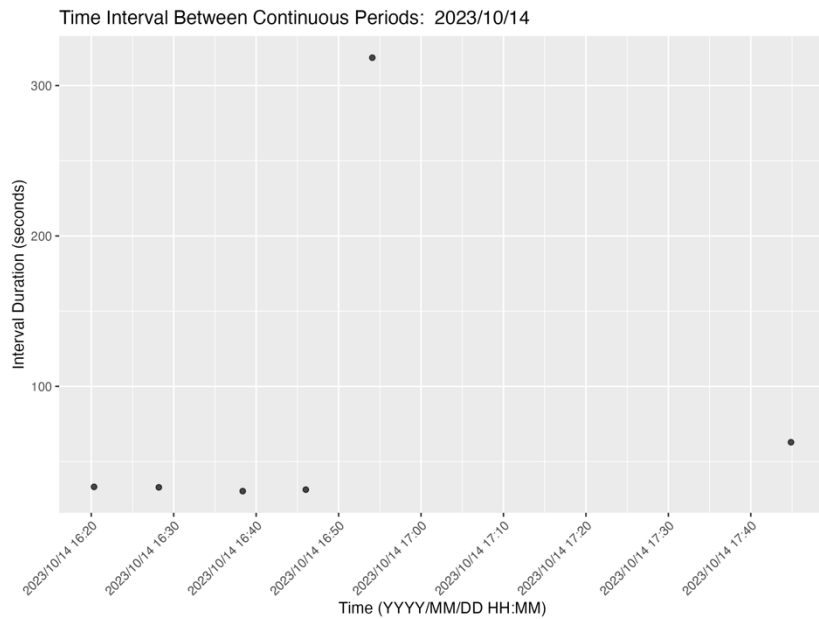


Figure 27. The time interval between continuous periods for the nearest Rockhopper for Foundation ID AN38 on October 14th, 2023.

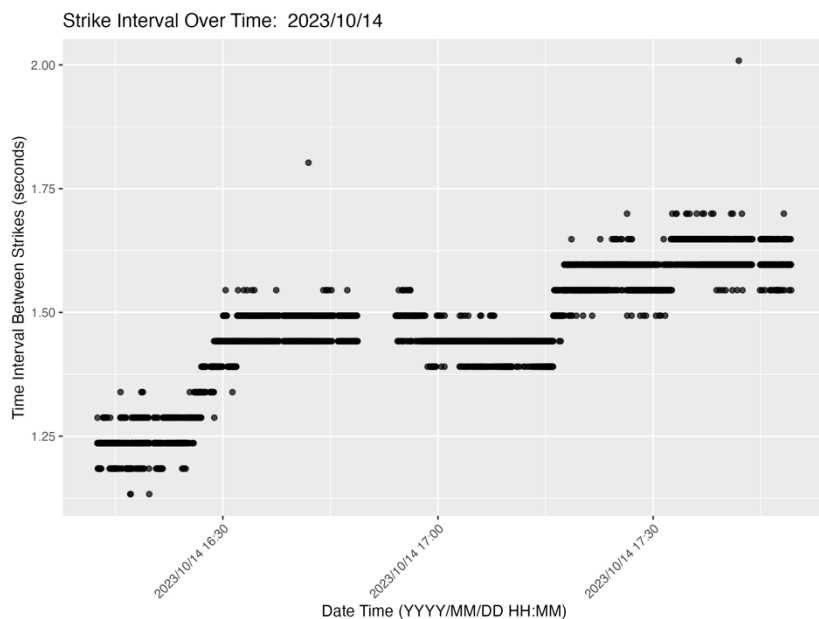


Figure 28. The time interval between strikes in a continuous period for the nearest Rockhopper for Foundation ID AN38 on October 14th, 2023.

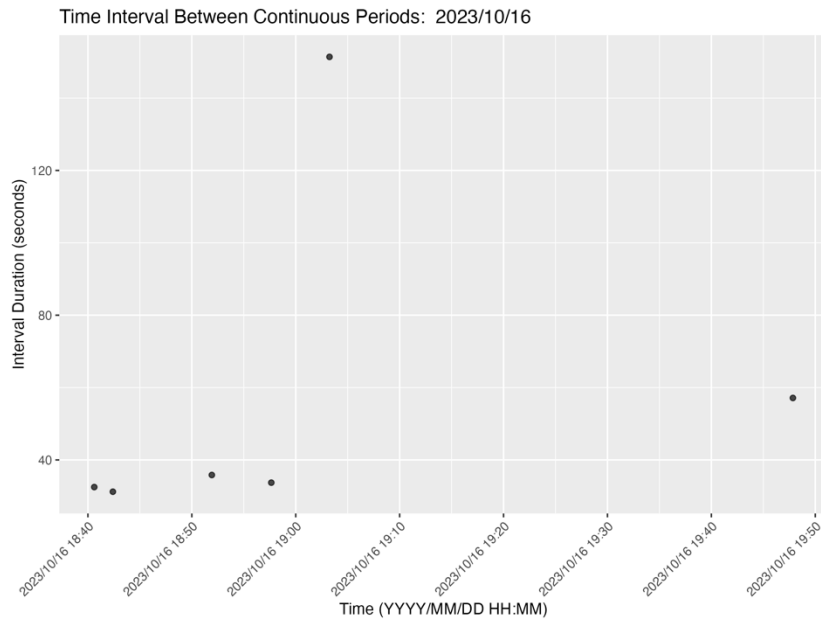


Figure 29. The time interval between continuous periods for the nearest Rockhopper for Foundation ID AR40 on October 16th, 2023.

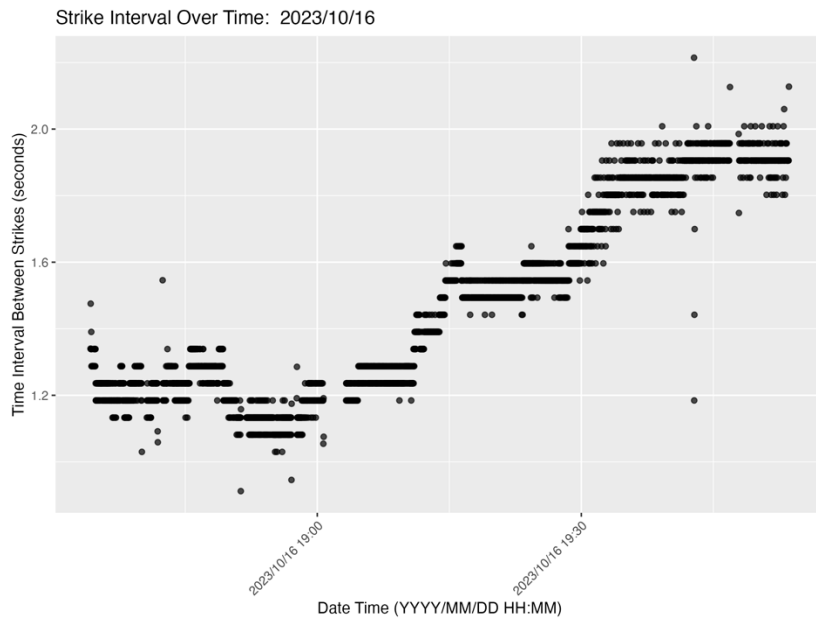


Figure 30. The time interval between strikes in a continuous period for the nearest Rockhopper for Foundation ID AR40 on October 16th, 2023.

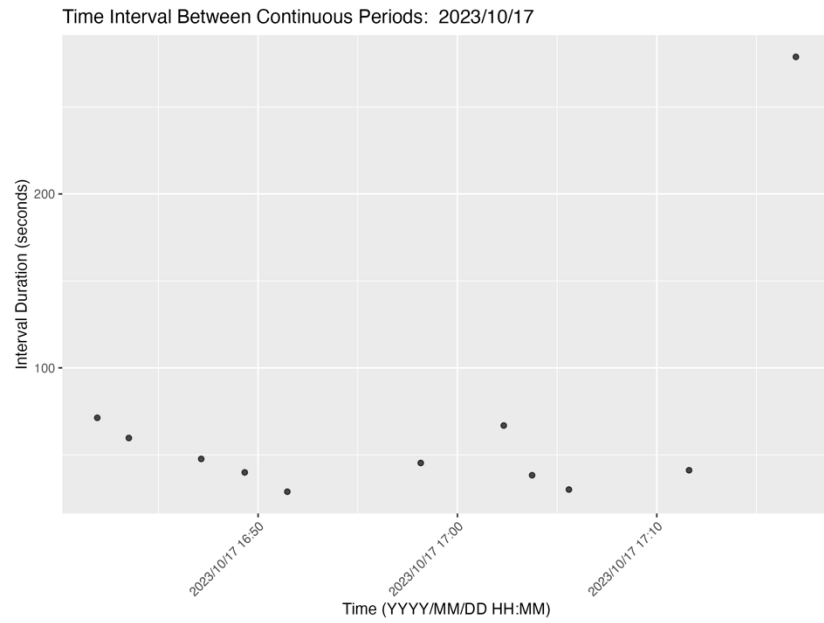


Figure 31. The time interval between continuous periods for the nearest Rockhopper for Foundation ID AR41 on October 17th, 2023.

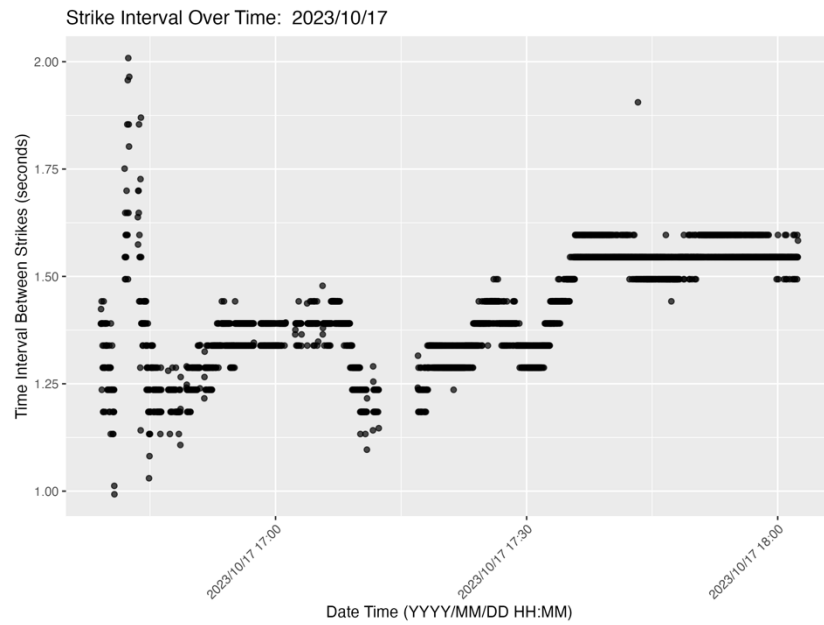


Figure 32. The time interval between strikes in a continuous period for the nearest Rockhopper for Foundation ID AR41 on October 17th, 2023.

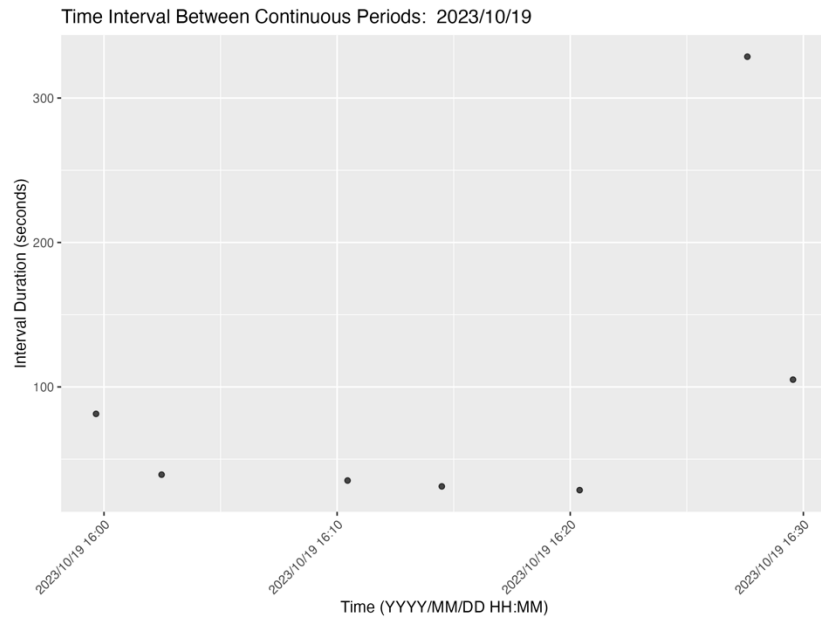


Figure 33. The time interval between continuous periods for the nearest Rockhopper for Foundation ID AU40 on October 19th, 2023.

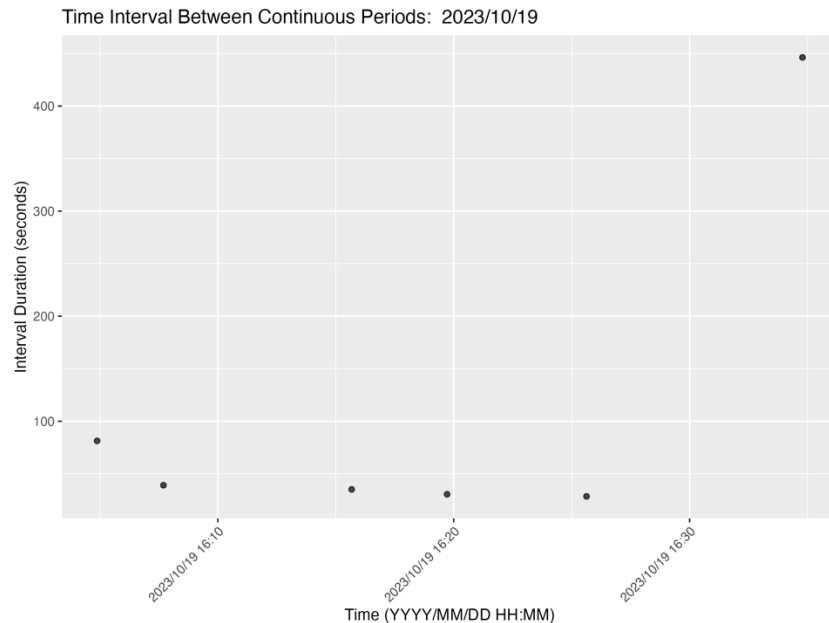


Figure 34. The time interval between continuous periods for the farthest Rockhopper for Foundation ID AU40 on October 19th, 2023.

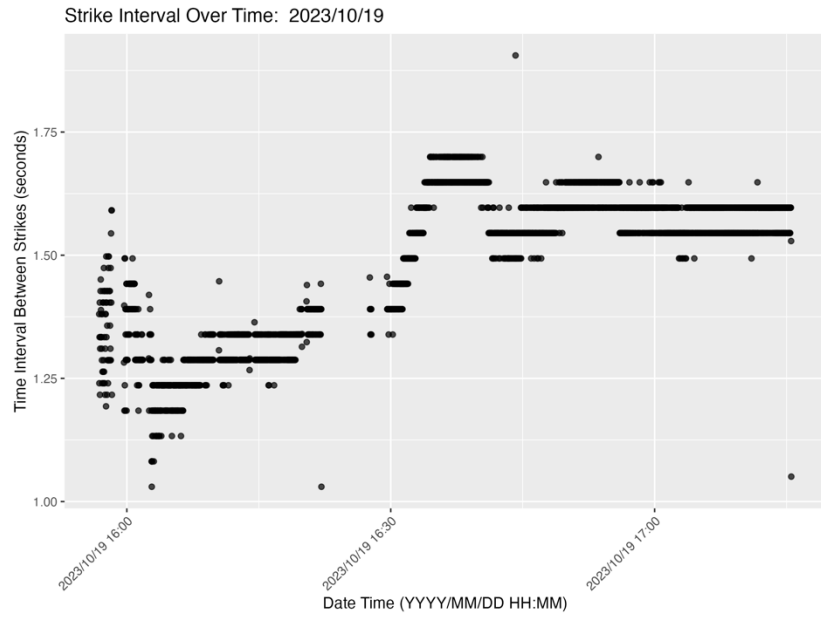


Figure 35. The time interval between strikes in a continuous period for the nearest Rockhopper for Foundation ID AU40 on October 19th, 2023.

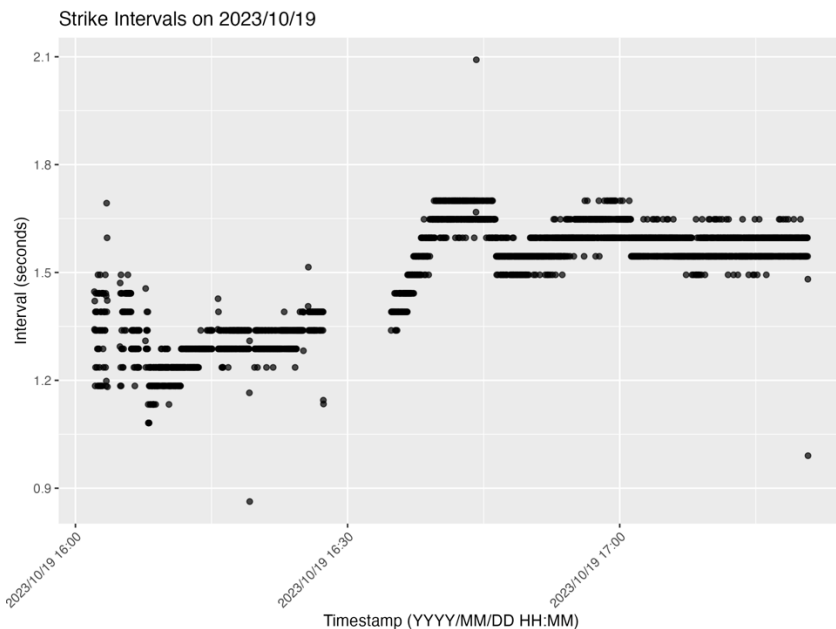


Figure 36. The time interval between strikes in a continuous period for the farthest Rockhopper for Foundation ID AU40 on October 19th, 2023.

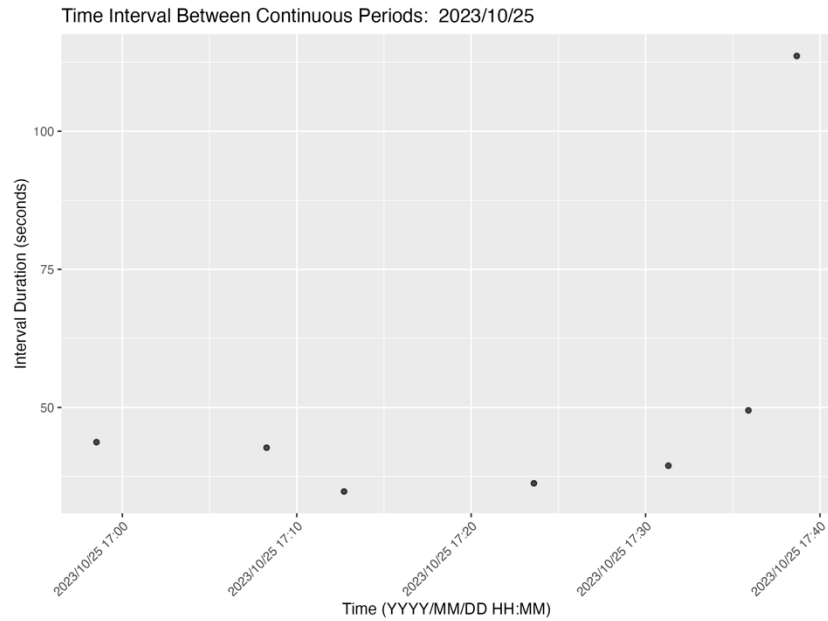


Figure 37. The time interval between continuous periods for the nearest Rockhopper for Foundation ID AQ42 on October 25th, 2023.

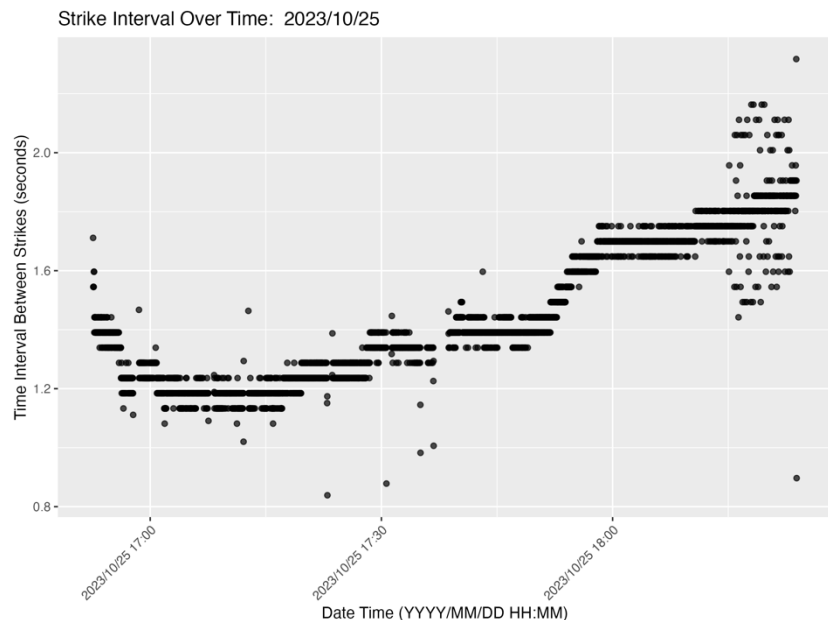


Figure 38. The time interval between strikes in a continuous period for the nearest Rockhopper for Foundation ID AQ42 on October 25th, 2023.

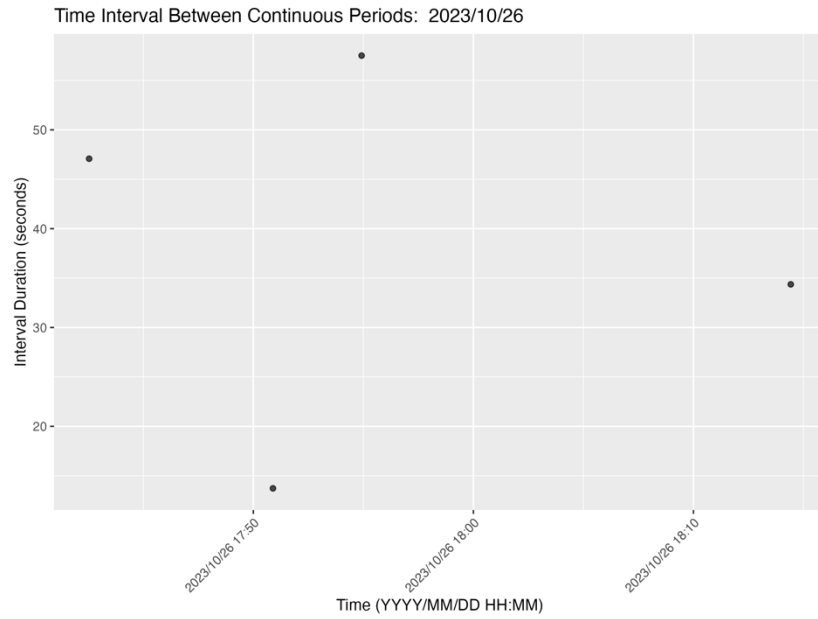


Figure 39. The time interval between continuous periods for the nearest Rockhopper for Foundation ID AM38 on October 26th, 2023.

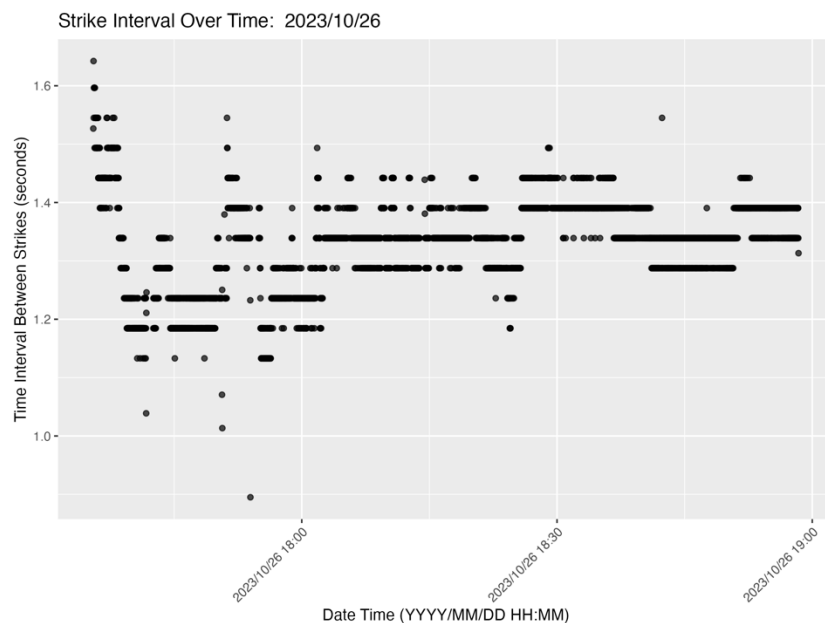


Figure 40. The time interval between strikes in a continuous period for the nearest Rockhopper for Foundation ID AM38 on October 26th, 2023.

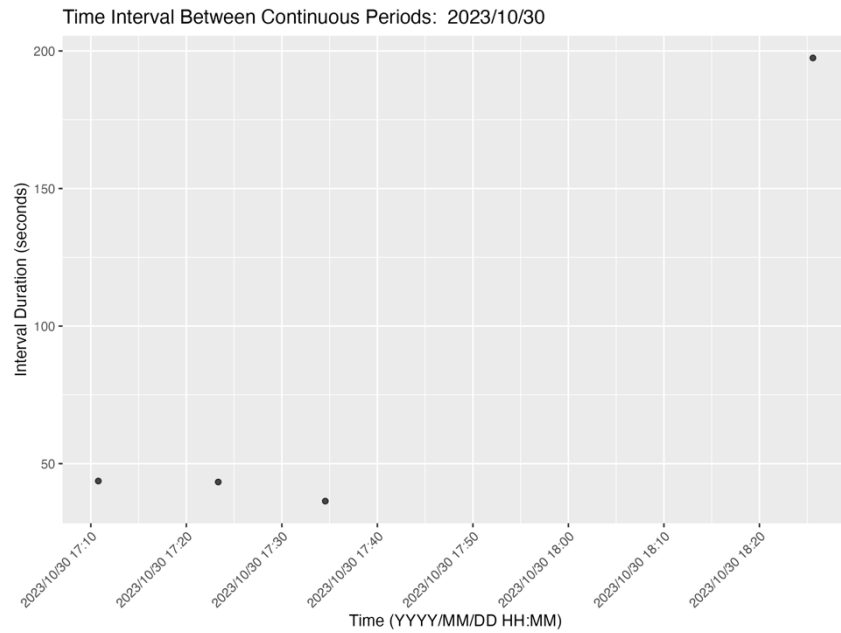


Figure 41. The time interval between continuous periods for the nearest Rockhopper for Foundation ID AQ41 on October 30th, 2023.

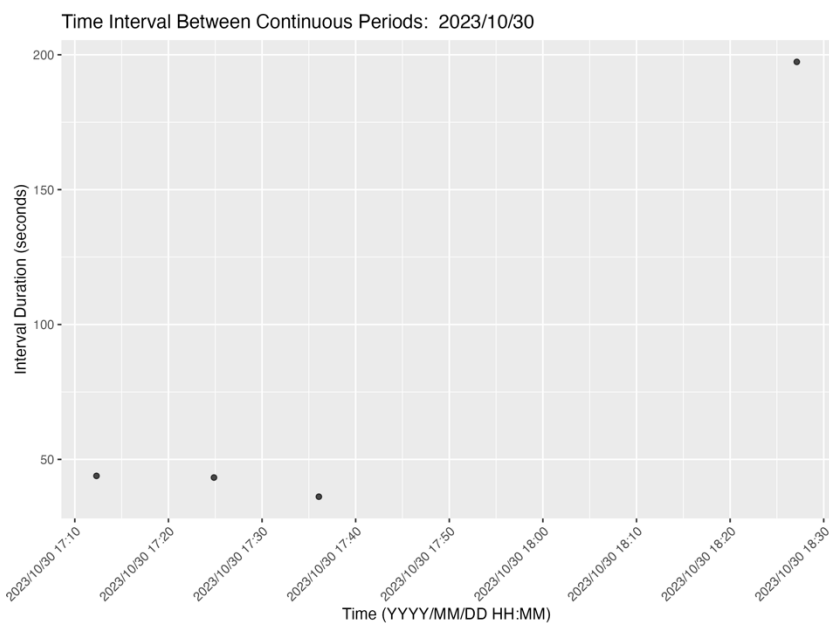


Figure 42. The time interval between continuous periods for the farthest Rockhopper for Foundation ID AQ41 on October 30th, 2023.

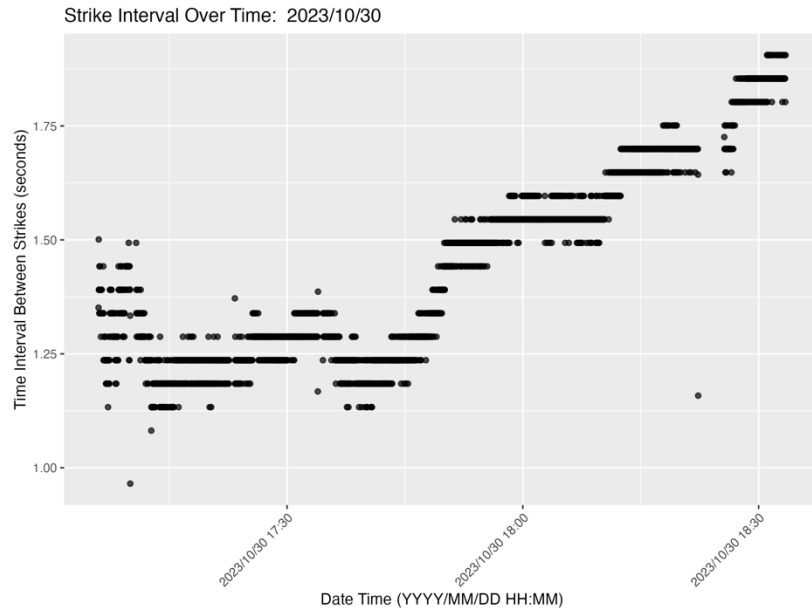


Figure 43. The time interval between strikes in a continuous period for the nearest Rockhopper for Foundation ID AQ41 on October 30th, 2023.

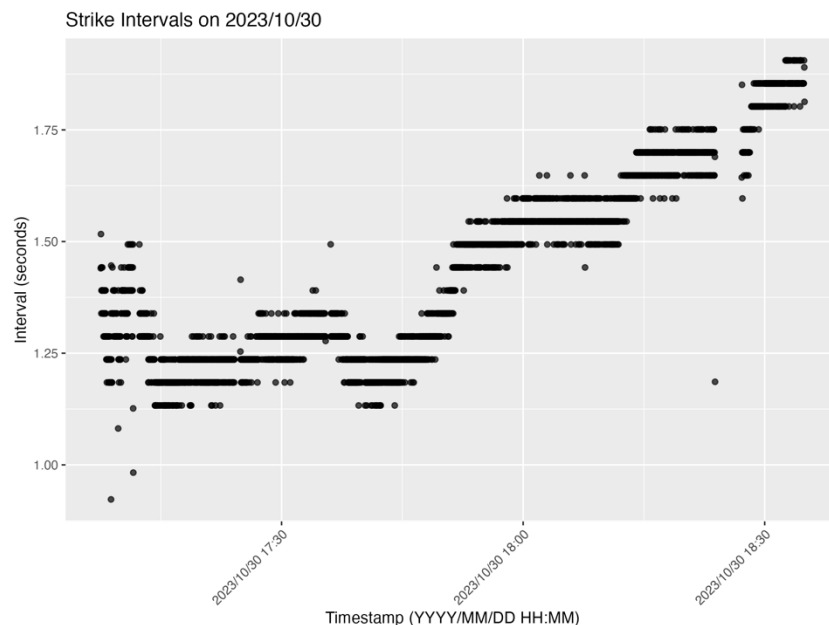


Figure 44. The time interval between strikes in a continuous period for the farthest Rockhopper for Foundation ID AQ41 on October 30th, 2023.

Time Interval Between Continuous Periods: 2023/10/31

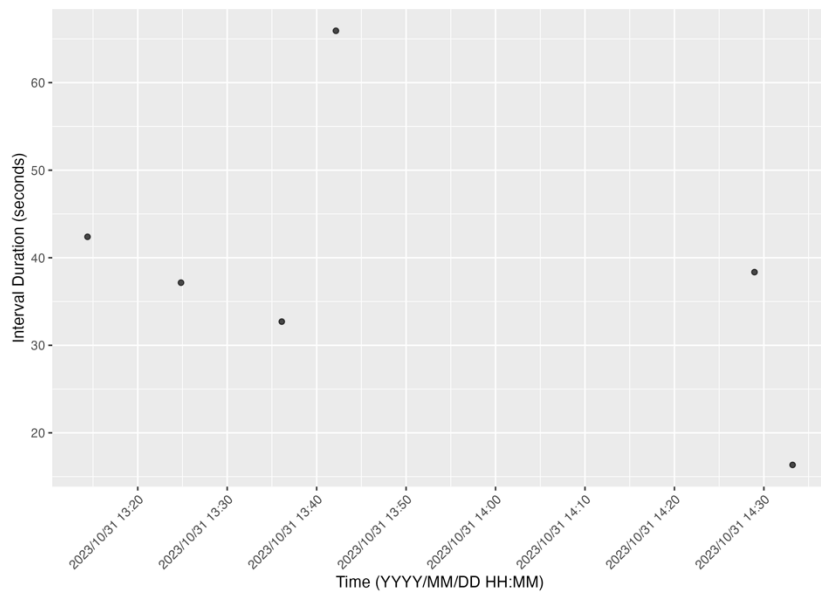


Figure 45. The time interval between continuous periods for the nearest Rockhopper for Foundation ID AQ40 on October 31st, 2023.

Strike Interval Over Time: 2023/10/31

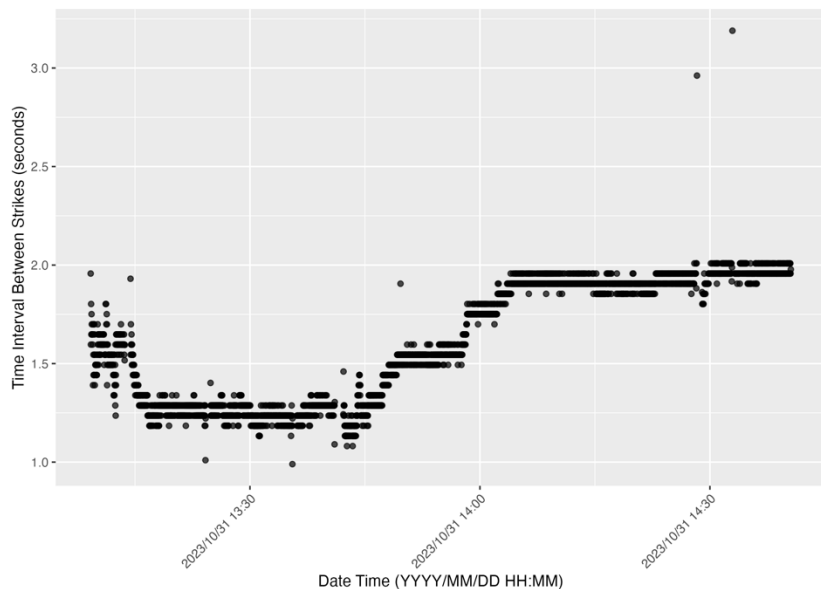


Figure 46. The time interval between strikes in a continuous period for the nearest Rockhopper for Foundation ID AQ40 on October 31st, 2023.

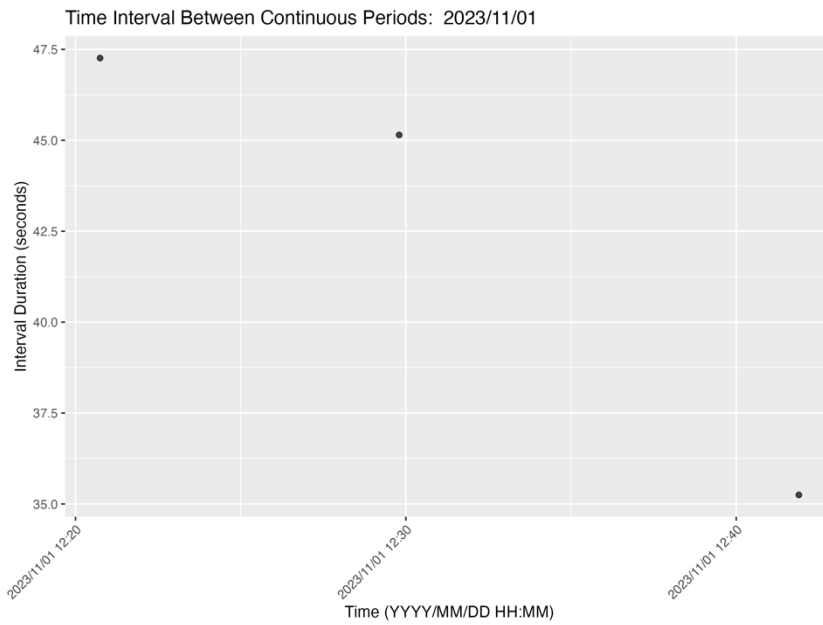


Figure 47. The time interval between continuous periods for the nearest Rockhopper for Foundation ID AR42 on November 1st, 2023.

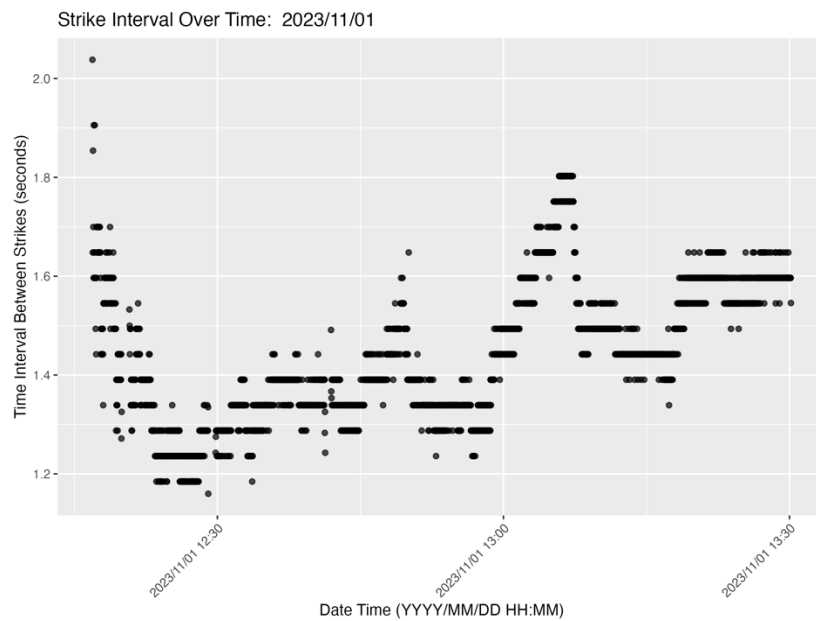


Figure 48. The time interval between strikes in a continuous period for the nearest Rockhopper for Foundation ID AR42 on November 1st, 2023.

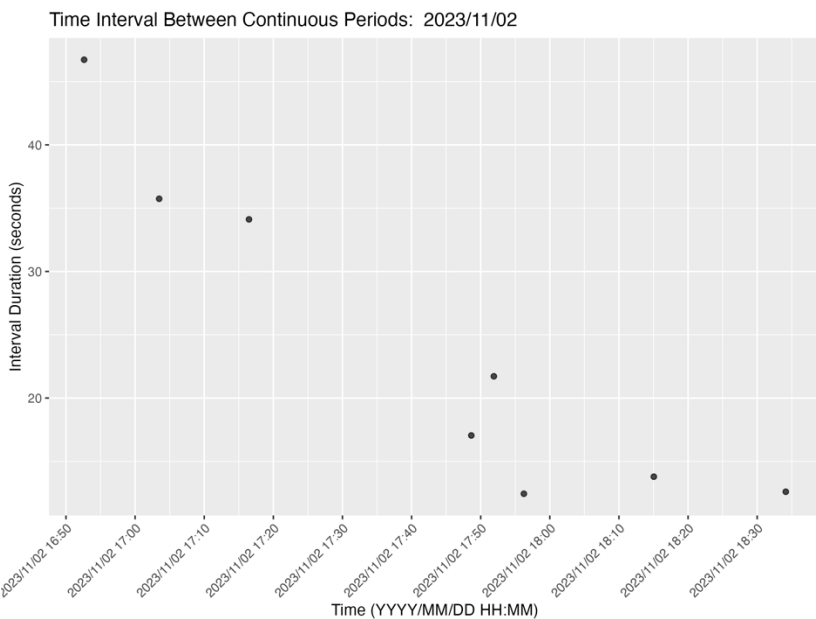


Figure 49. The time interval between continuous periods for the nearest Rockhopper for Foundation ID AP40 on November 2nd, 2023.

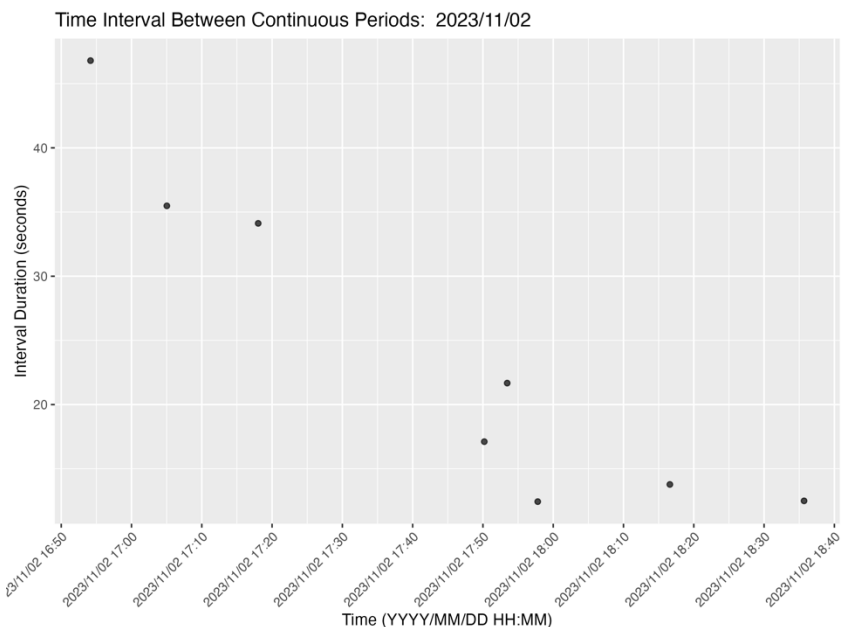


Figure 50. The time interval between continuous periods for the farthest Rockhopper for Foundation ID AP40 on November 2nd, 2023.

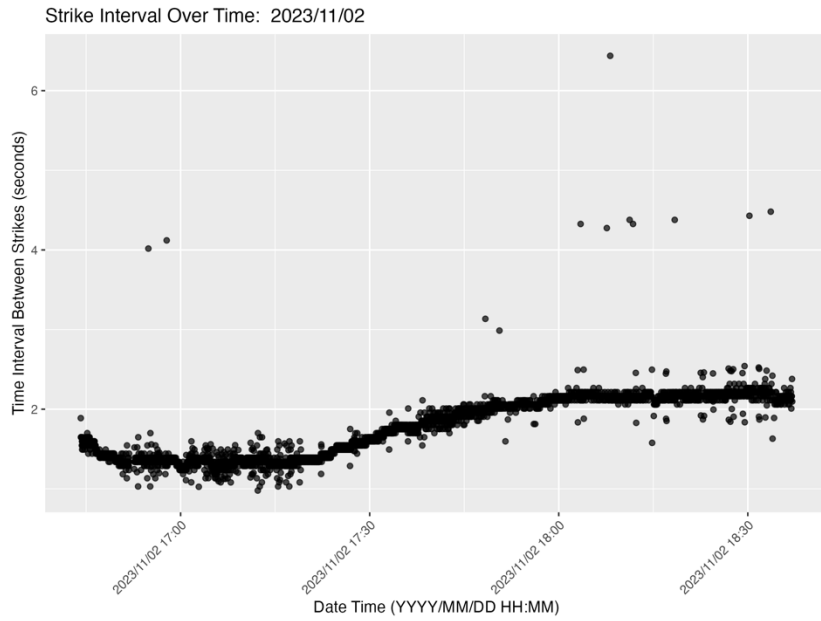


Figure 51. The time interval between strikes in a continuous period for the nearest Rockhopper for Foundation ID AP40 on November 2nd, 2023.

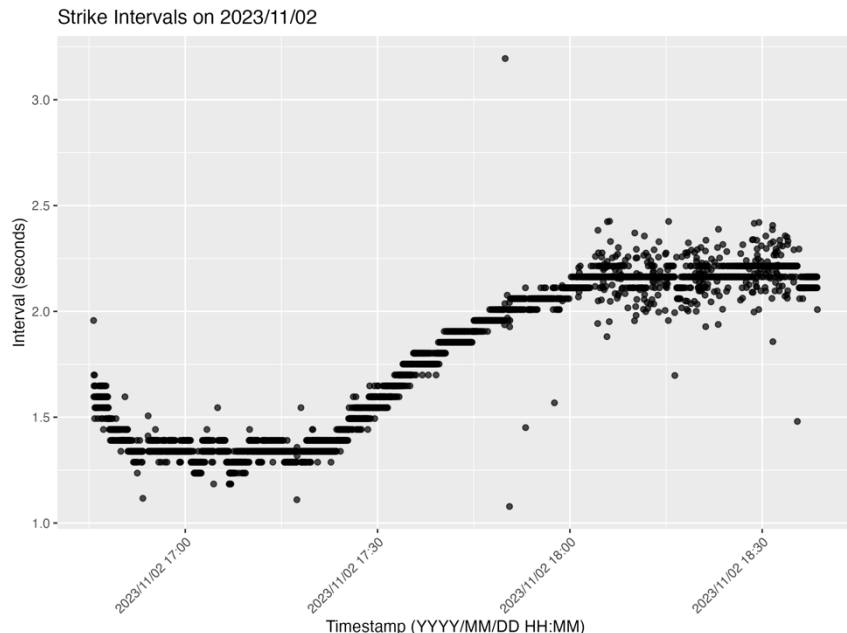


Figure 52. The time interval between strikes in a continuous period for the farthest Rockhopper for Foundation ID AP40 on November 2nd, 2023.

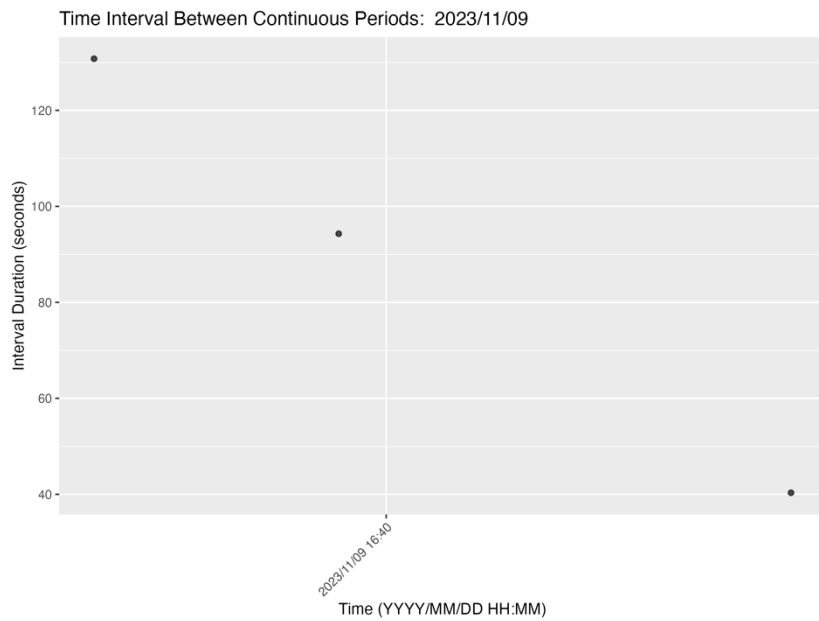


Figure 53. The time interval between continuous periods for the nearest Rockhopper for Foundation ID AN39 on November 9th, 2023.

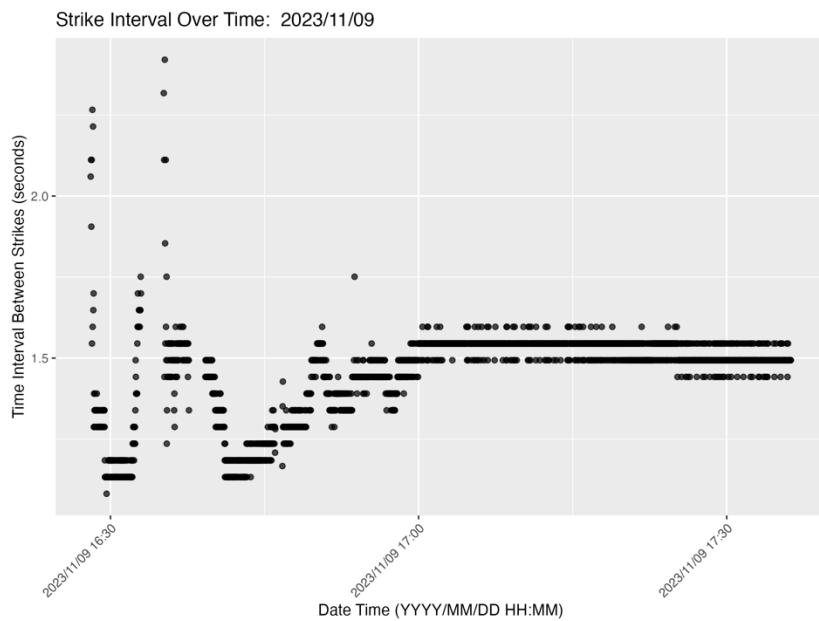


Figure 54. The time interval between strikes in a continuous period for the nearest Rockhopper for Foundation ID AN39 on November 9th, 2023.

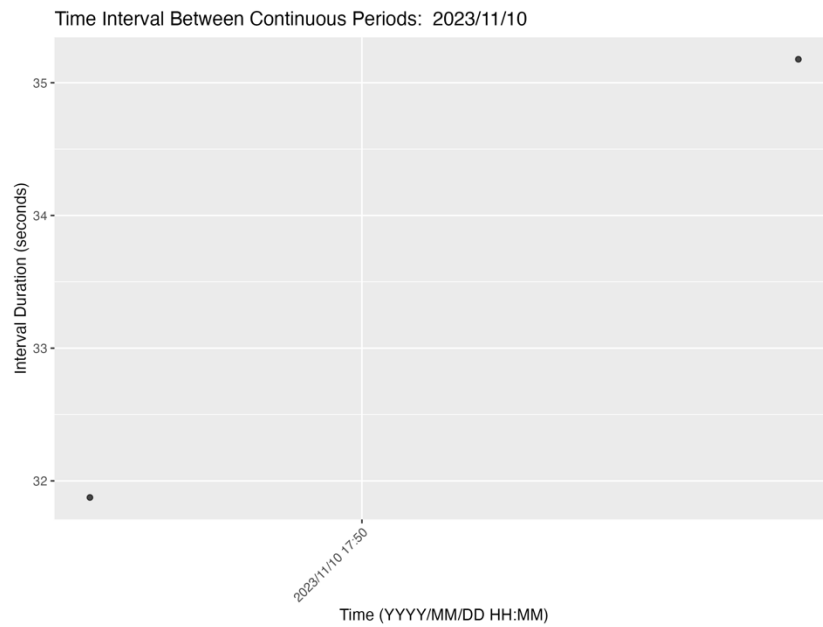


Figure 55. The time interval between continuous periods for the nearest Rockhopper for Foundation ID AP41 on November 10th, 2023.

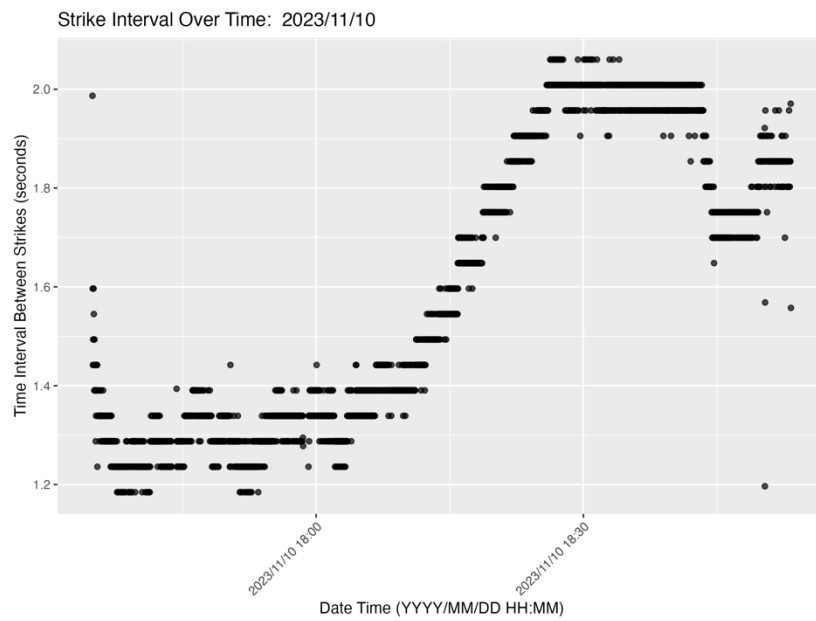


Figure 56. The time interval between strikes in a continuous period for the nearest Rockhopper for Foundation ID AP41 on November 10th, 2023.

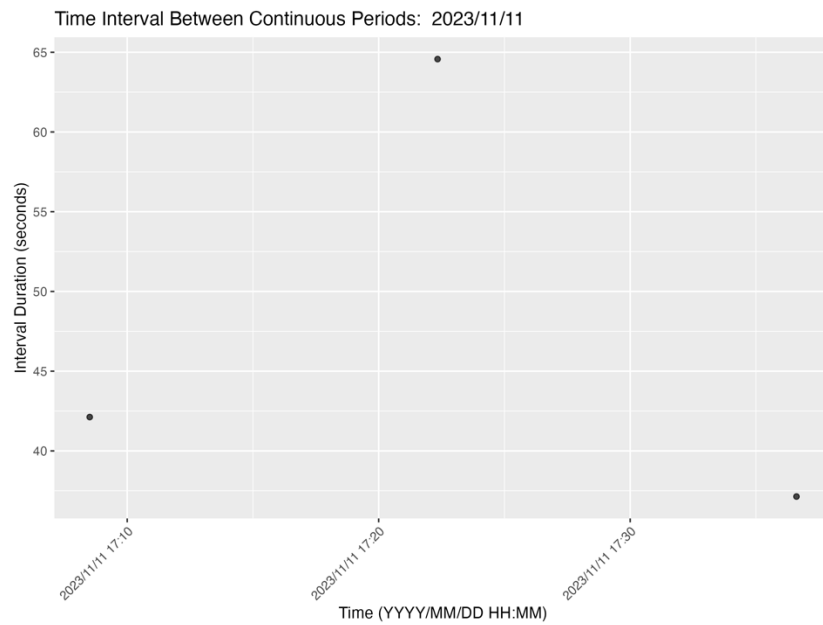


Figure 57. The time interval between continuous periods for the nearest Rockhopper for Foundation ID AM39 on November 11th, 2023.

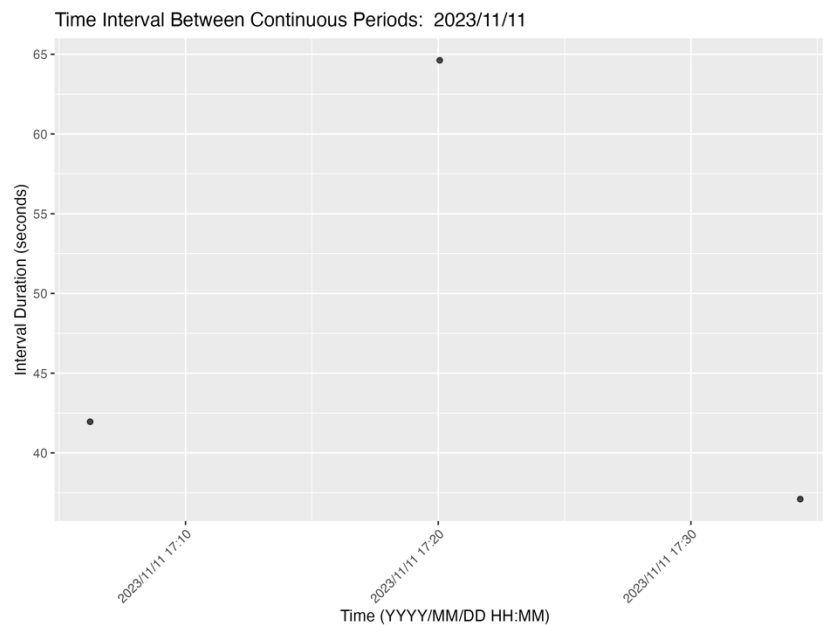


Figure 58. The time interval between continuous periods for the farthest Rockhopper for Foundation ID AM39 on November 11th, 2023.

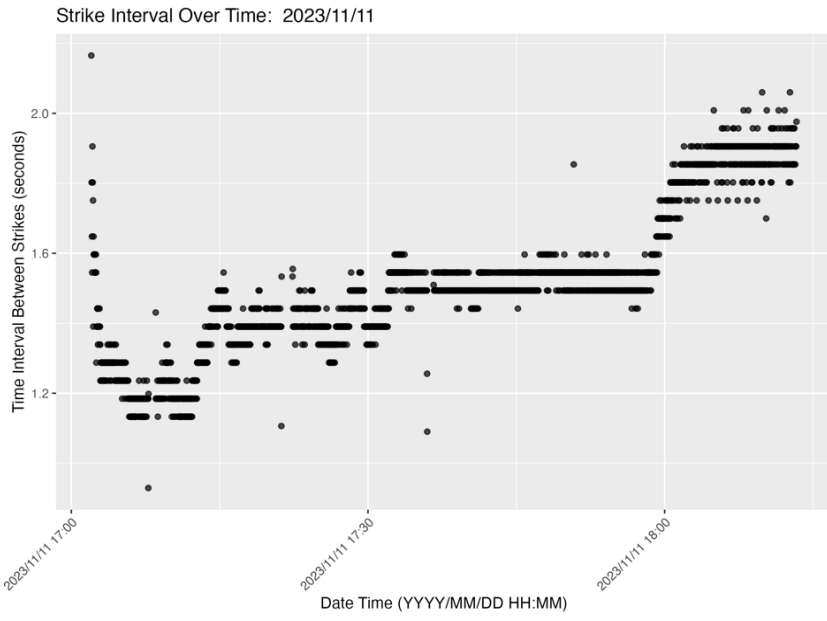


Figure 59. The time interval between strikes in a continuous period for the nearest Rockhopper for Foundation ID AM39 on November 11th, 2023.

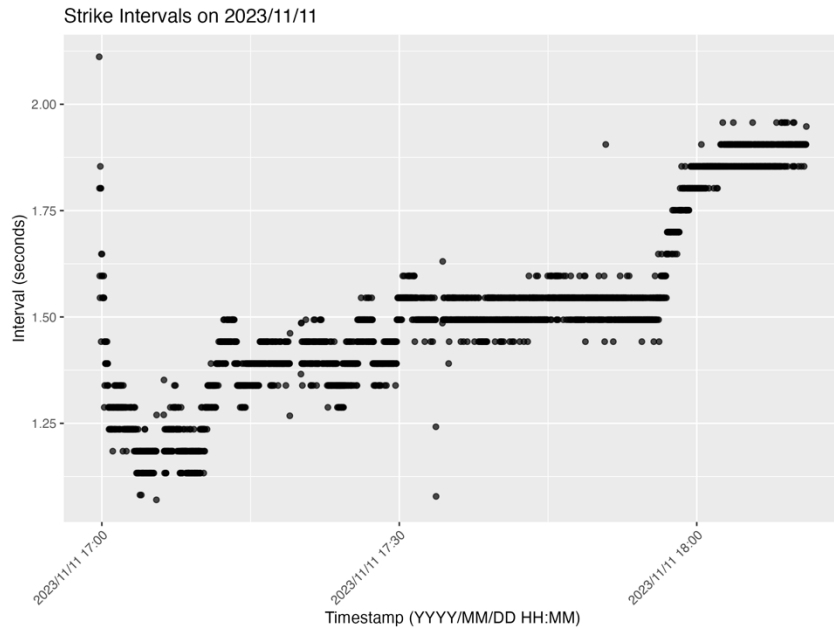


Figure 60. The time interval between strikes in a continuous period for the farthest Rockhopper for Foundation ID AM39 on November 11th, 2023.

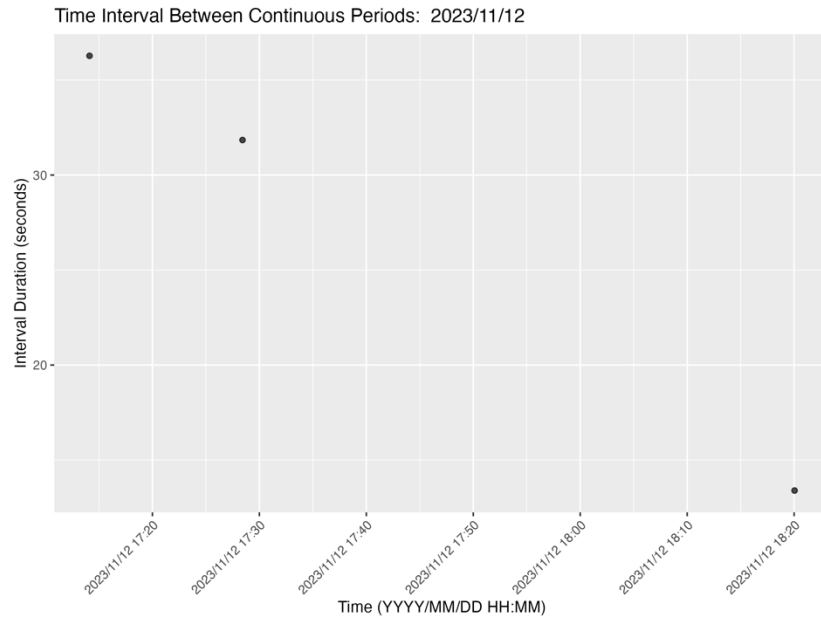


Figure 61. The time interval between continuous periods for the nearest Rockhopper for Foundation ID AT37 on November 12th, 2023.

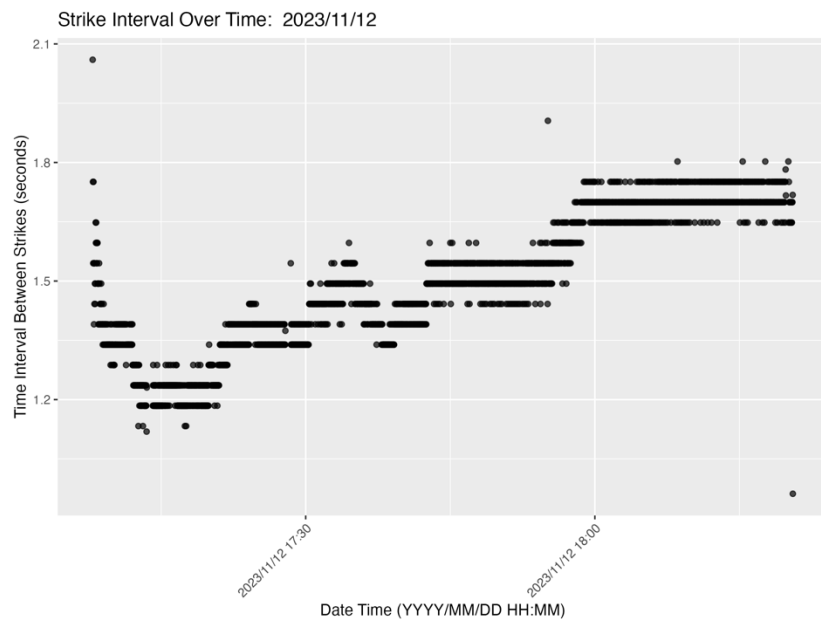


Figure 62. The time interval between strikes in a continuous period for the nearest Rockhopper for Foundation ID AT37 on November 12th, 2023.

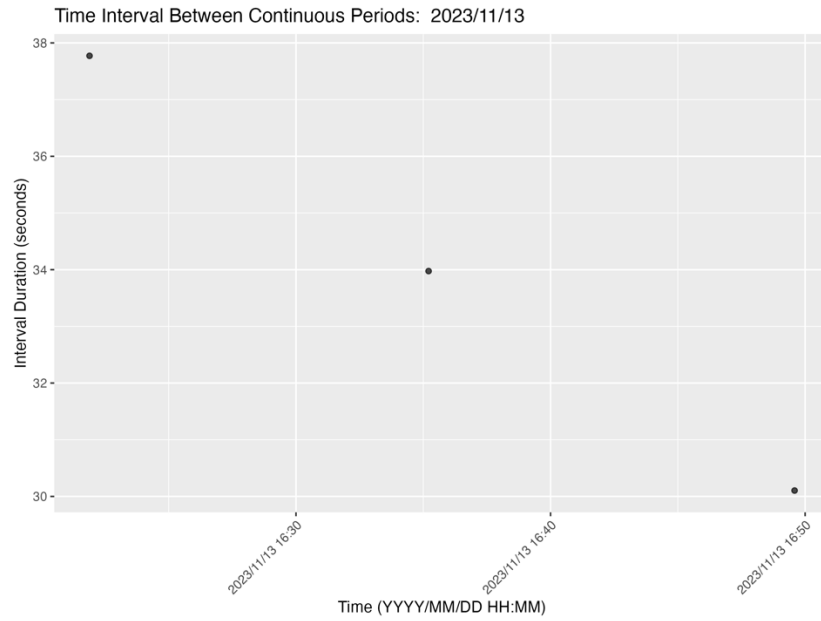


Figure 63. The time interval between continuous periods for the nearest Rockhopper for Foundation ID AL38 on November 13th, 2023.

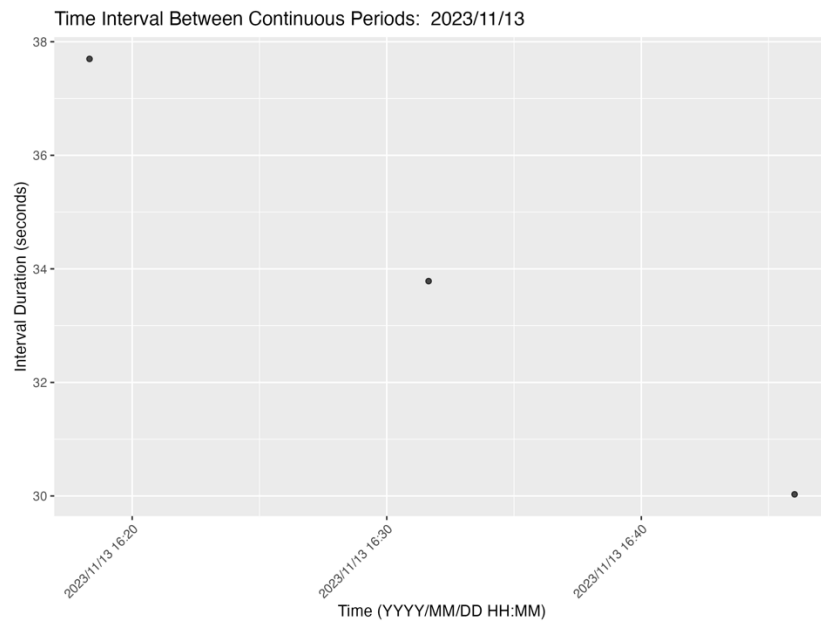


Figure 64. The time interval between continuous periods for the farthest Rockhopper for Foundation ID AL38 on November 13th, 2023.

Strike Interval Over Time: 2023/11/13

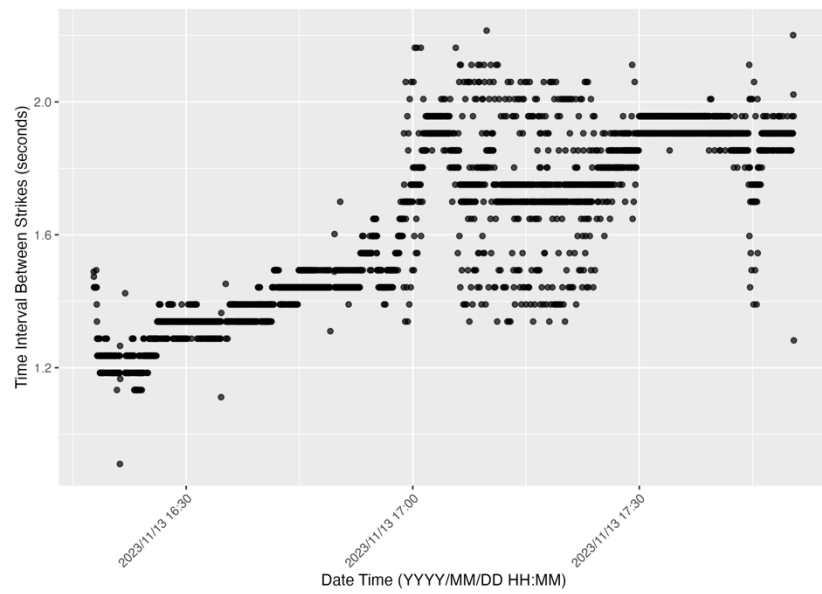


Figure 65. The time interval between strikes in a continuous period for the nearest Rockhopper for Foundation ID AL38 on November 13th, 2023.

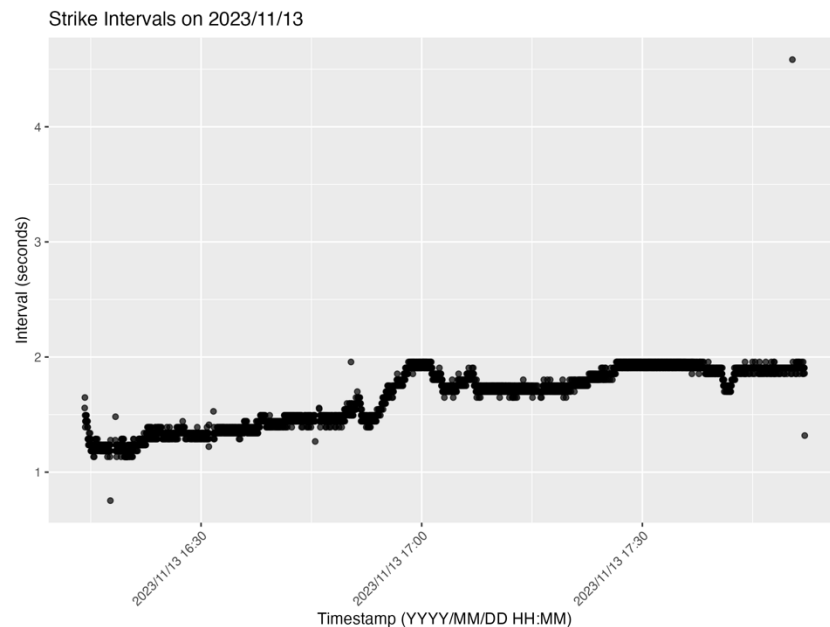


Figure 66. The time interval between strikes in a continuous period for the farthest Rockhopper for Foundation ID AL38 on November 13th, 2023.

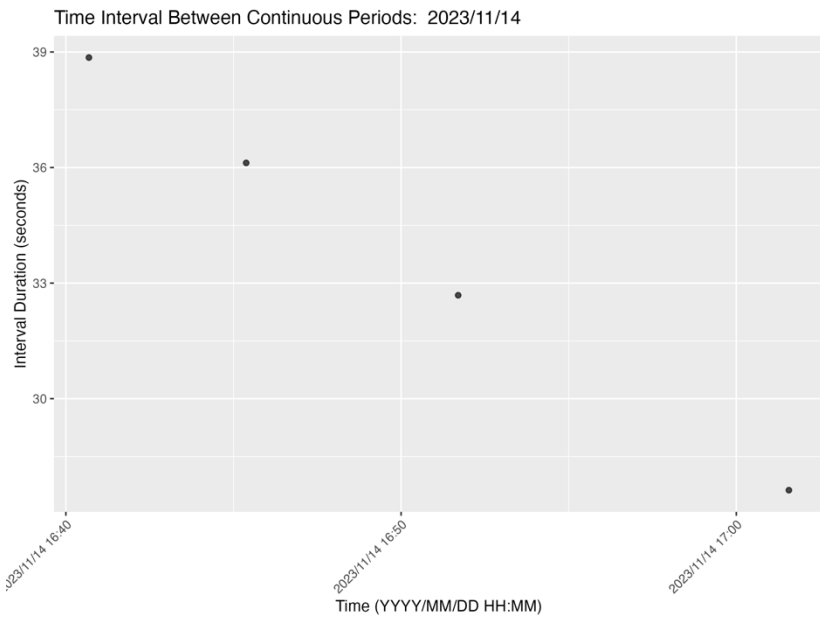


Figure 67. The time interval between continuous periods for the nearest Rockhopper for Foundation ID AS37 on November 14th, 2023.

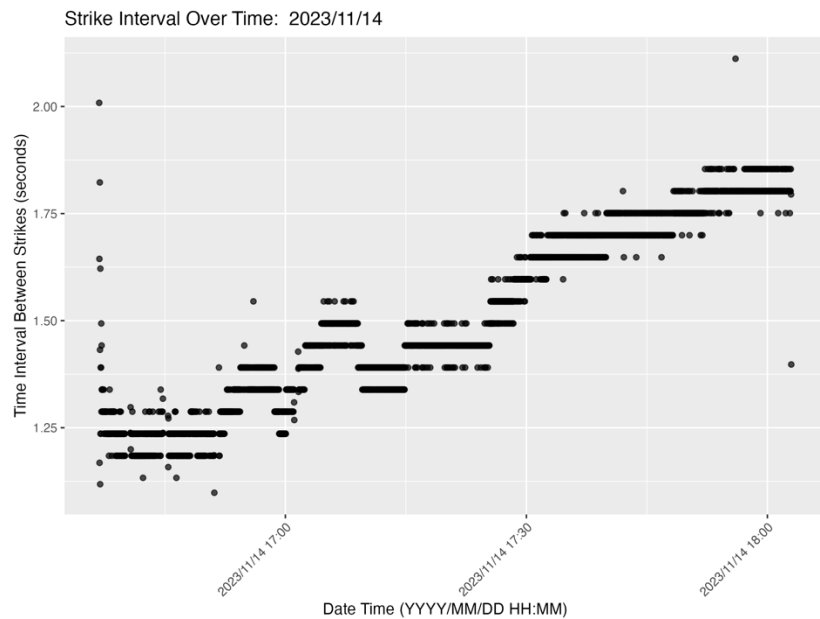


Figure 68. The time interval between strikes in a continuous period for the nearest Rockhopper for Foundation ID AS37 on November 14th, 2023.

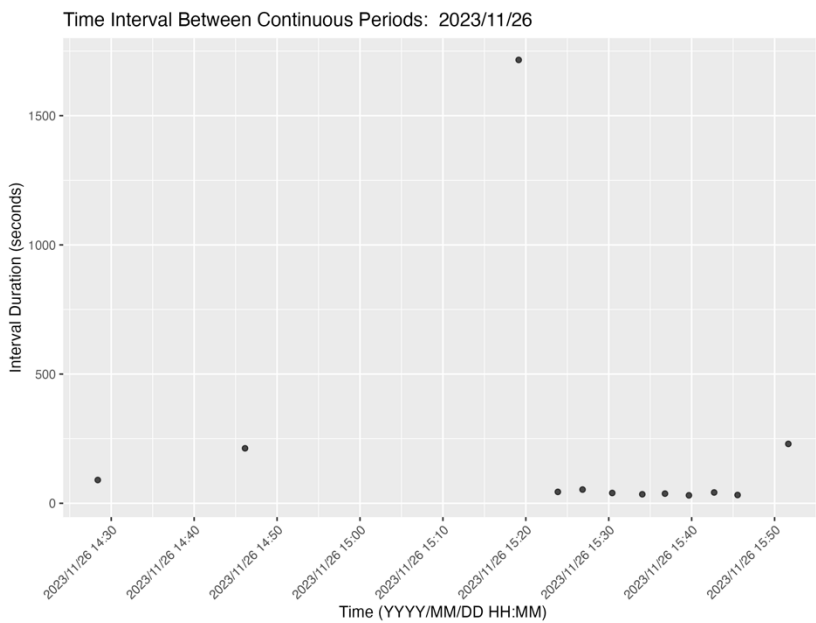


Figure 69. The time interval between continuous periods for the nearest Rockhopper for Foundation ID AQ34 on November 26th, 2023.

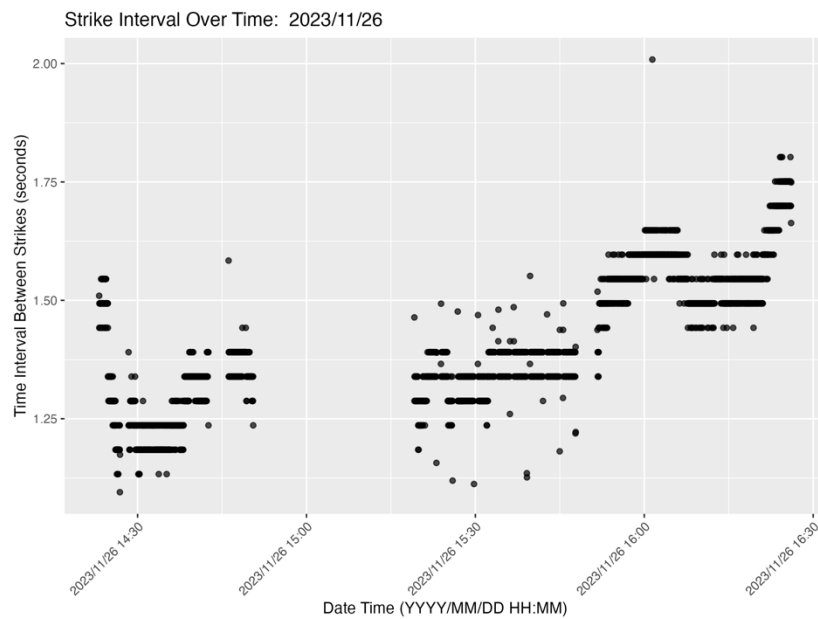


Figure 70. The time interval between strikes in a continuous period for the nearest Rockhopper for Foundation ID AQ34 on November 26th, 2023.

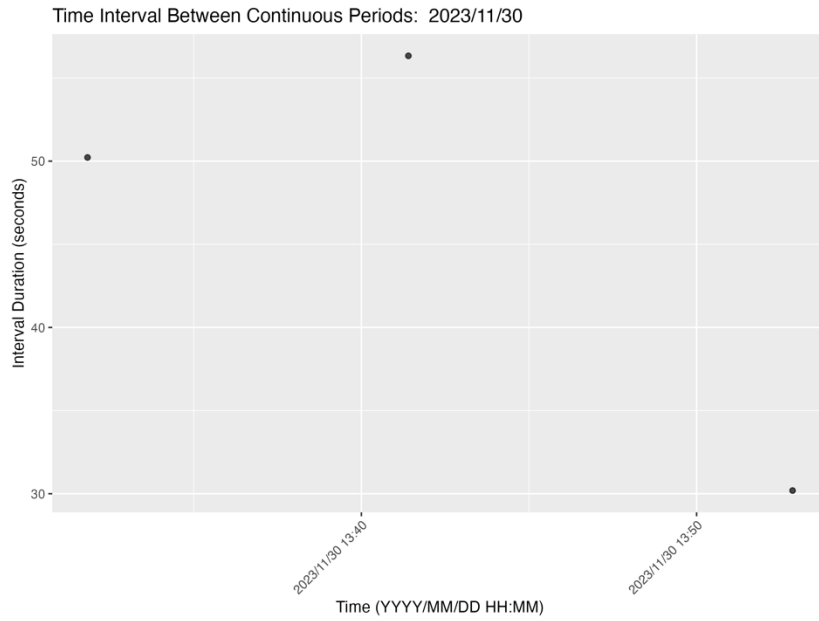


Figure 71. The time interval between continuous periods for the nearest Rockhopper for Foundation ID AP35 on November 30th, 2023.

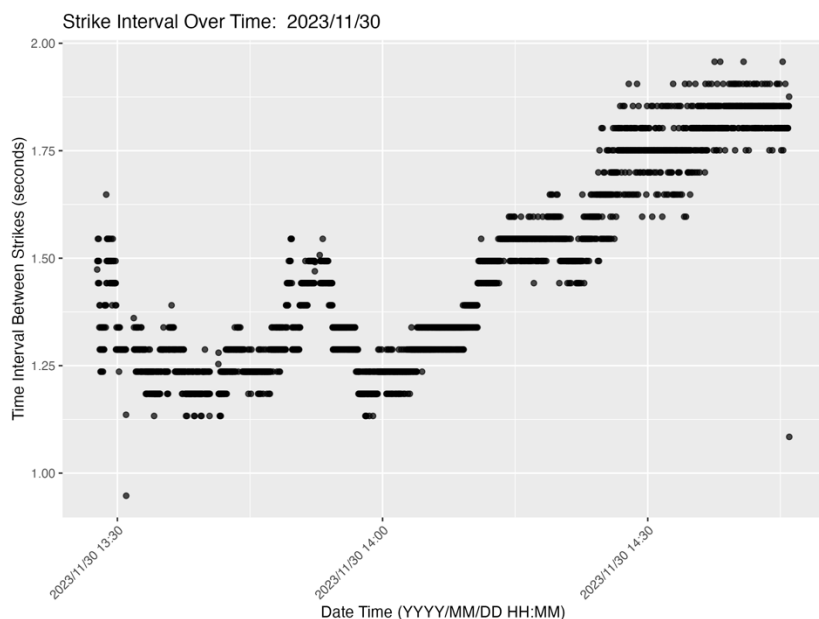


Figure 72. The time interval between strikes in a continuous period for Foundation ID AP35 on November 30th, 2023.

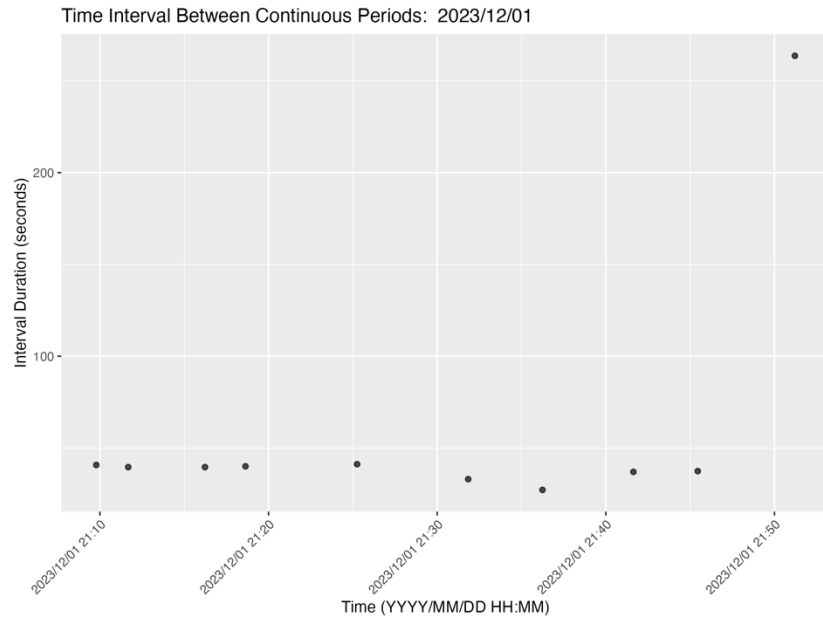


Figure 73. The time interval between continuous periods for the nearest Rockhopper for Foundation ID AN36 on December 1st, 2023.

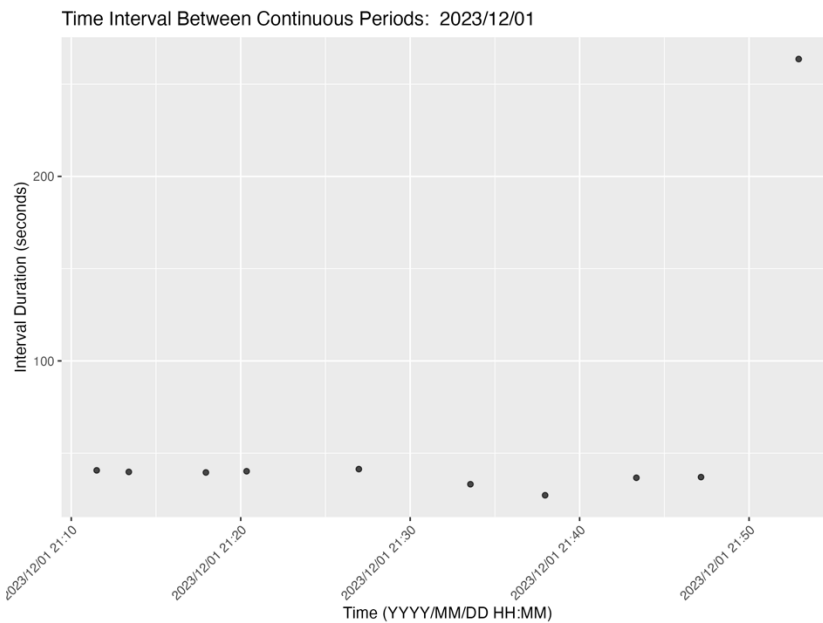


Figure 74. The time interval between continuous periods for the farthest Rockhopper for Foundation ID AN36 on December 1st, 2023.

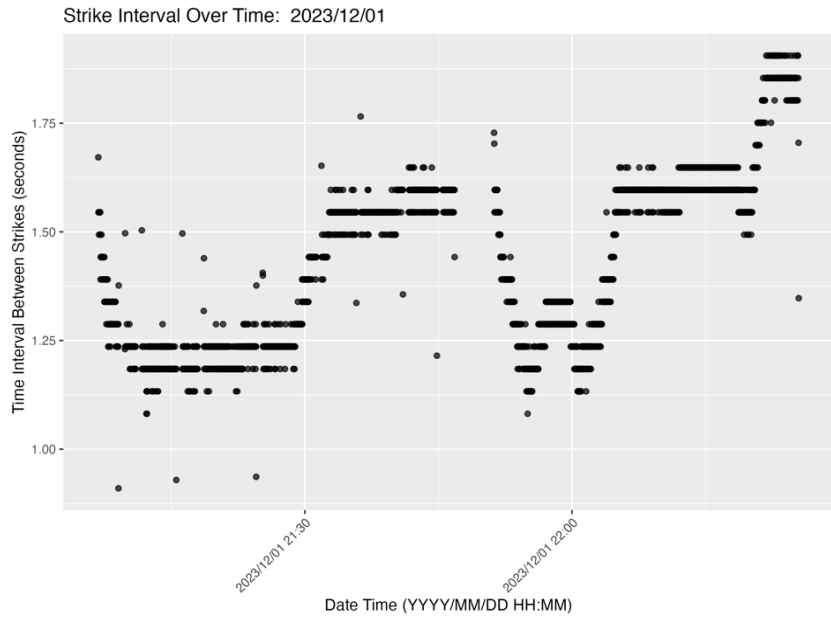


Figure 75. The time interval between strikes in a continuous period for the nearest Rockhopper for Foundation ID AN36 on December 1st, 2023.

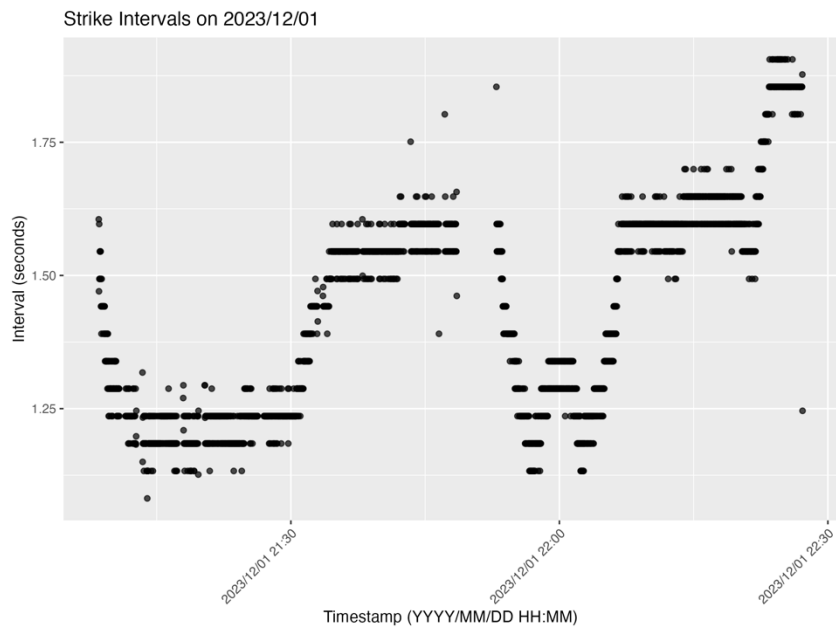


Figure 76. The time interval between strikes in a continuous period for the farthest Rockhopper for Foundation ID AN36 on December 1st, 2023.

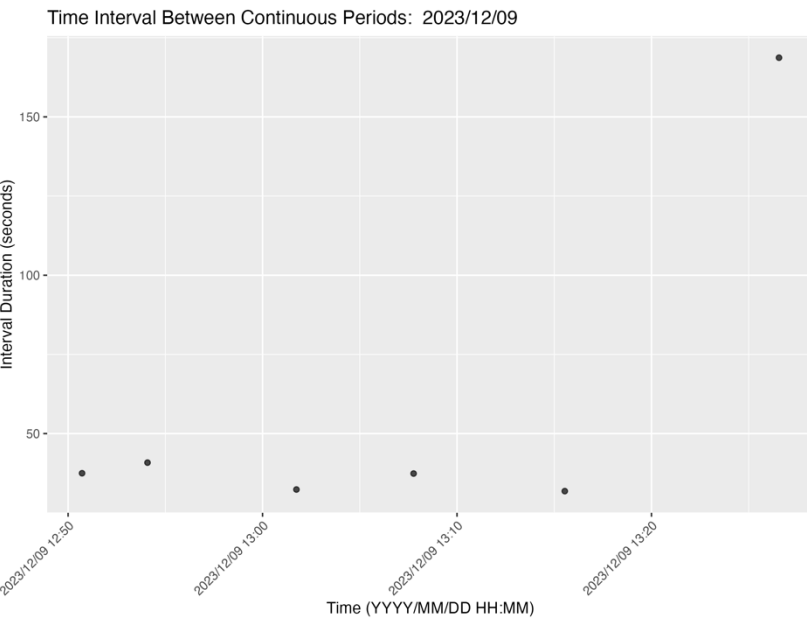


Figure 77. The time interval between continuous periods for the nearest Rockhopper for Foundation ID AR34 on December 9th, 2023.

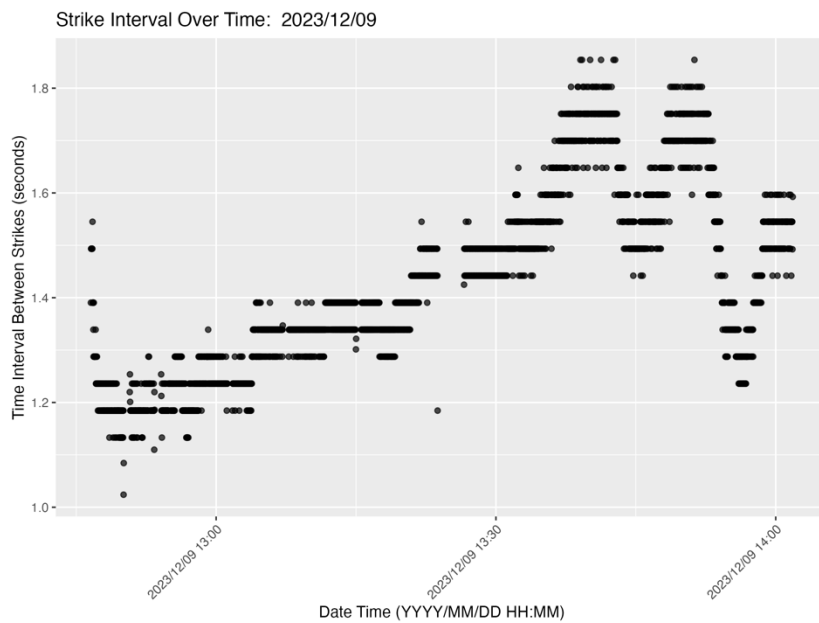


Figure 78. The time interval between strikes in a continuous period for the nearest Rockhopper for Foundation ID AR34 on December 9th, 2023.

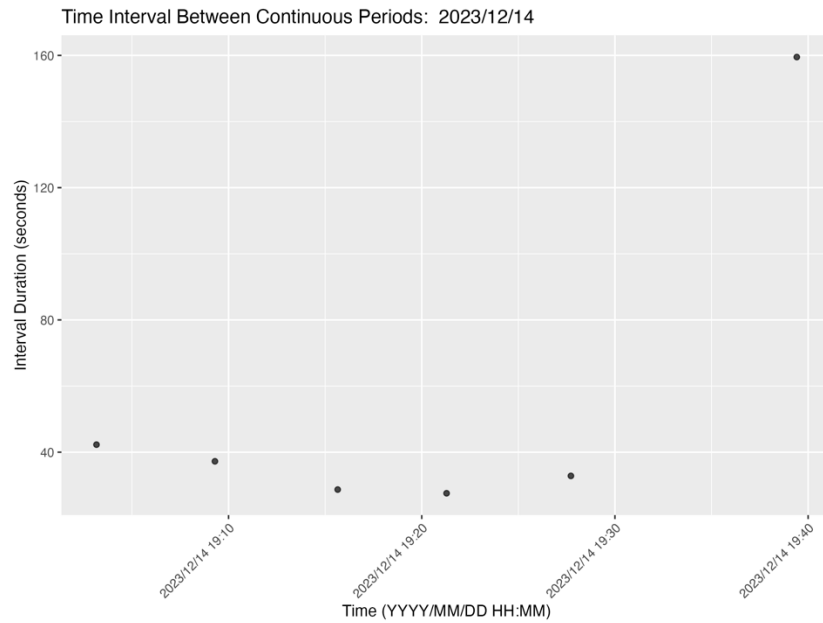


Figure 79. The time interval between continuous periods for the nearest Rockhopper for Foundation ID AR37 on December 14th, 2023.

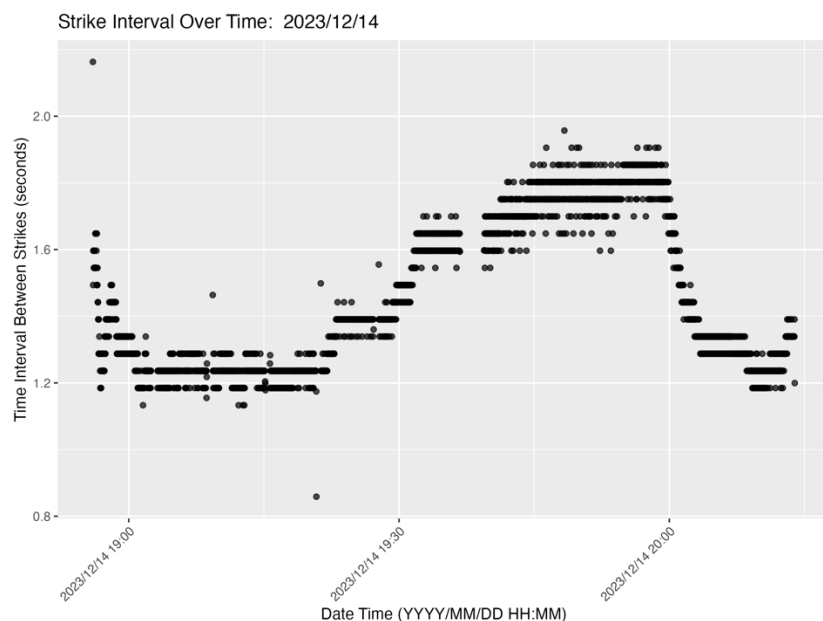


Figure 80. The time interval between strikes in a continuous period for the nearest Rockhopper for Foundation ID AR37 on December 14th, 2023.

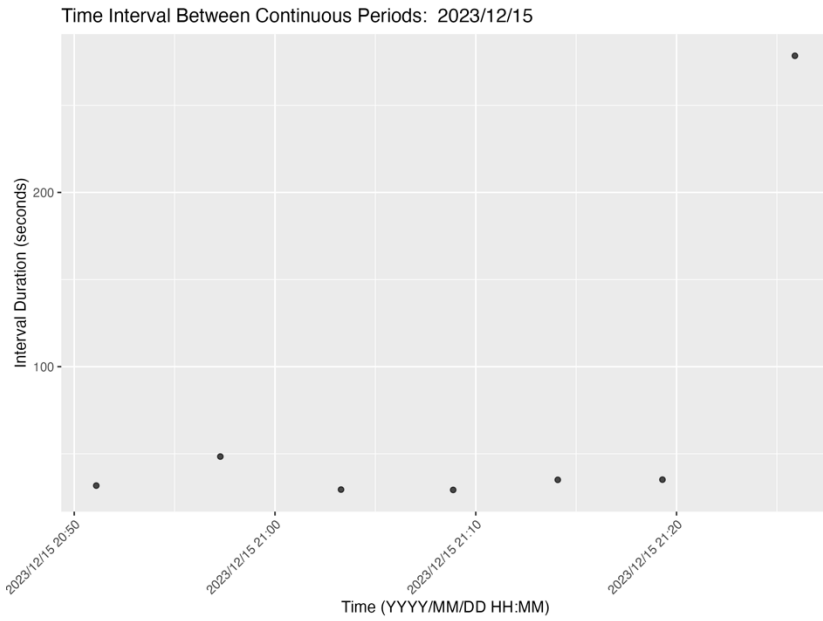


Figure 81. The time interval between continuous periods for the nearest Rockhopper for Foundation ID AT33 on December 15th, 2023.

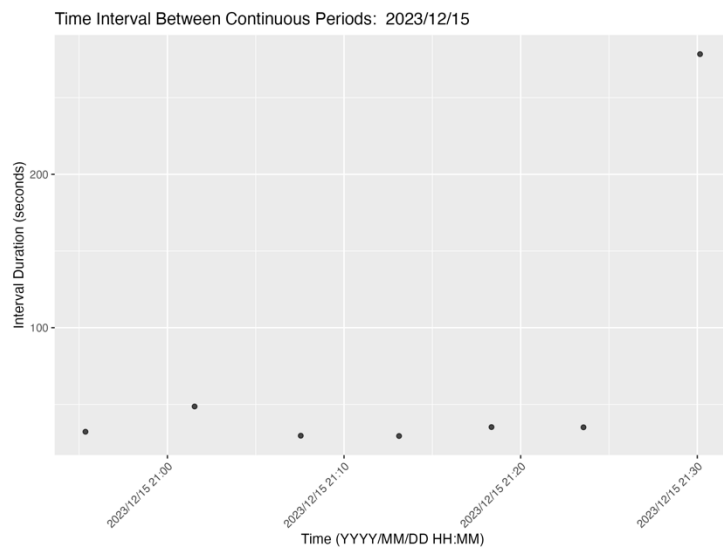


Figure 82. The time interval between continuous periods for the farthest Rockhopper for Foundation ID AT33 on December 15th, 2023.

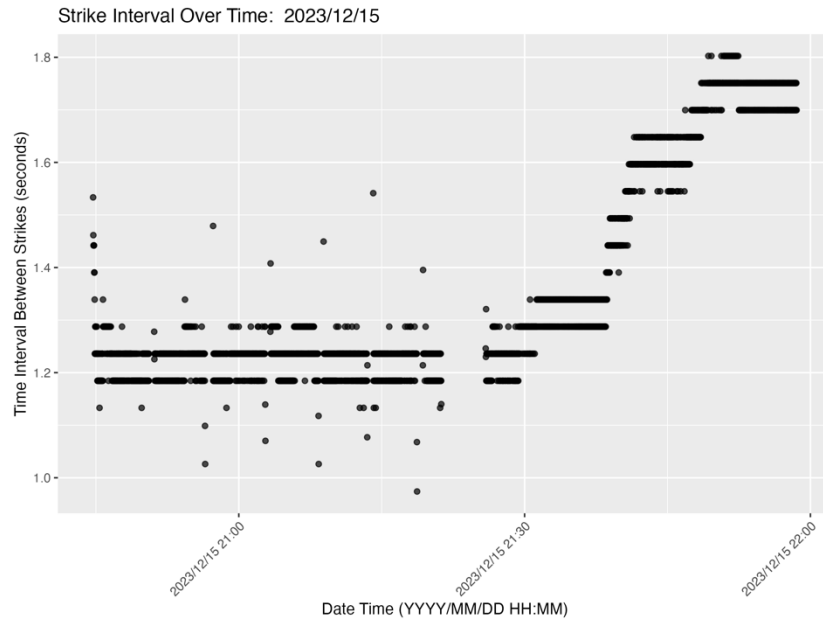


Figure 83. The time interval between strikes in a continuous period for the nearest Rockhopper for Foundation ID AT33 on December 15th, 2023.

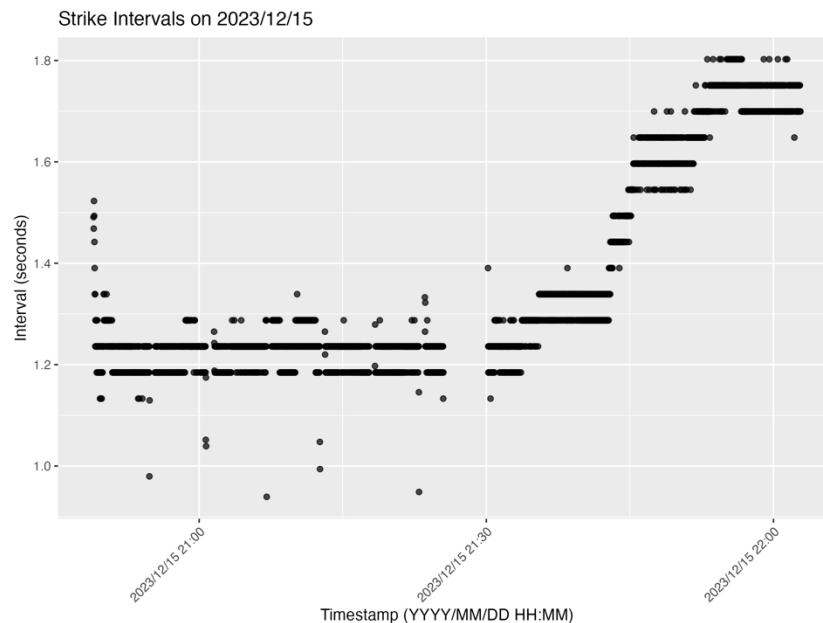


Figure 84. The time interval between strikes in a continuous period for the farthest Rockhopper for Foundation ID AT33 on December 15th, 2023.

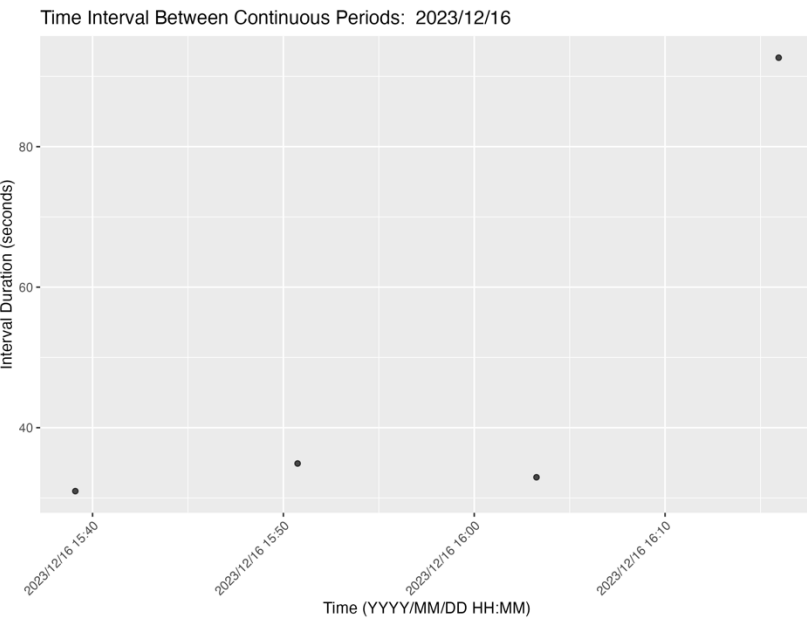


Figure 85. The time interval between continuous periods for the nearest Rockhopper for Foundation ID AS32 on December 16th, 2023.

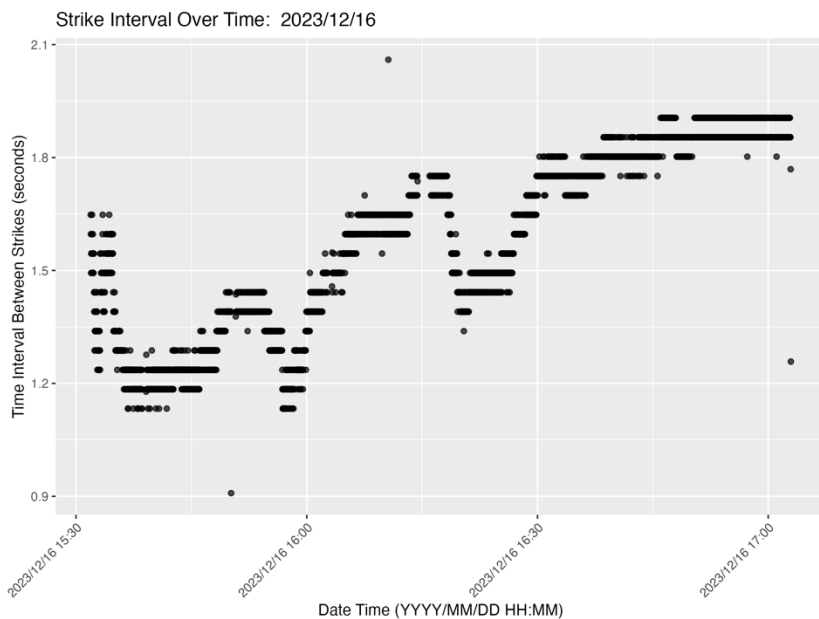


Figure 86. The time interval between strikes in a continuous period for the nearest Rockhopper for Foundation ID AS32 on December 16th, 2023.

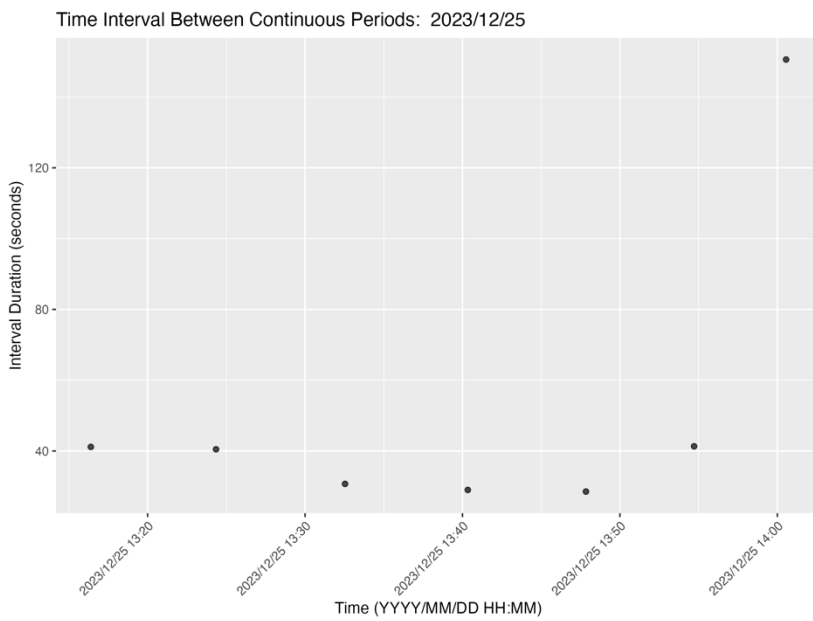


Figure 87. The time interval between continuous periods for the nearest Rockhopper for Foundation ID AQ35 on December 25th, 2023.

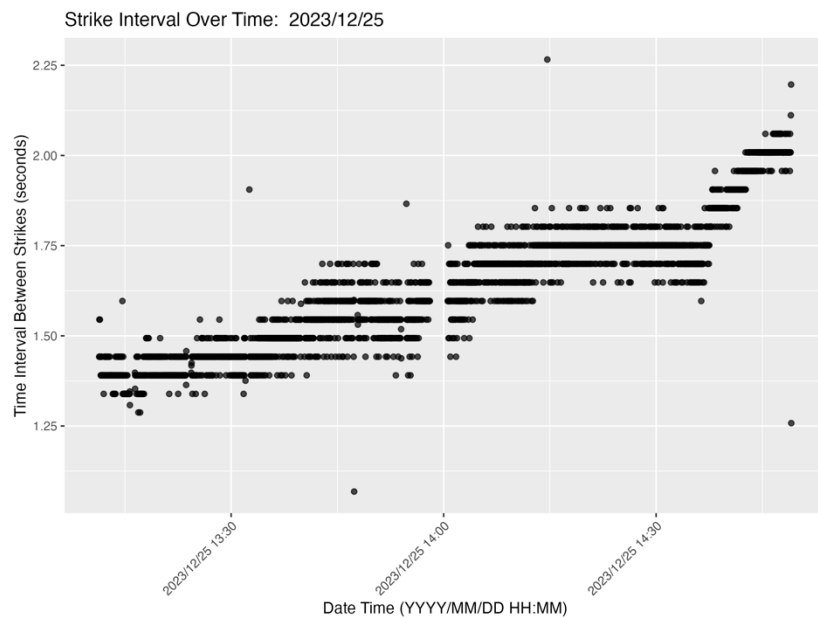


Figure 88. The time interval between strikes in a continuous period for the nearest Rockhopper for Foundation ID AQ35 on December 25th, 2023.

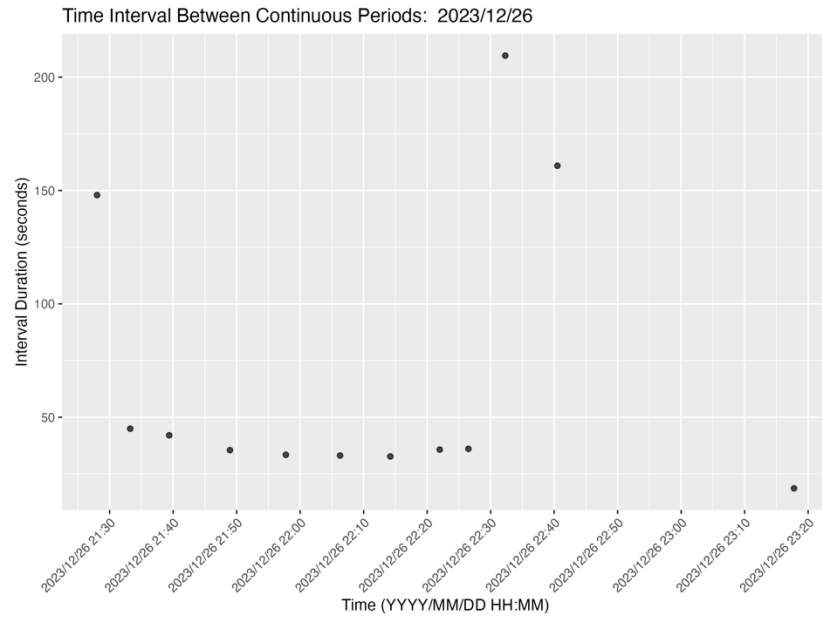


Figure 89. The time interval between continuous periods for the nearest Rockhopper for Foundation ID AS34 on December 26th, 2023.

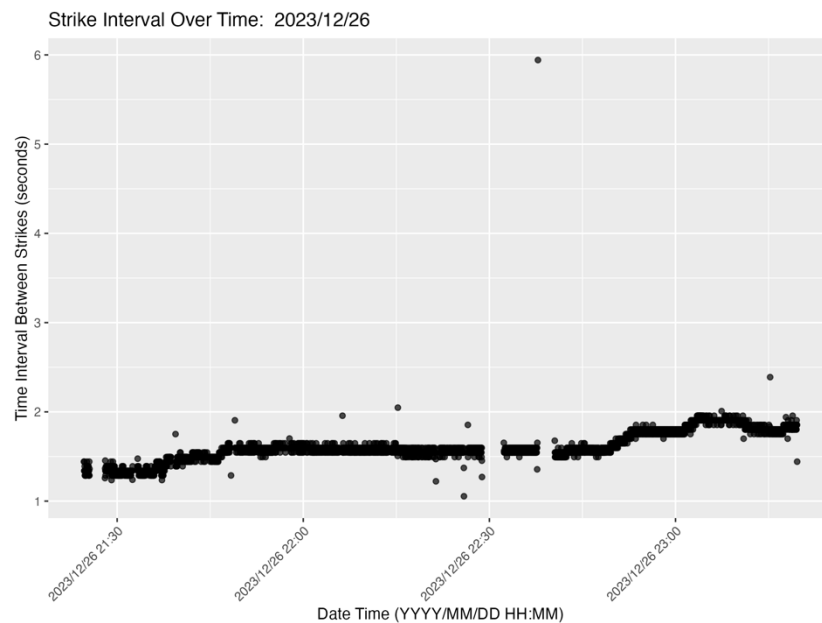


Figure 90. The time interval between strikes in a continuous period for the nearest Rockhopper for Foundation ID AS34 on December 26th, 2023.

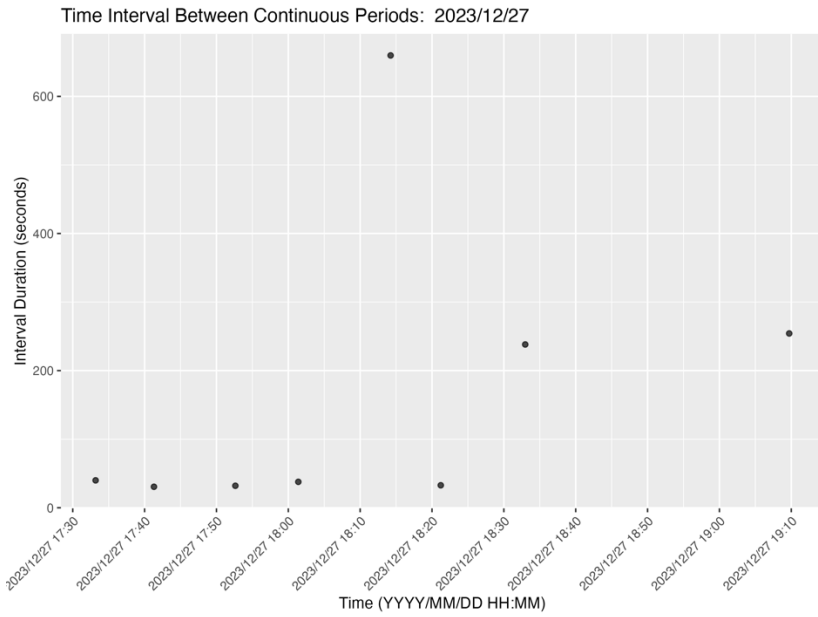


Figure 91. The time interval between continuous periods for the nearest Rockhopper for Foundation ID AR33 on December 27th, 2023.

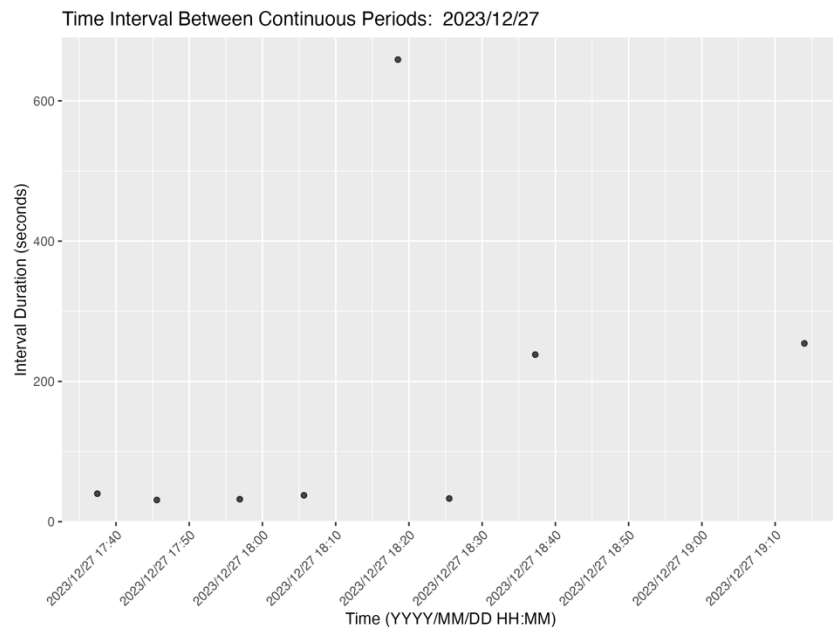


Figure 92. The time interval between continuous periods for the farthest Rockhopper for Foundation ID AR33 on December 27th, 2023.

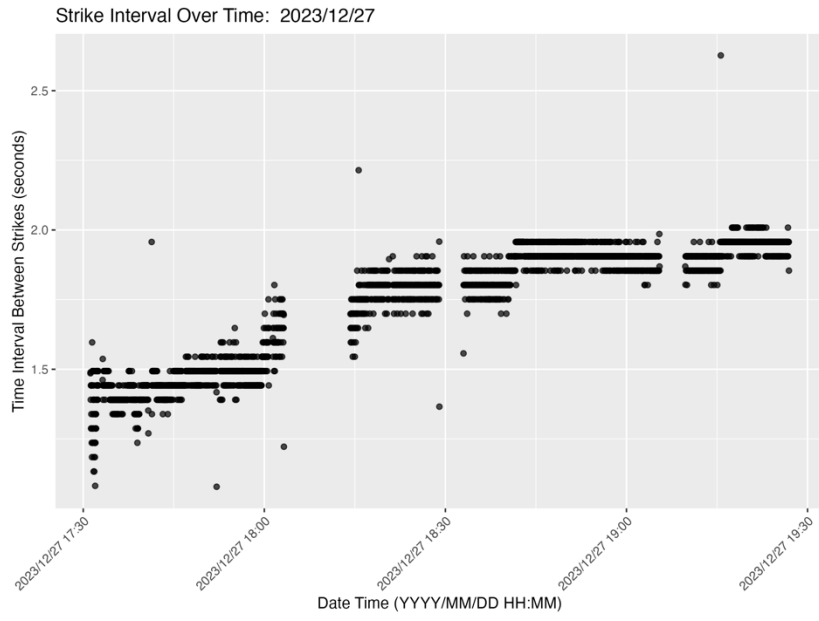


Figure 93. The time interval between strikes in a continuous period for the nearest Rockhopper for Foundation ID AR33 on December 27th, 2023.

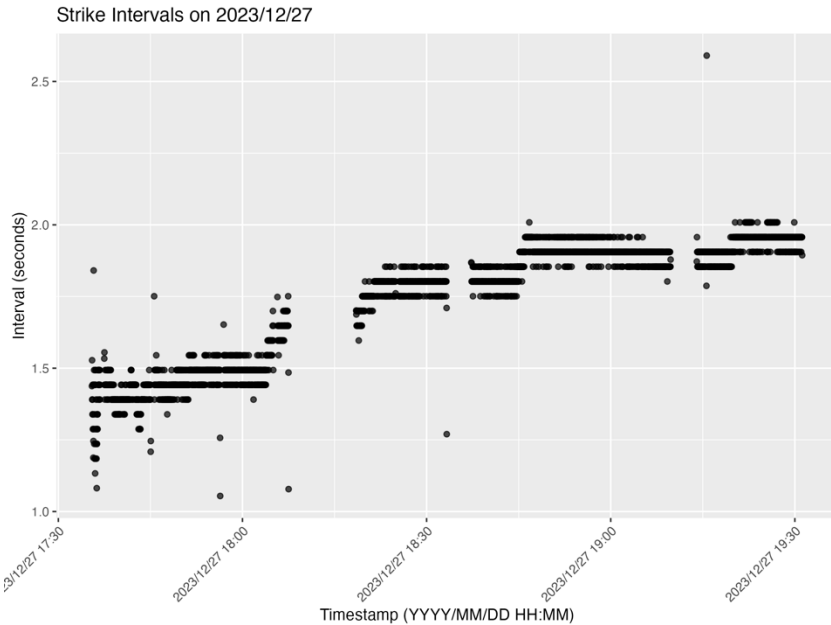


Figure 94. The time interval between strikes in a continuous period for the farthest Rockhopper for Foundation ID AR33 on December 27th, 2023.

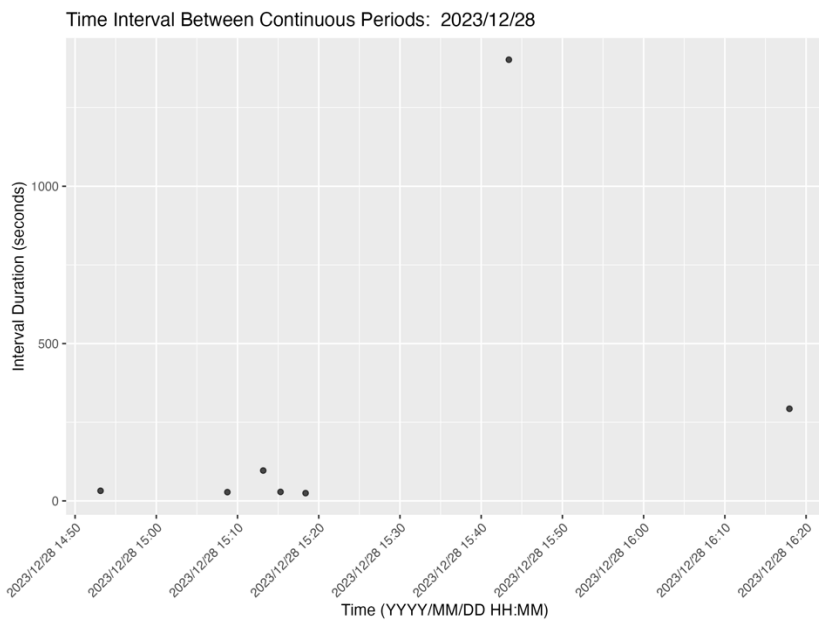


Figure 95. The time interval between continuous periods for the nearest Rockhopper for Foundation ID AS33 on December 28th, 2023.

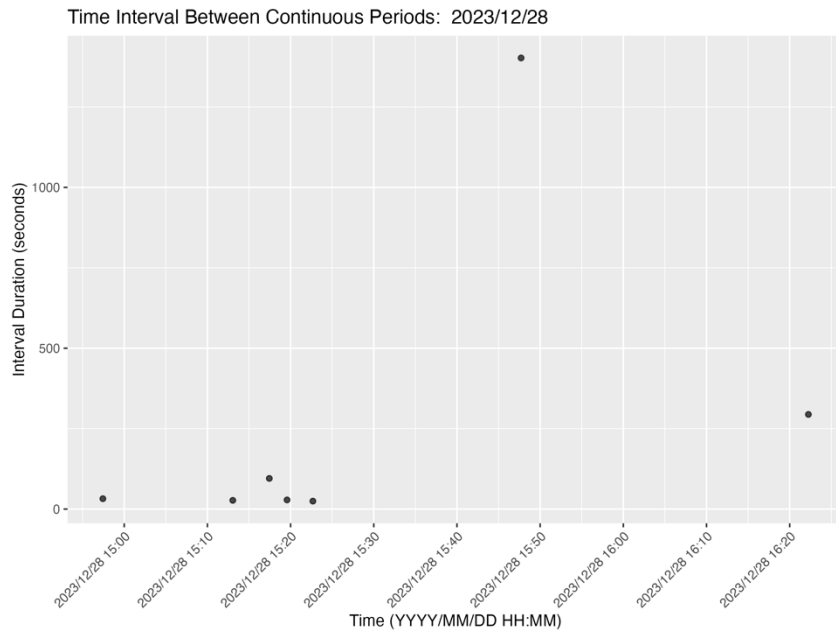


Figure 96. The time interval between continuous periods for the farthest Rockhopper for Foundation ID AS33 on December 28th, 2023.

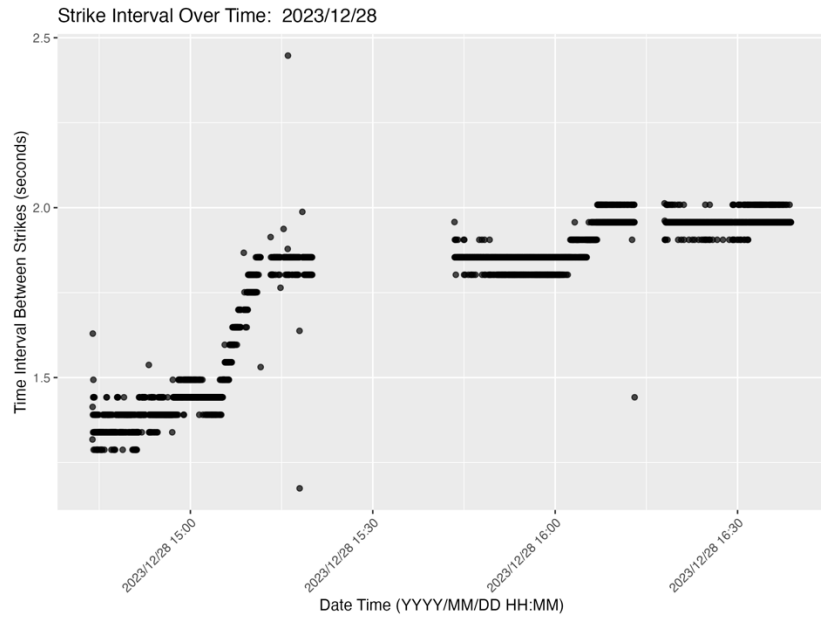


Figure 97. The time interval between strikes in a continuous period for the nearest Rockhopper for Foundation ID AS33 on December 28th, 2023.

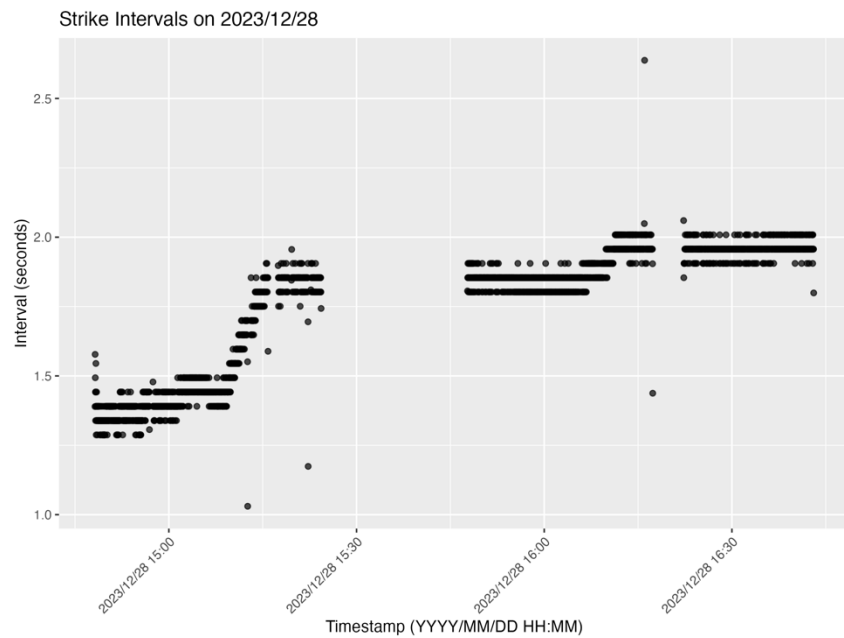


Figure 98. The time interval between strikes in a continuous period for the farthest Rockhopper for Foundation ID AS33 on December 28th, 2023.